Advances in Internal Dosimetry

Michael G. Stabin
Dept of Radiology/Radiological Sciences
Vanderbilt University
Nashville, TN, USA

HPS Savannah River Chapter Technical Seminar
Aiken, SC
April 16, 2010

Marinelli/Quimby method

Publications by Marinelli et al. and Quimby and Feitelberg, gave the dose from a beta emitter that decays completely in a tissue as

$$D_\beta = 73.8\, C\, E_\beta\, T$$

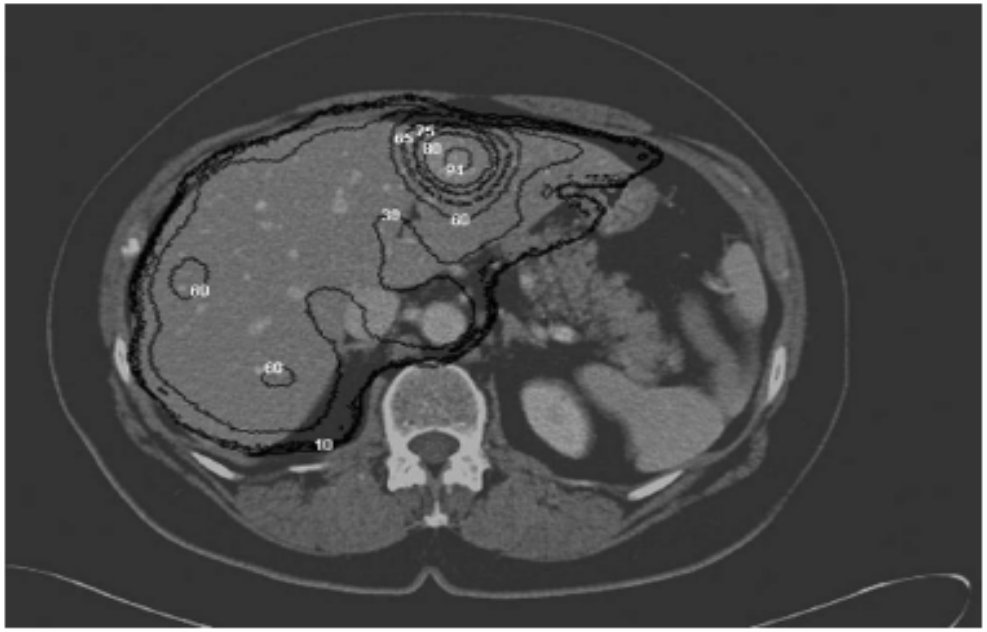

FIG. 7. Calculated dose distribution after administration of ^{131}I-MIBG superimposed on axial CT scan.

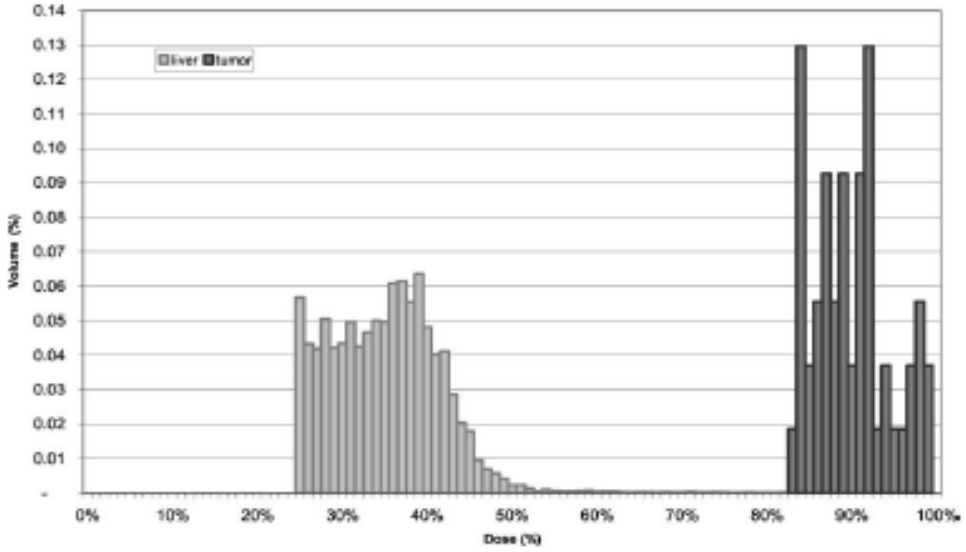

FIG. 8. Differential dose volume histogram for normal liver and metastasis of the case presented in this study.

Strigari *et al.*: Tumor control probability in systemic radiotherapy Medical Physics, Vol. 33, No. 6, June 2006

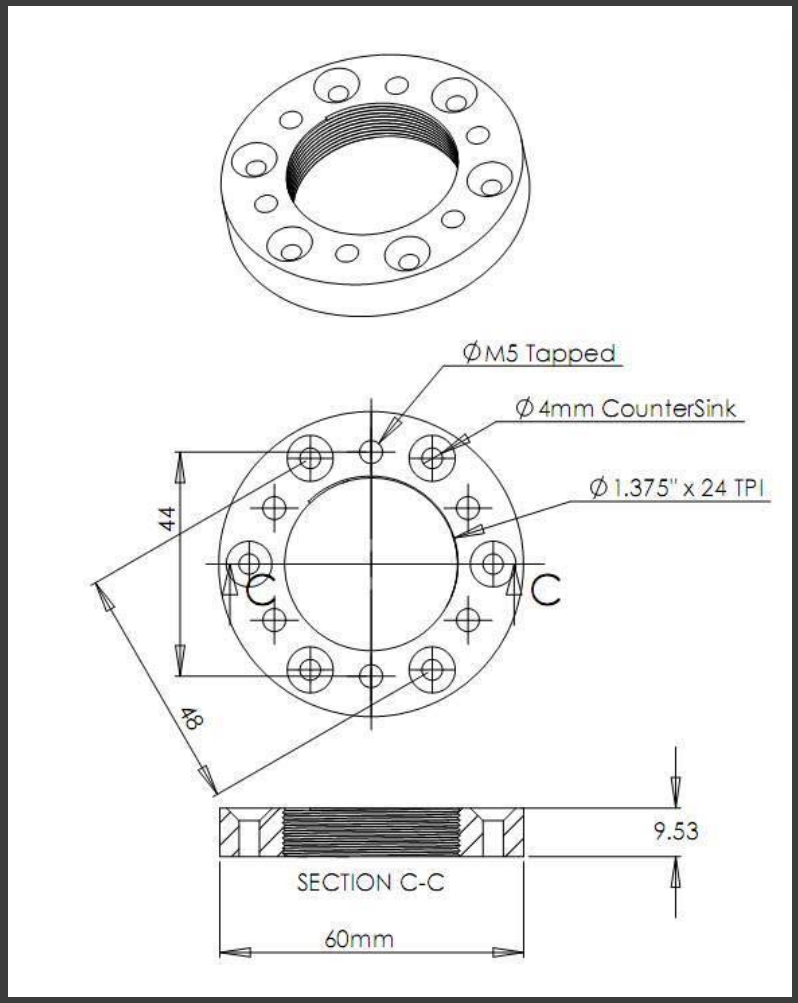

Standardization

SPECIAL CONTRIBUTION

MIRD Pamphlet No. 16: Techniques for Quantitative Radiopharmaceutical Biodistribution Data Acquisition and Analysis for Use in Human Radiation Dose Estimates

Jeffry A. Siegel, Stephen R. Thomas, James B. Stubbs, Michael G. Stabin, Marguerite T. Hays, Kenneth F. Koral, James S. Robertson, Roger W. Howell, Barry W. Wessels, Darrell R. Fisher, David A. Weber and A. Bertrand Brill

Nuclear Physics Enterprises, Cherry Hill, New Jersey; University of Cincinnati, Division of Medical Physics, Cincinnati, Ohio; Radiation Dosimetry Systems of Oak Ridge, Inc., Knoxville, Tennessee; Oak Ridge Institute for Science and Education, Radiation Internal Dose Information Center, Oak Ridge, Tennessee; Veterans Affairs Medical Center 640/151, Palo Alto, California; Department of Nuclear Medicine, University of Michigan, Ann Arbor, Michigan; Gaithersburg, Maryland; Division of Radiation Research, Department of Radiology, University of Medicine and Dentistry of New Jersey, Newark, New Jersey; Department of Radiology, George Washington University Medical Center, Washington, DC; Pacific Northwest National Laboratory, Richland, Washington; Department of Radiation Research, University of California Davis Medical Center, Sacramento, California; Department of Radiology, Vanderbilt University School of Medicine, Nashville, Tennessee

This report describes recommended techniques for radiopharmaceutical biodistribution data acquisition and analysis in human subjects to estimate radiation absorbed dose using the Medical Internal Radiation Dose (MIRD) schema. The document has been prepared in a format to address two audiences: individuals with a primary interest in designing clinical trials who are not experts in pling error analysis techniques and selected calculational examples. The utilization of the presented approach should aid in the standardization of protocol design for collecting kinetic data and in the calculation of absorbed dose estimates.

J Nucl Med 1999; 40:37S–61S

Standardized method and resources

- **RADAR** is the **RAdiation Dose Assessment Resource**, which is an task group of the US Society of Nuclear Medicine that maintains resources for internal and external dose calculations, on a US and European web site, and in a number of open literature publications.
- The **Organ Level INternal Dose Assessment** code, **OLINDA**, with an **EXponential Modeling** (EXM) function, is the update and replacement of the MIRDOSE personal computer software.

RADAR is all about……..

….helping people get standardized, high quality dose information!

The RADAR Web Site www.doseinfo-radar.com

- Standardized information
- Reliable information
- Information when people need it, which is generally “right now, please”.
- Consistency over time
- Minimizing confusion
- Teaching and training

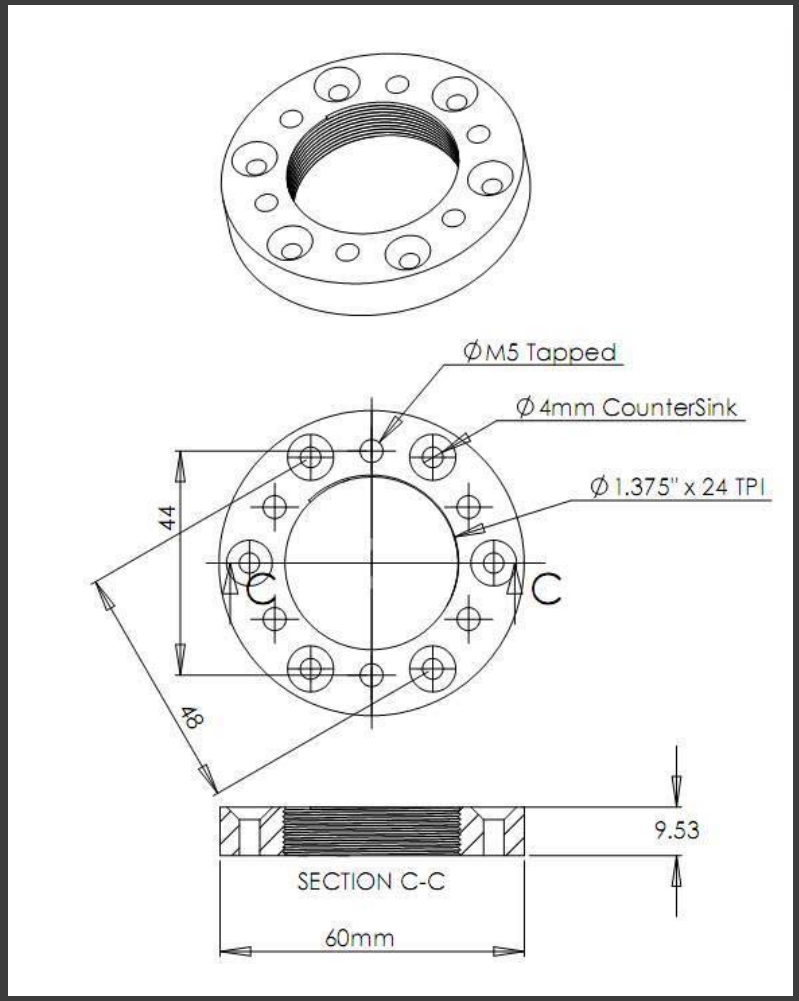

standardized, but…….

MIRD

$$D(r_T, T_D) = \int_0^{T_D} \dot{D}(r_T, t)dt$$

$$= \sum_{r_S} \int_0^{T_D} A(r_S, t) S(r_T \leftarrow r_S, t)dt,$$

$$S(r_T \leftarrow r_S, t) = \frac{1}{M(r_T, t)} \sum_i E_i Y_i \phi(r_T \leftarrow r_S, E_i, t)$$

ICRP

$$H_{50,T} = \sum_S U_S \, SEE(T \leftarrow S)$$

$$SEE = \frac{k \sum_i n_i E_i \phi_i Q_i}{m}$$

$$D = N \times DF$$

N is the number of disintegrations that occur in a source region

DF is the dose factor, which gives the dose absorbed in a target per disintegration in a source

Stabin and Siegel, HPJ 85(3):294-310, 2003.

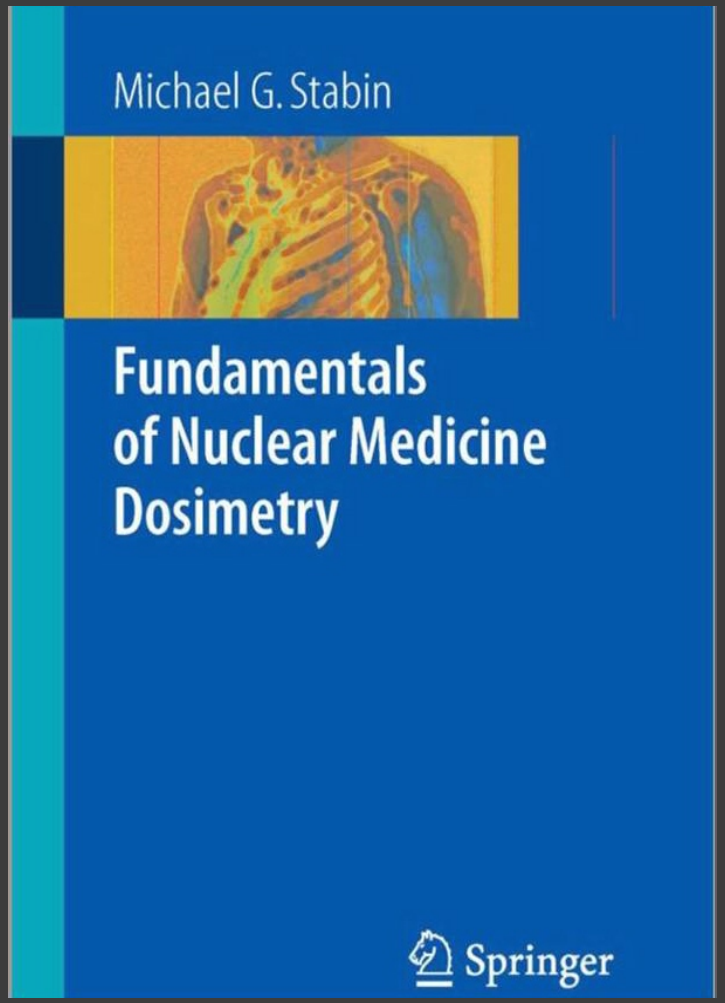

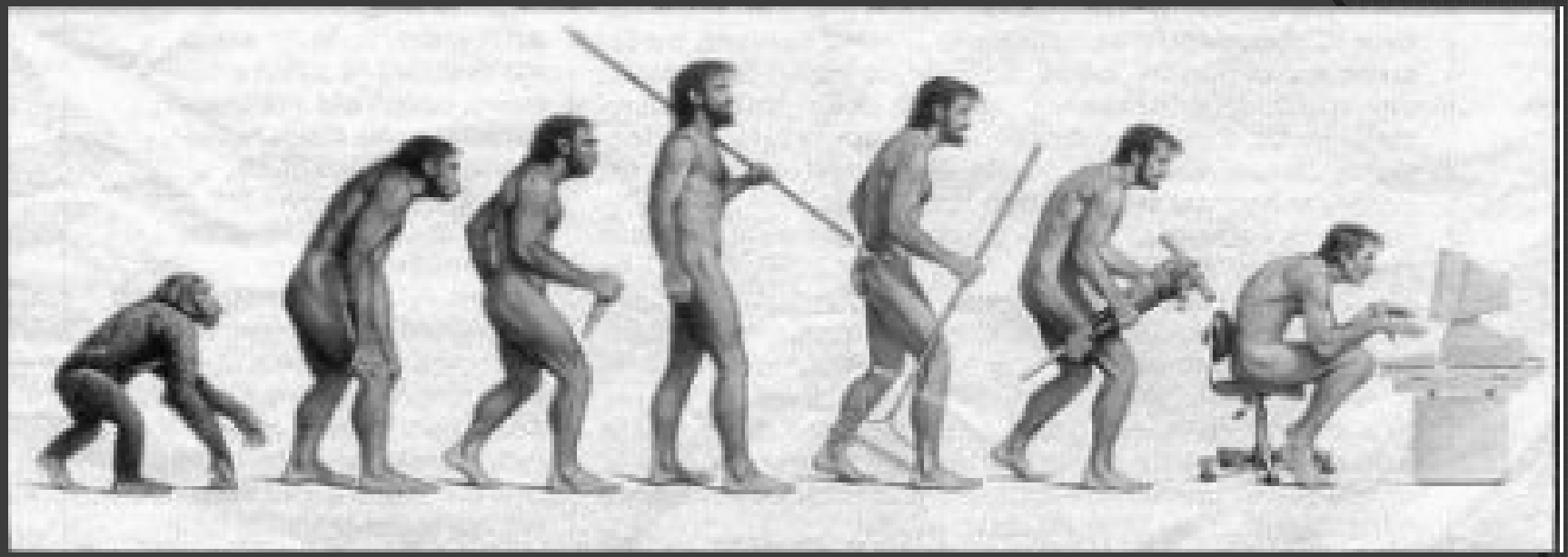

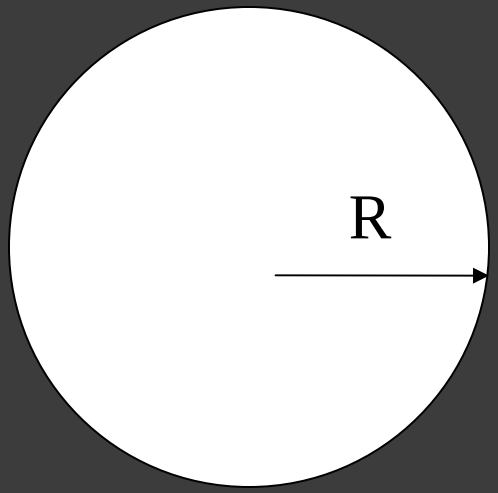

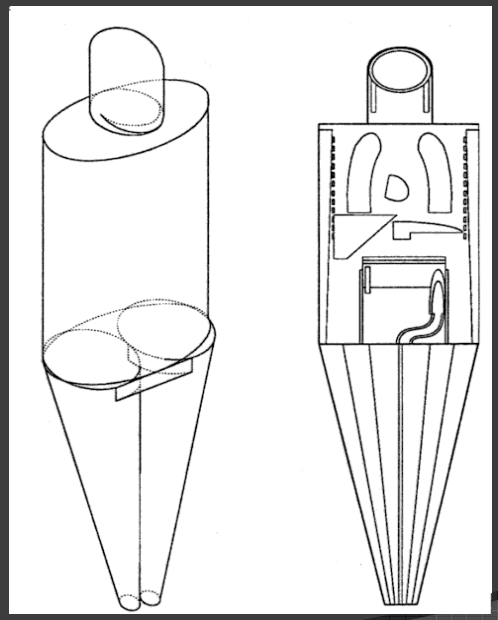

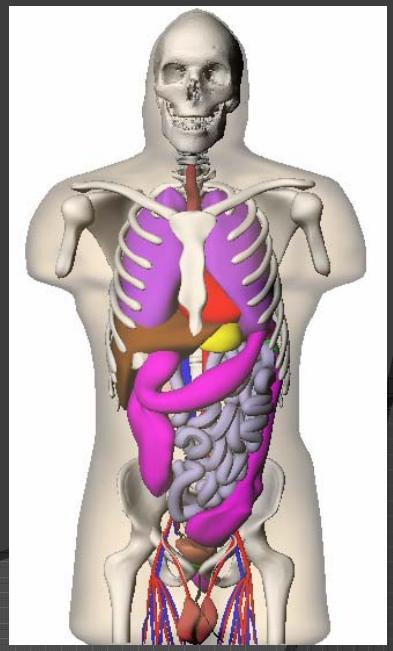

1959 **1975** **2001**

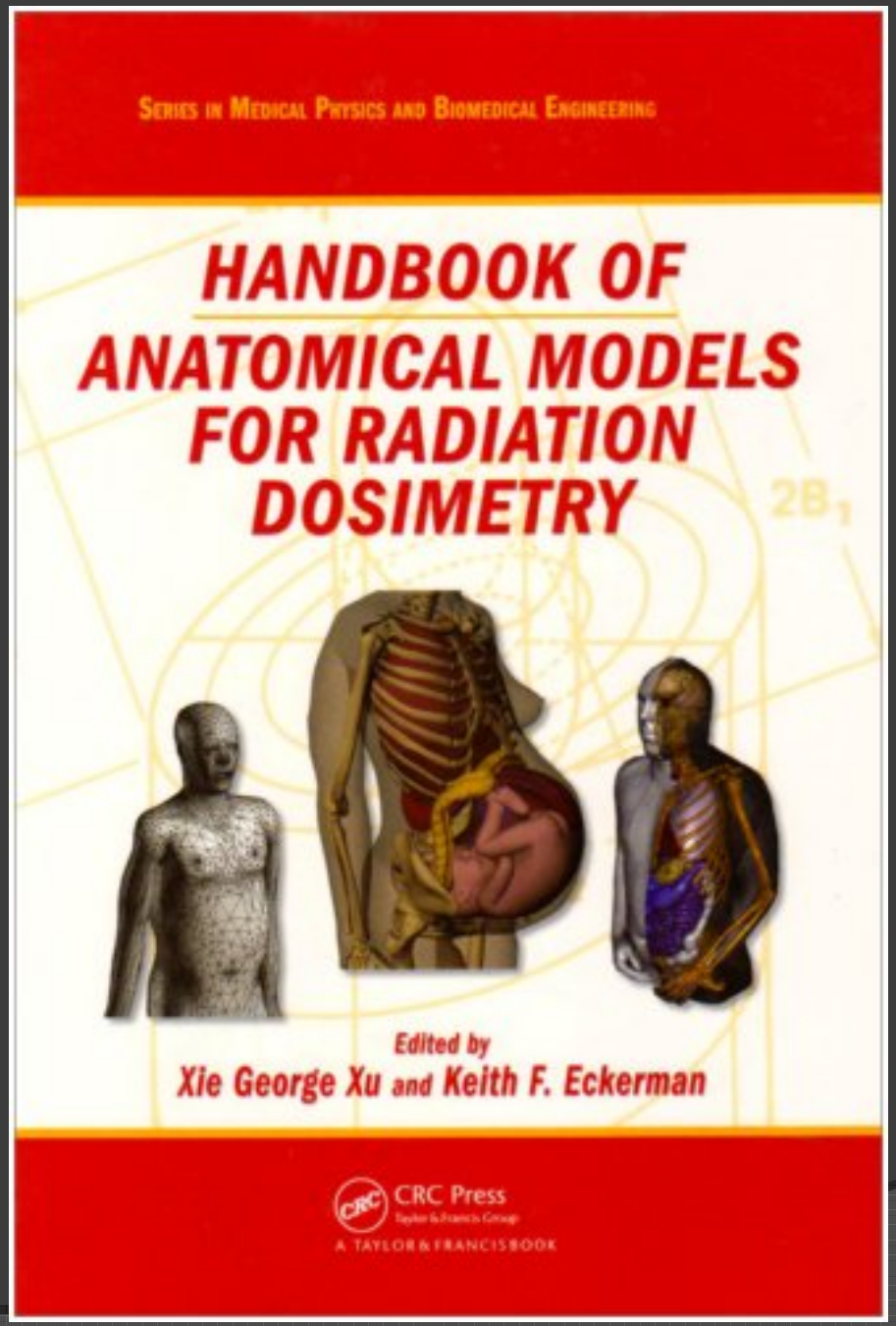
Series in Medical Physics and Biomedical Engineering
HANDBOOK OF
ANATOMICAL MODELS
FOR RADIATION
DOSIMETRY
Edited by
Xie George Xu and Keith F. Eckerman
CRC Press
A TAYLOR & FRANCIS BOOK

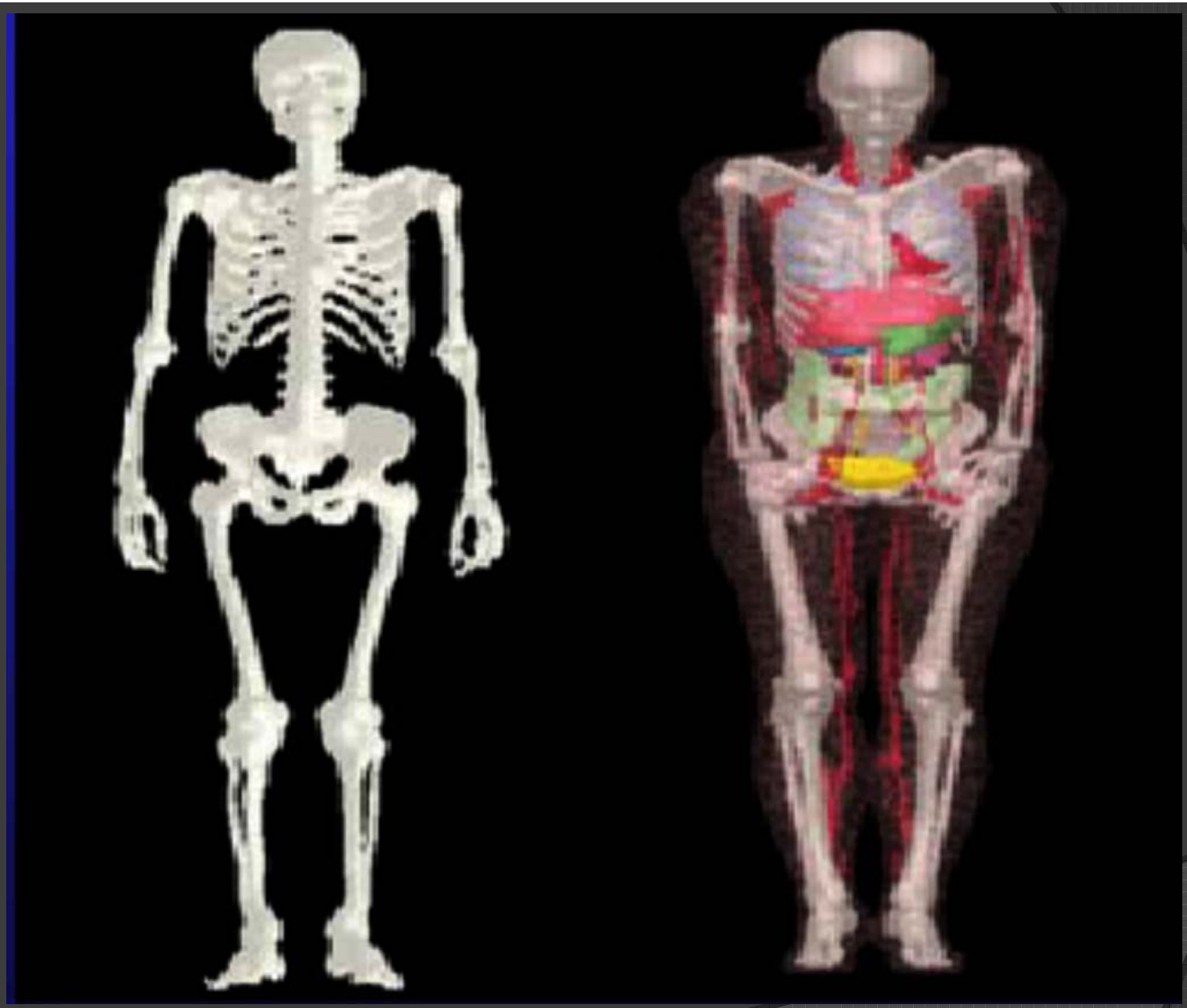

GSF Reference Adult Male and Female

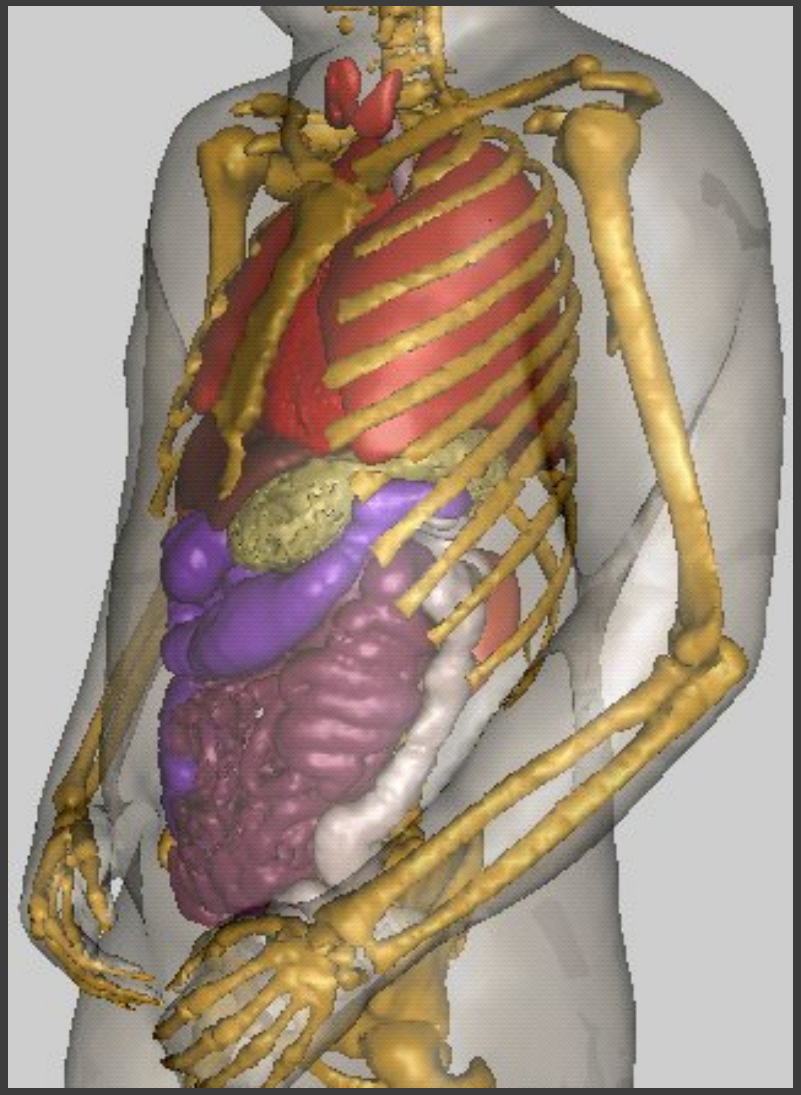

Xu and colleagues – Rensselaer Polytechnic Institute
VIP man realistic model

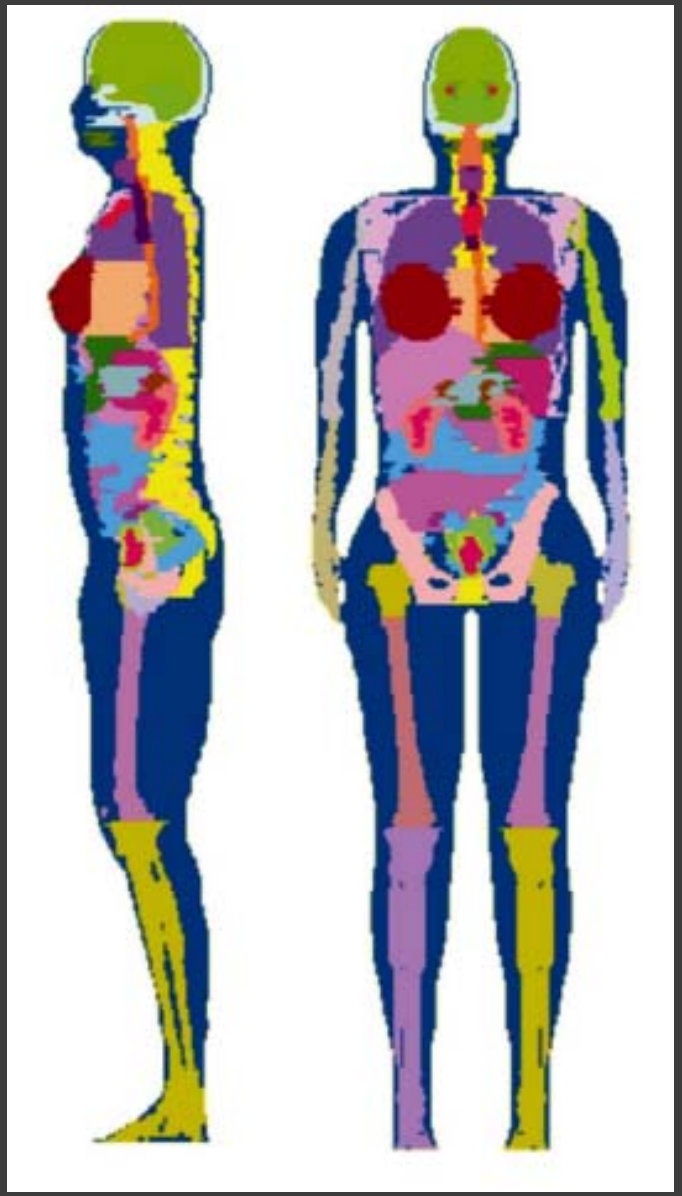

Kramer et al. The FAX phantom: frontal and lateral view with skeleton and internal organs. Phys. Med. Biol. 49 (2004) 5203–5216.

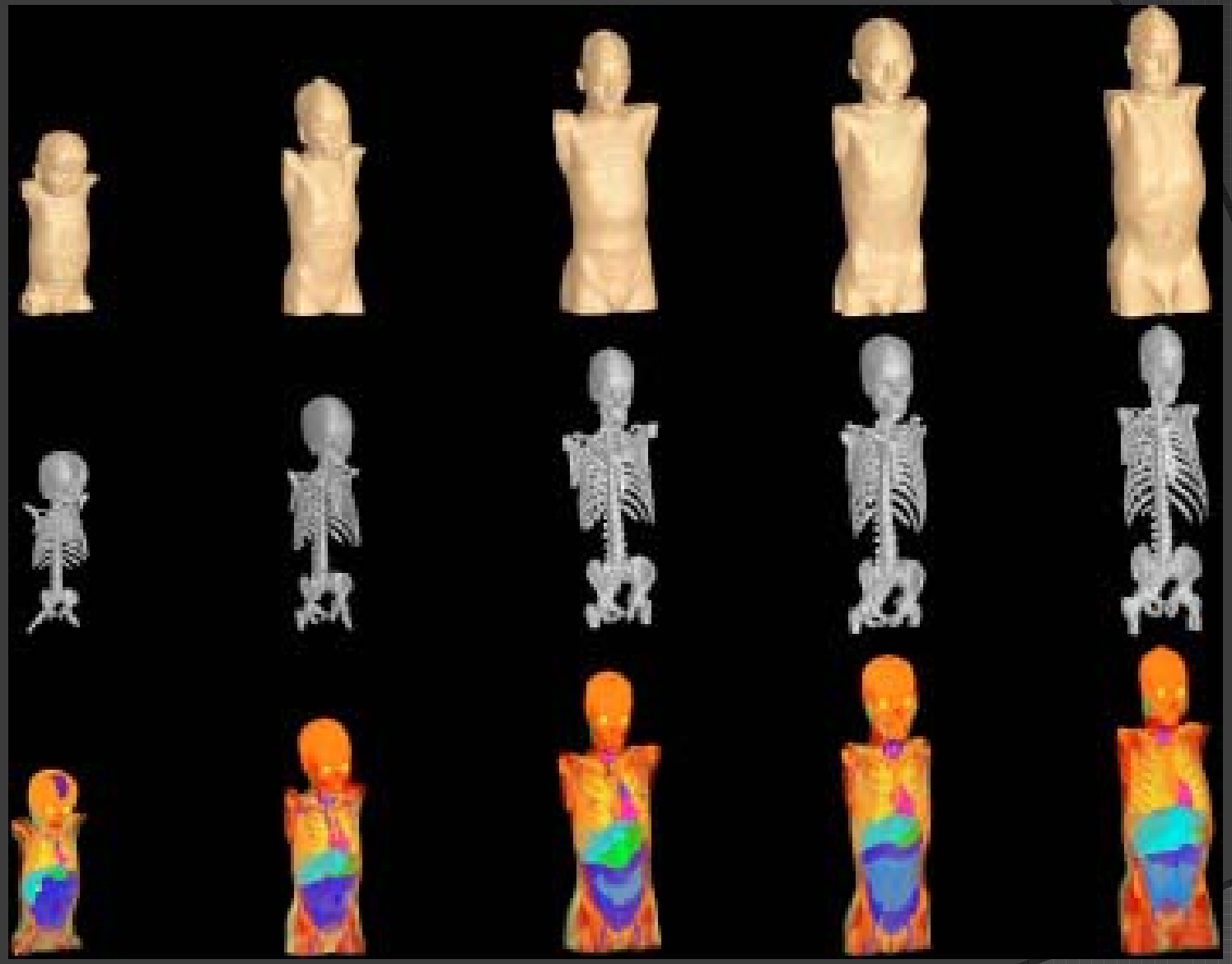

Lee C, Williams JL, Lee C, Bolch WE. The UF series of tomographic computational phantoms of pediatric patients. Med Phys. 2005 Dec;32(12):3537-48.

NURBS Phantoms

- Developed by William Paul Segars, Johns Hopkins Medical Institutes.
- 4D NURBS-based cardiac-torso (NCAT) phantom: realistic and flexible model of the human anatomy and physiology for medical imaging research.
- Organ models are based on NURBS, non-uniform rational B-splines, as used in computer graphics.
- NURBS, which define continuous surfaces, allow the phantom to be defined at any spatial resolution.
- A nice innovation is the extension of NURBS to a fourth dimension, time, to model the cardiac and respiratory motions.

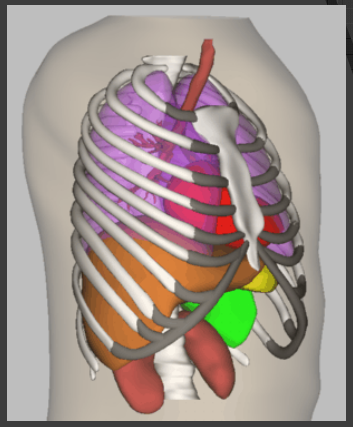

Respiratory Motion

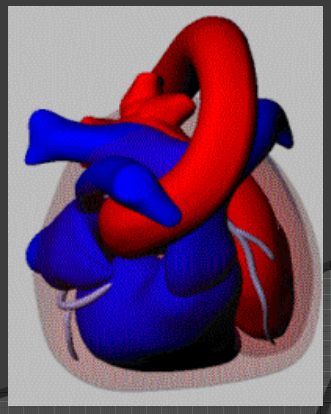

Cardiac Motion

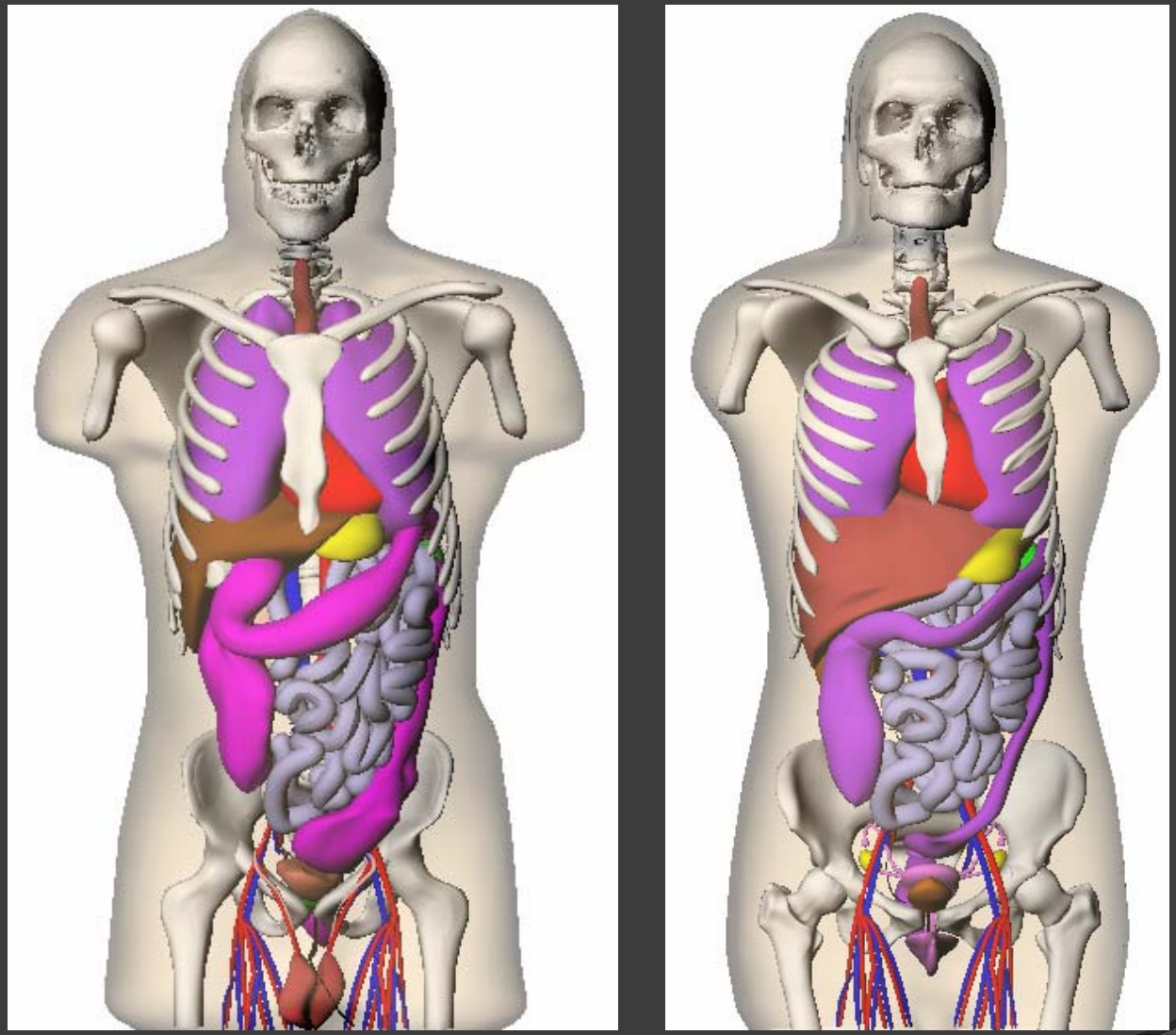

Anterior views of the NURBS models of the adult male (left) and adult female (right)

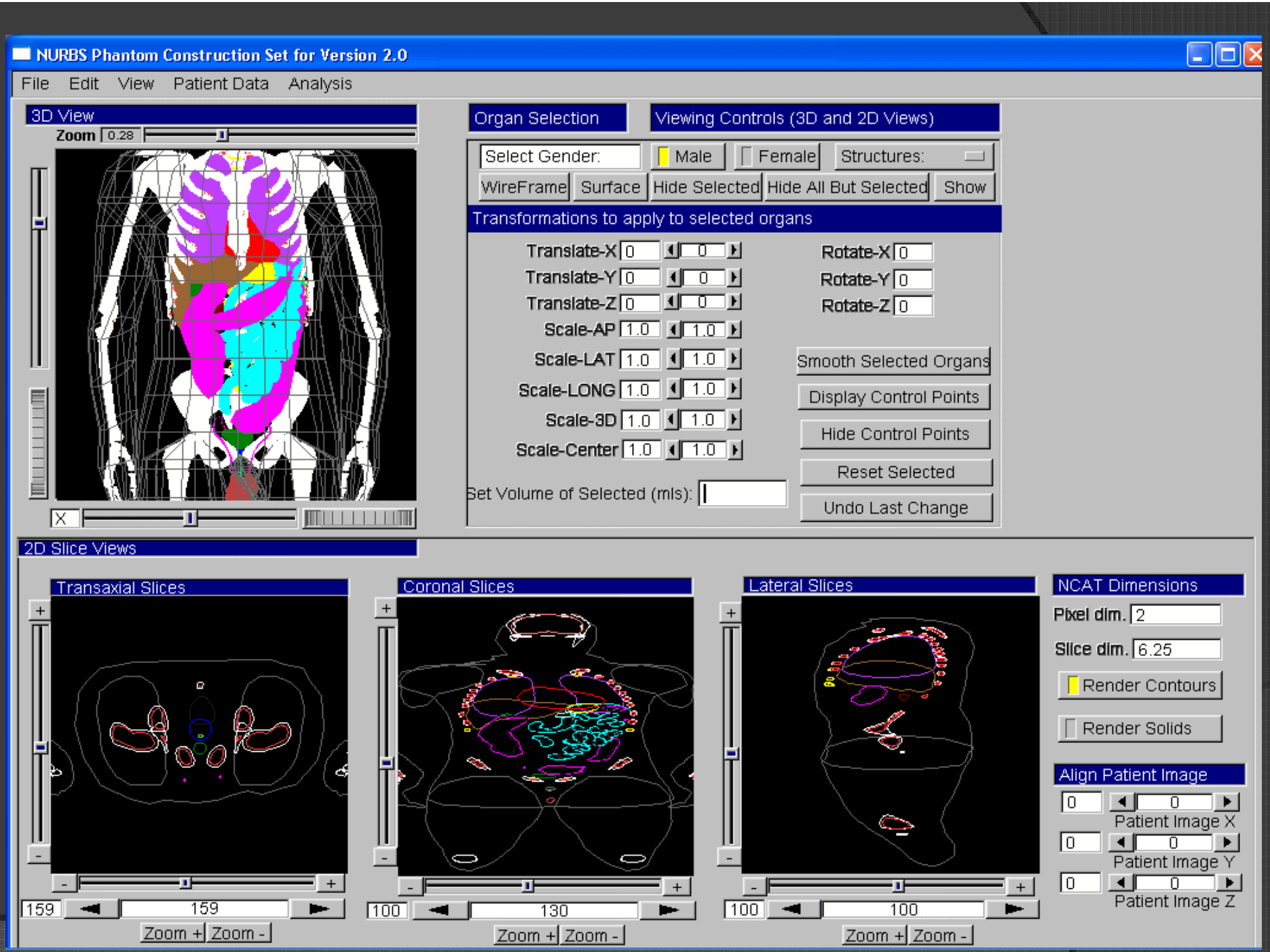
NURBS Phantom Construction Set for Version 2.0
File
Edit
View
Patient Data
Analysis
3D View
Zoom
0.28
X
Organ Selection
Viewing Controls (3D and 2D Views)
Select Gender:
Male
Female
Structures:
WireFrame
Surface
Hide Selected
Hide All But Selected
Show
Transformations to apply to selected organs
Translate-X
Translate-Y
Translate-Z
Scale-AP
Scale-LAT
Scale-LONG
Scale-3D
Scale-Center
Rotate-X
Rotate-Y
Rotate-Z
Smooth Selected Organs
Display Control Points
Hide Control Points
Reset Selected
Undo Last Change
Set Volume of Selected (mls):
2D Slice Views
Transaxial Slices
Coronal Slices
Lateral Slices
159
130
100
Zoom +
Zoom -
NCAT Dimensions
Pixel dim.
2
Slice dim.
6.25
Render Contours
Render Solids
Align Patient Image
Patient Image X
Patient Image Y
Patient Image Z

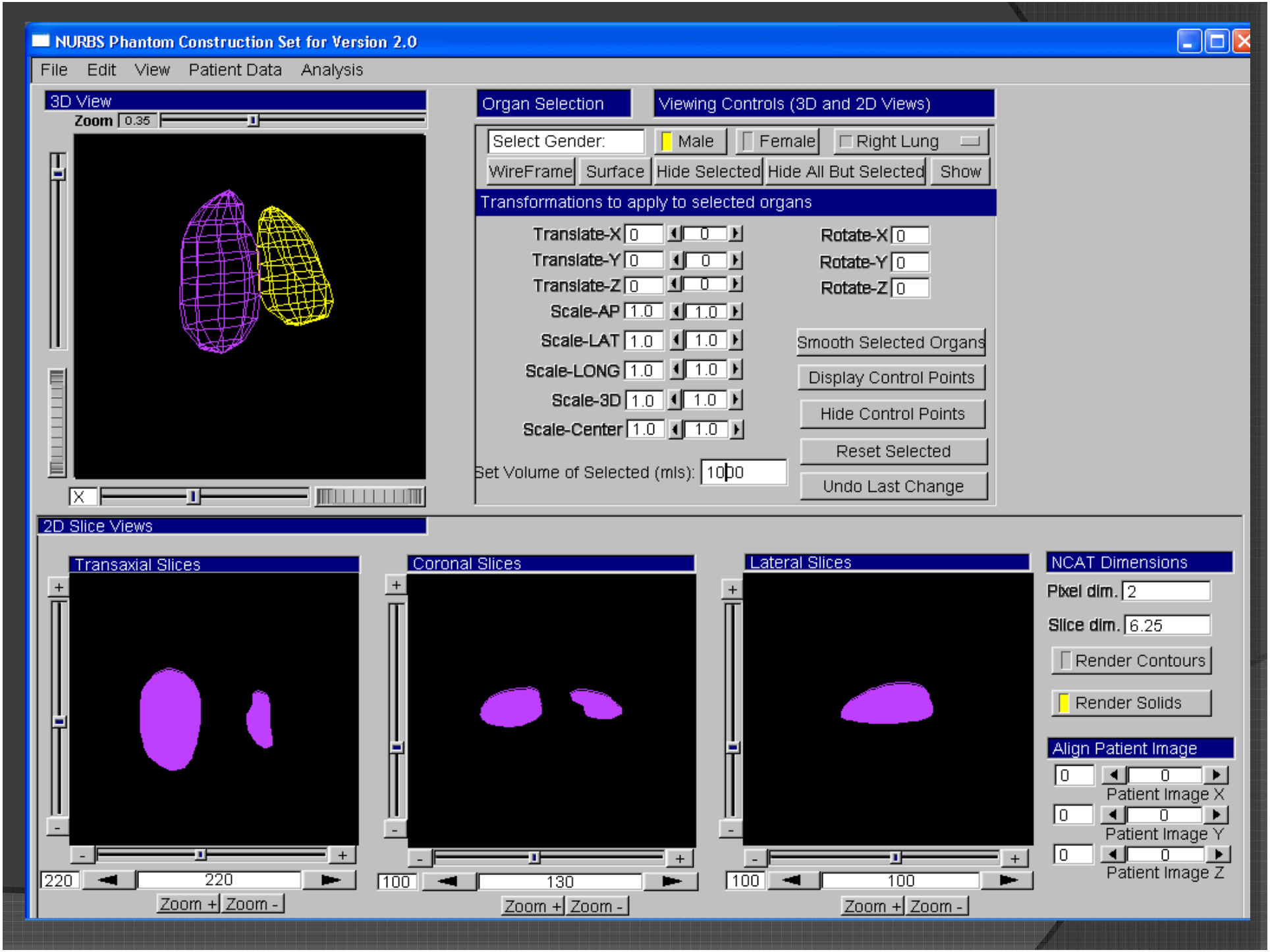
NURBS Phantom Construction Set for Version 2.0
File
Edit
View
Patient Data
Analysis
3D View
Zoom
0.35
X
Organ Selection
Viewing Controls (3D and 2D Views)
Select Gender:
Male
Female
Right Lung
WireFrame
Surface
Hide Selected
Hide All But Selected
Show
Transformations to apply to selected organs
Translate-X
Translate-Y
Translate-Z
Scale-AP
Scale-LAT
Scale-LONG
Scale-3D
Scale-Center
Rotate-X
Rotate-Y
Rotate-Z
Smooth Selected Organs
Display Control Points
Hide Control Points
Reset Selected
Undo Last Change
Set Volume of Selected (mls):
1000
2D Slice Views
Transaxial Slices
Coronal Slices
Lateral Slices
220
220
100
130
100
100
Zoom +
Zoom -
NCAT Dimensions
Pixel dim.
2
Slice dim.
6.25
Render Contours
Render Solids
Align Patient Image
Patient Image X
Patient Image Y
Patient Image Z

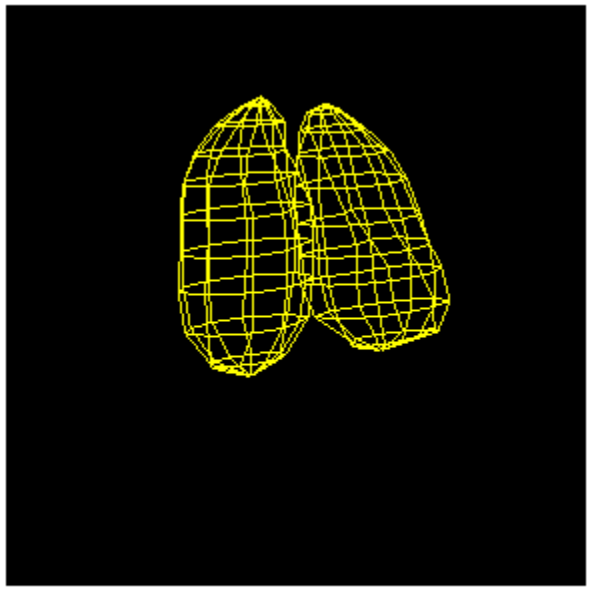

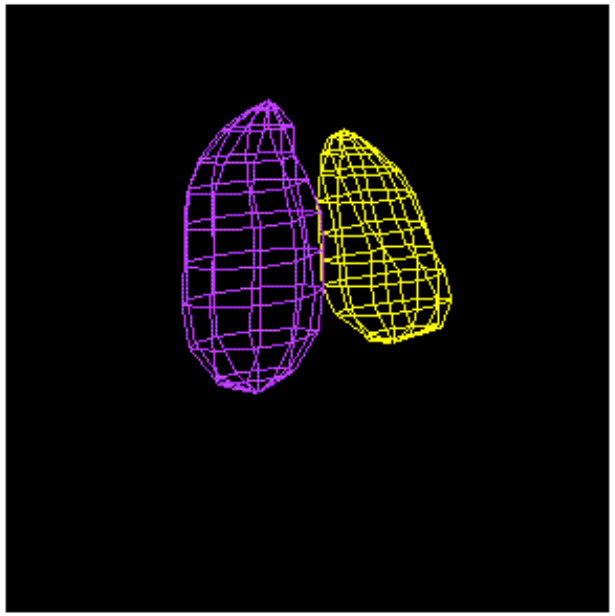

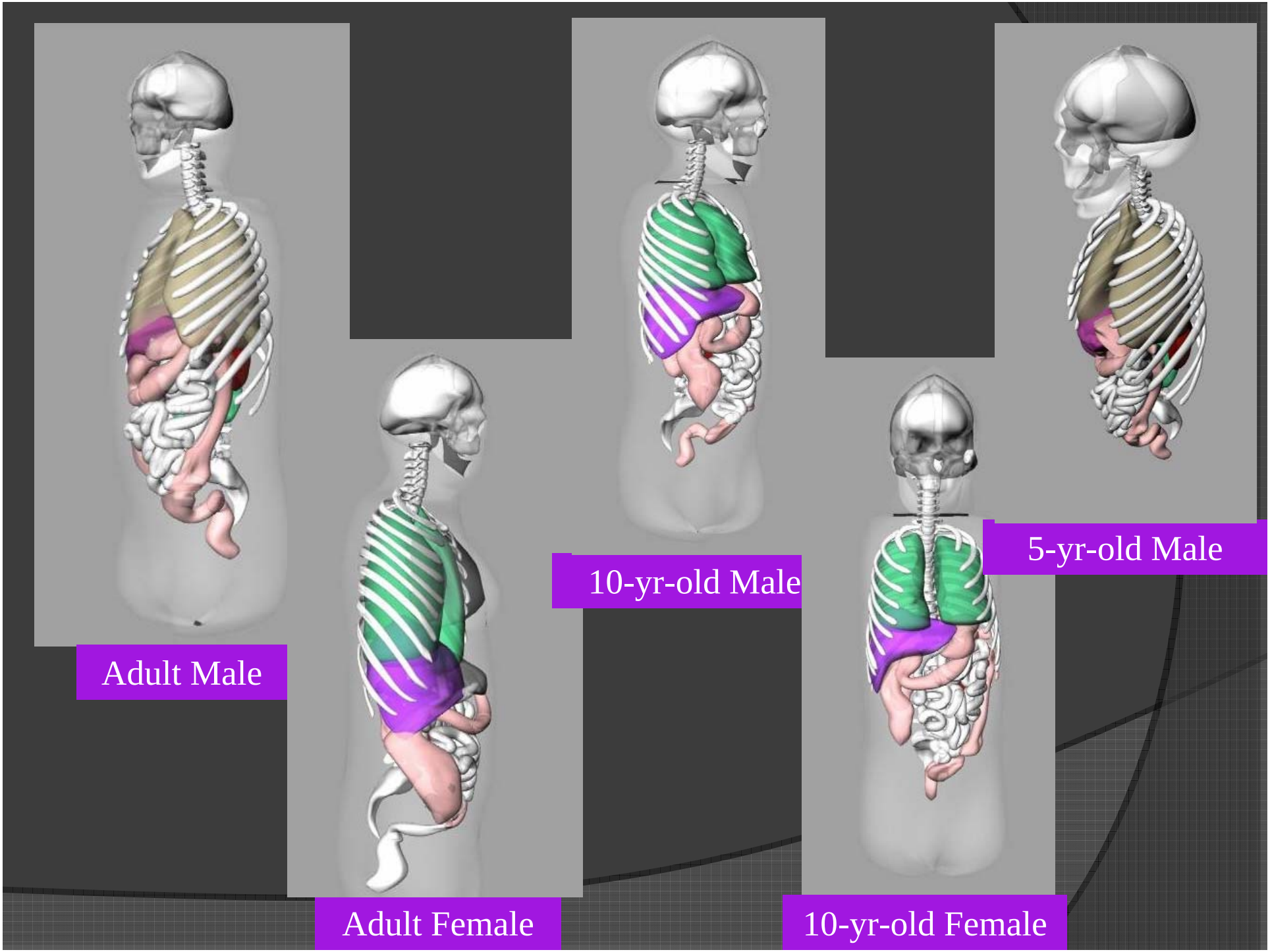
Adult Male
Adult Female
10-yr-old Male
5-yr-old Male
10-yr-old Female

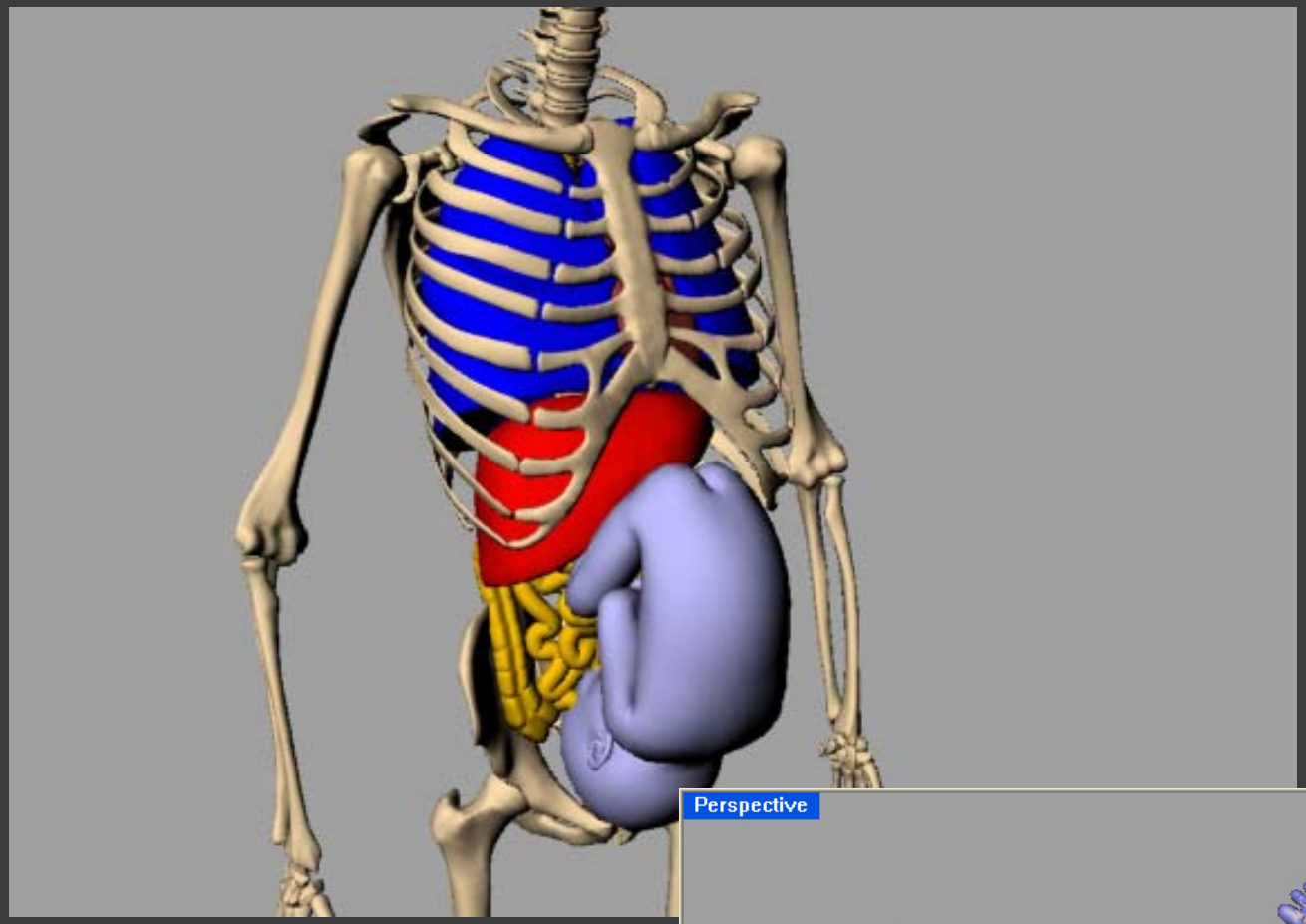

Xu et al., Rensselaer Polytechnic Institute, Troy, NY

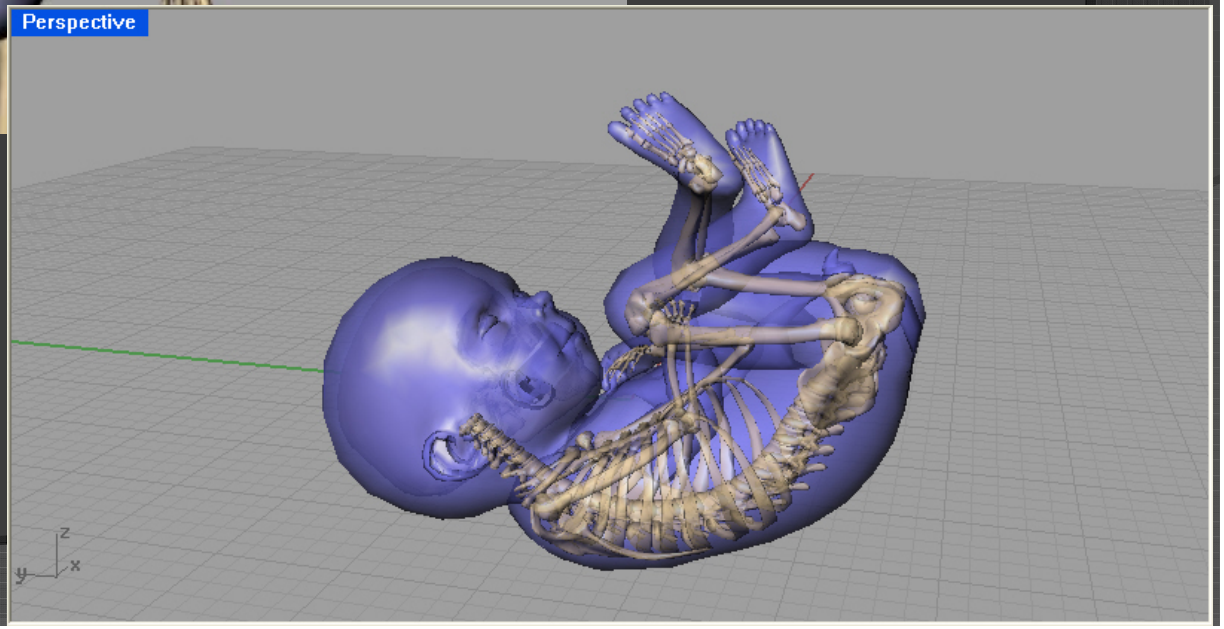

RADAR Dose Factors

We have calculated dose factors for our >800 radionuclides for the traditional models:

Adult Male	Adult Female
15-year-old	3 month pregnant female
10-year-old	6 month pregnant female
5-year-old	9 month pregnant female
1-year-old	MIRD Head and Brain Model
Newborn	Prostate Gland Model
Unit Density Sphere Model	Peritoneal Cavity Model

- Get the data free, by electronic download, at our site.
- Data for the new models will arrive soon.

	ICRP 89 Organ Masses (g)					
	NB female	NB male	1 yr female	1 yr male	5 yr female	5 yr male
Brain	380	380	950	950	1180	1310
Salivary Glands	6	6	24	24	34	34
Lungs	60	60	151	151	300	300
Liver	130	130	330	330	570	570
Kidneys	25	25	70	70	110	110
Adrenals	6	6	4	4	5	5
Thyroid	1.3	1.3	1.8	1.8	3.4	3.4
Thymus	13	13	30	30	30	30
Esophagus	2	2	5	5	10	10

	NURBS Organ Masses (g)					
	NB female	NB male	1 yr female	1 yr male	5 yr female	5 yr male
Brain	381	381	928	928	1177	1258
Salivary Glands	6.1	6.1	23.9	23.9	33.6	33.6
Lungs	58.7	58.7	149	149	300	300
Liver	129	129	334	334	557	557
Kidneys	23.8	23.8	69.7	70.9	108	108
Adrenals	5.7	5.7	3.9	4.0	4.8	4.8
Thyroid	1.3	1.3	1.7	1.8	3.3	3.4
Thymus	13.1	13.1	30.0	30.1	29.6	29.6
Esophagus	1.9	1.9	5.0	5.0	10.0	10.0

	ICRP 89 Organ Masses (g)					
	10 yr female	10 yr male	15 yr female	15 yr male	Adult female	Adult male
Brain	1220	1400	1300	1420	1300	1450
Salivary Glands	44	44	65	68	70	85
Lungs	500	500	750	900	950	1200
Liver	830	830	1300	1300	1400	1800
Kidneys	180	180	240	250	276	310
Adrenals	7	7	9	10	13	14
Thyroid	7.9	7.9	12	12	17	20
Thymus	35	35	30	35	20	25
Esophagus	18.0	18	30	30	35	40

	NURBS Organ Masses (g)					
	10 yr female	10 yr male	15 yr female	15 yr male	Adult female	Adult male
Brain	1193	1350	1291	1336	1242	1404
Salivary Glands	43.7	43.7	66.7	67.9	68.8	83.0
Lungs	505	505	758	875	937	1189
Liver	824	824	1275	1304	1403	1766
Kidneys	182	182	243	244	277	299
Adrenals	6.9	6.9	9.1	10.1	12.9	13.6
Thyroid	7.8	7.8	12.2	11.8	17.0	19.7
Thymus	34.0	34.0	29.8	33.6	19.5	24.2
Esophagus	17.7	17.7	30.3	28.5	35.2	38.3

Selected photon SAF values, adult female

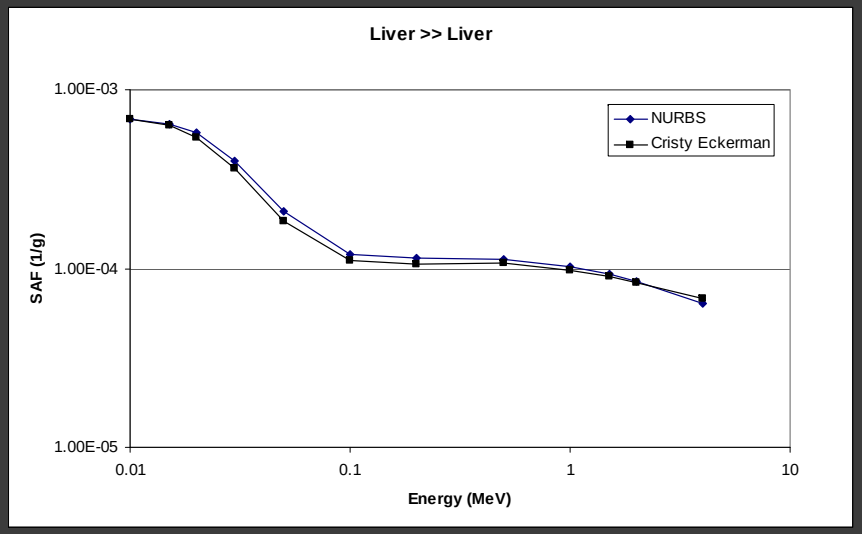

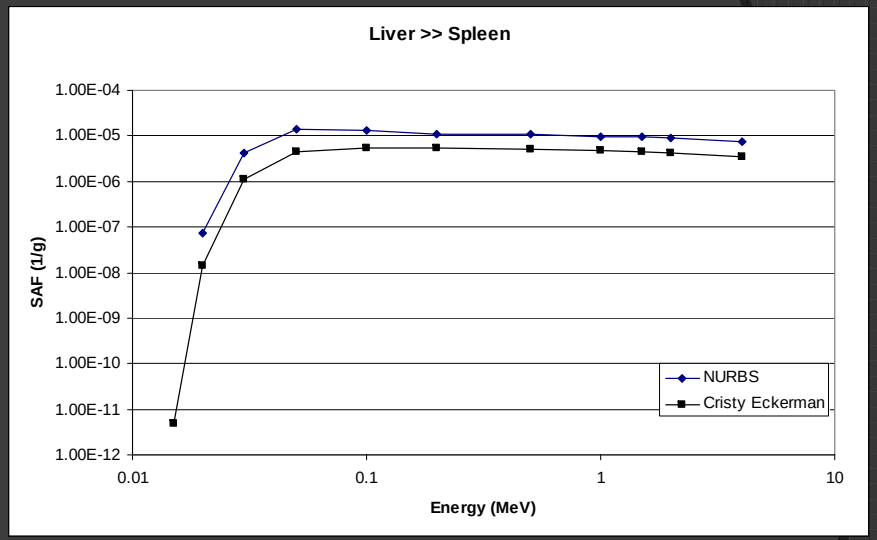

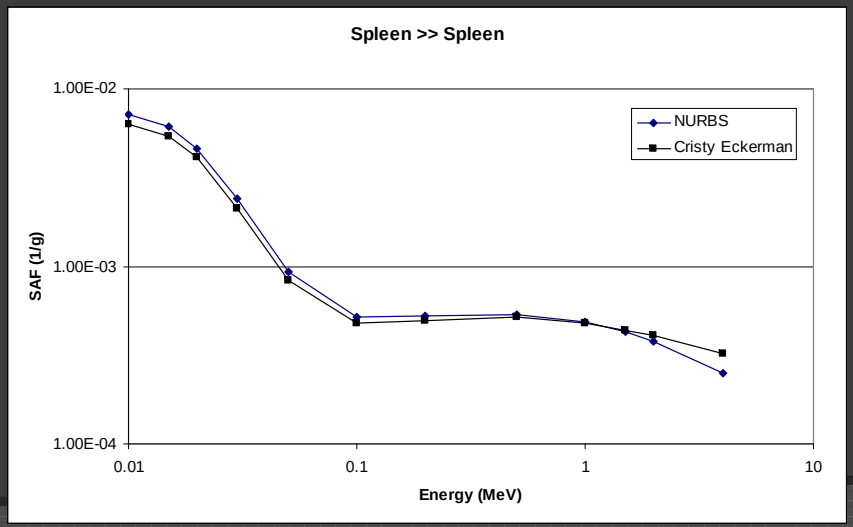

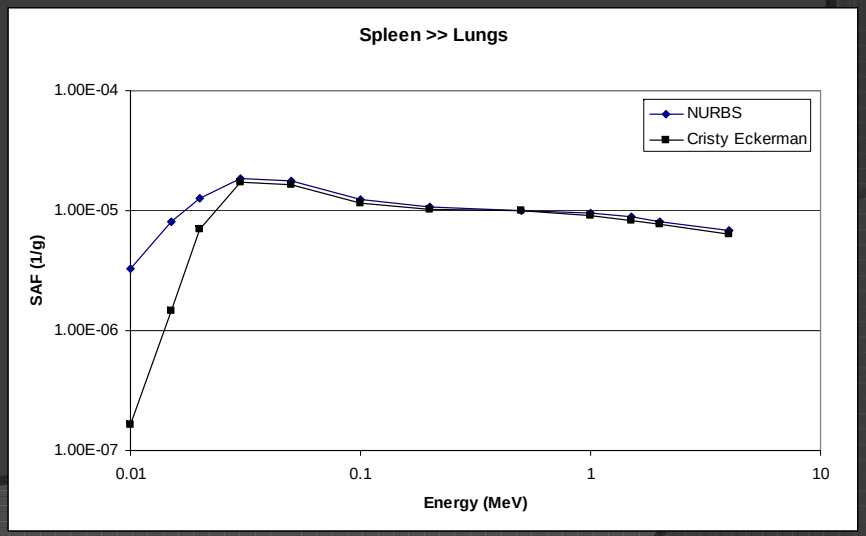

Selected photon SAF values, 10-yr-old female

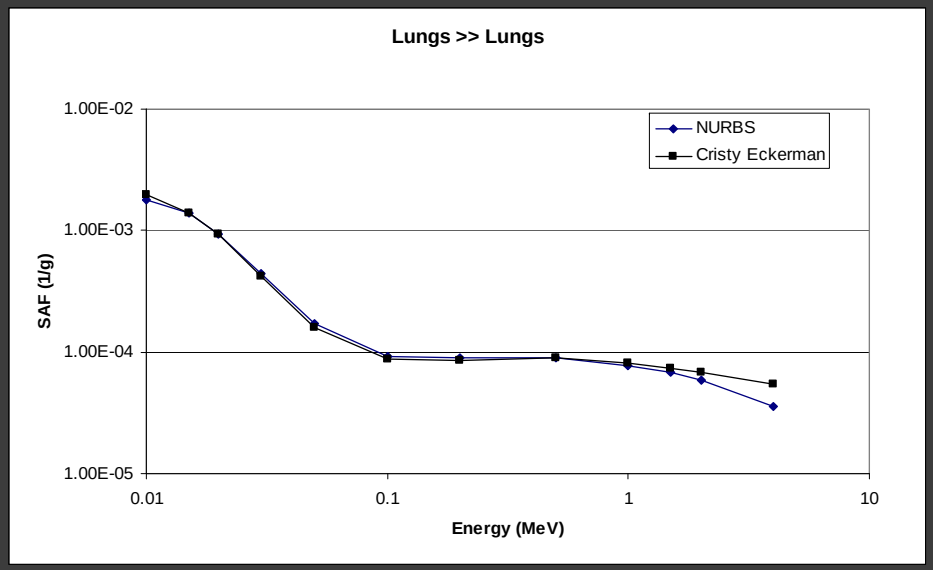

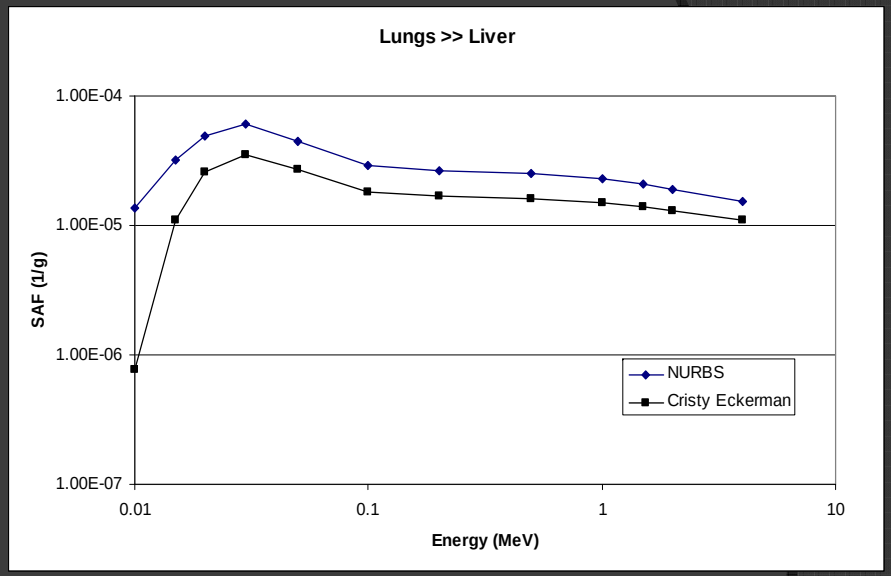

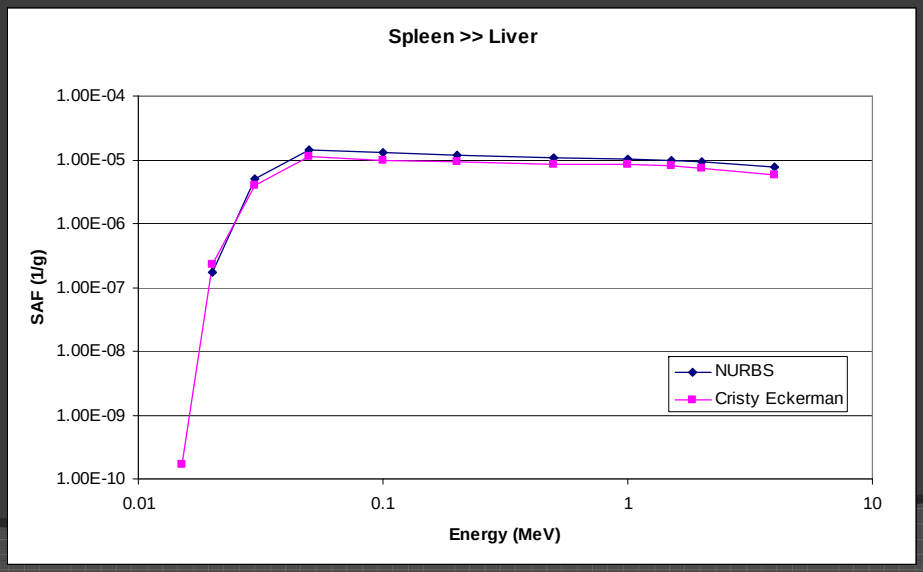

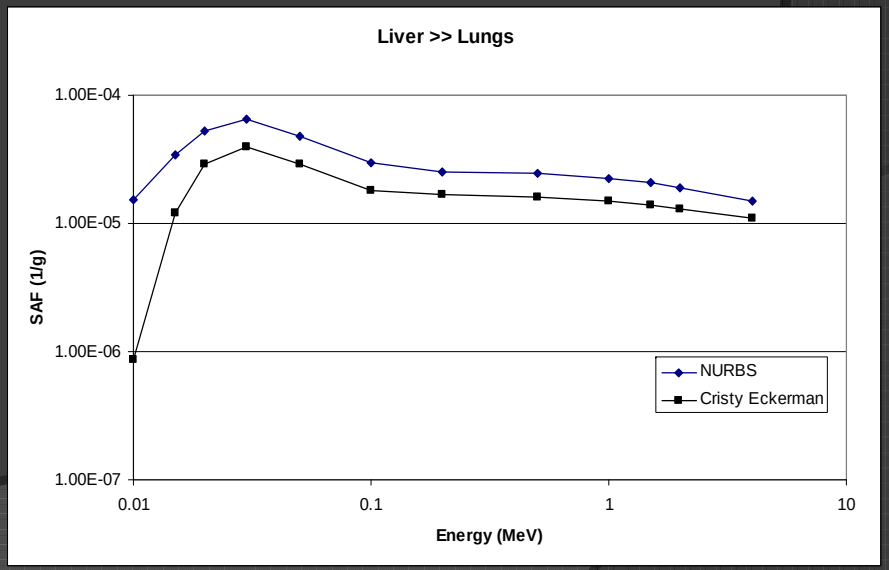

Selected electron SAF values

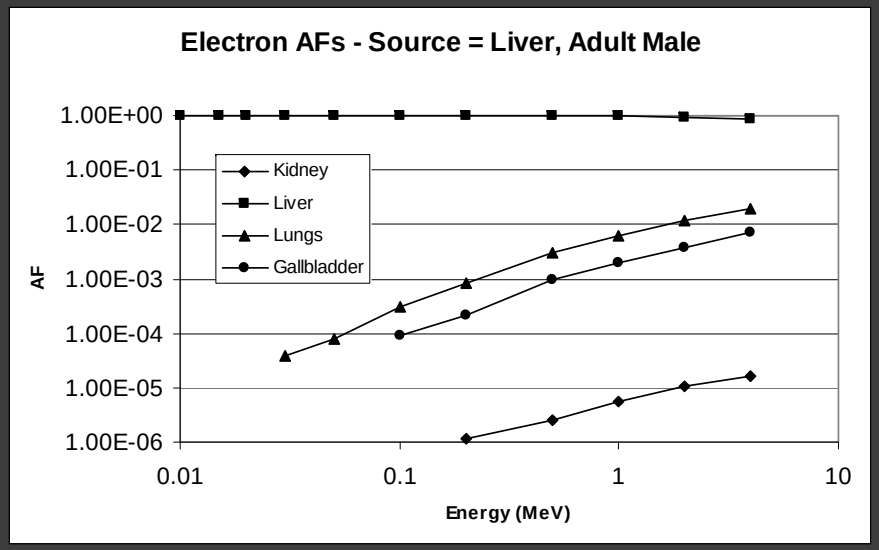

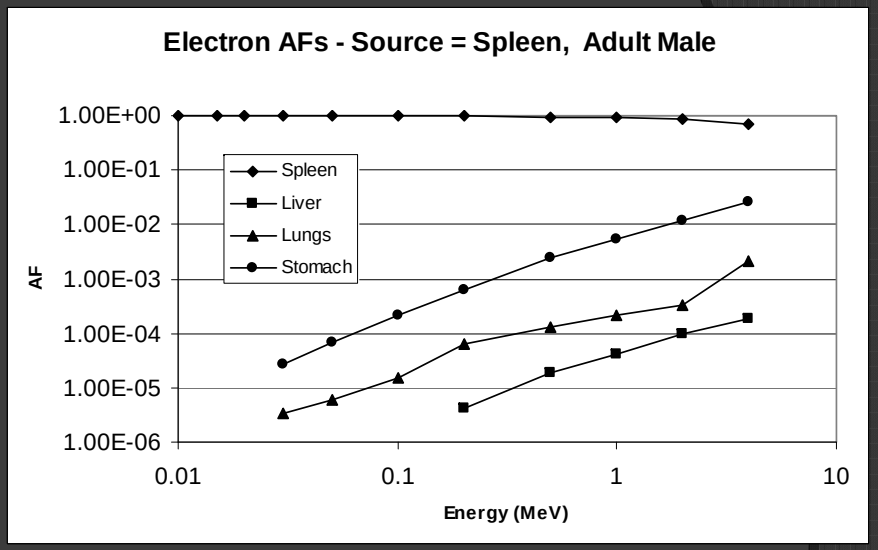

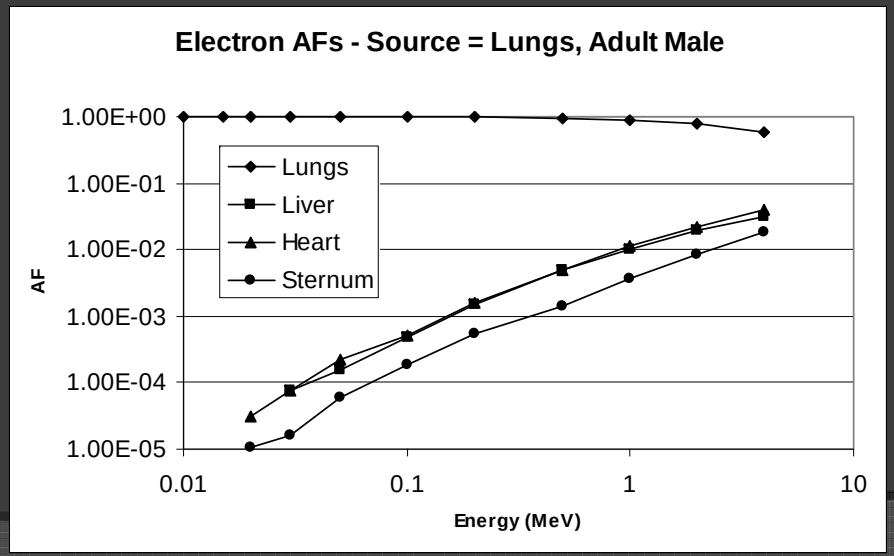

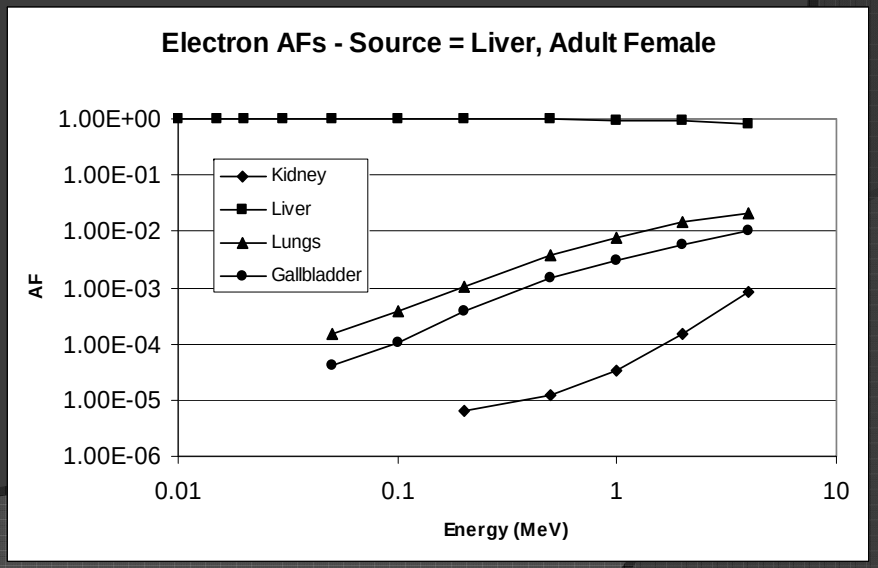

Normal weight adult female models of different stature: modeled changes in organ mass

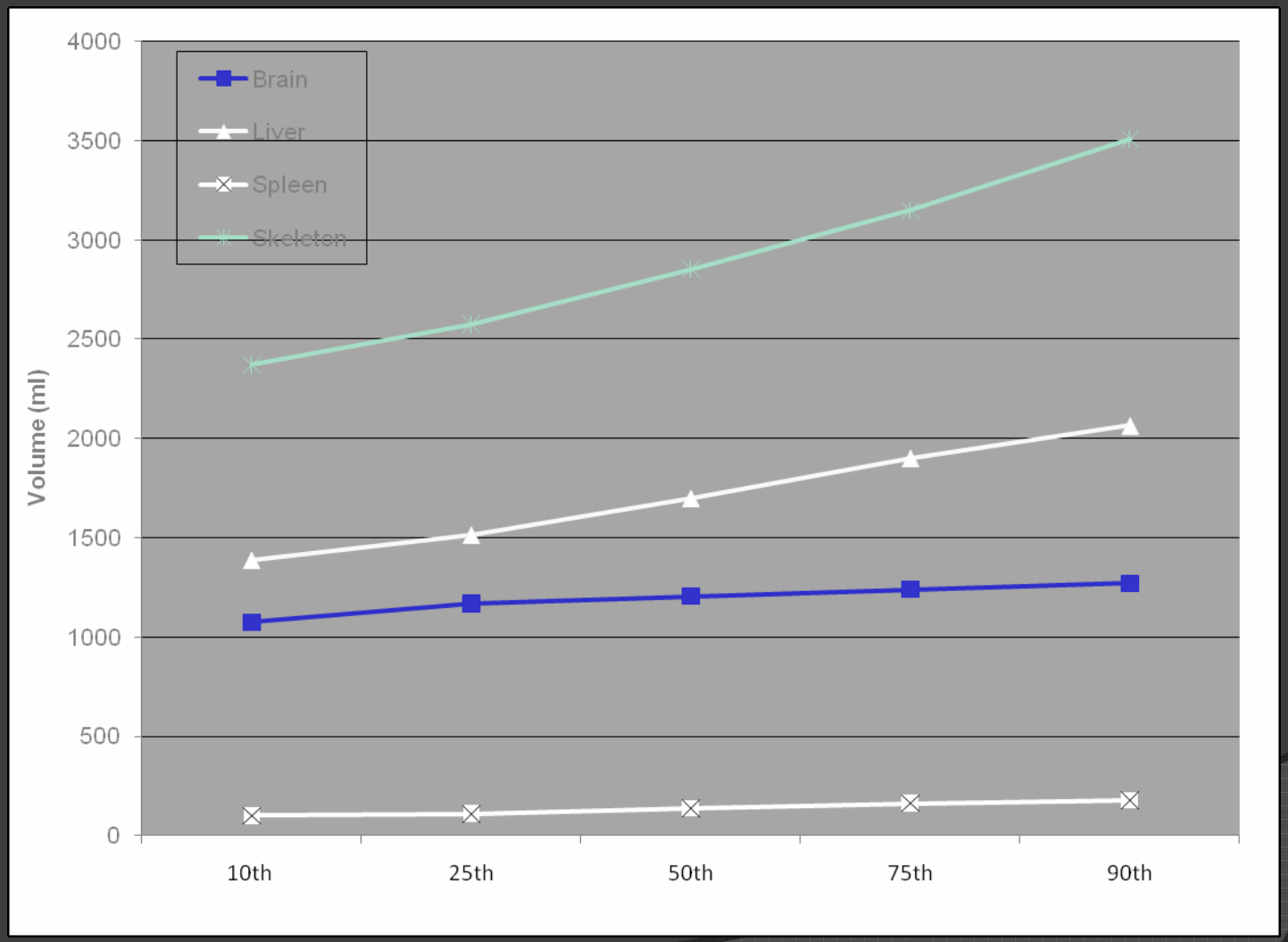

Selected photon SAFs, Normal Weight Adult Male Models of different stature

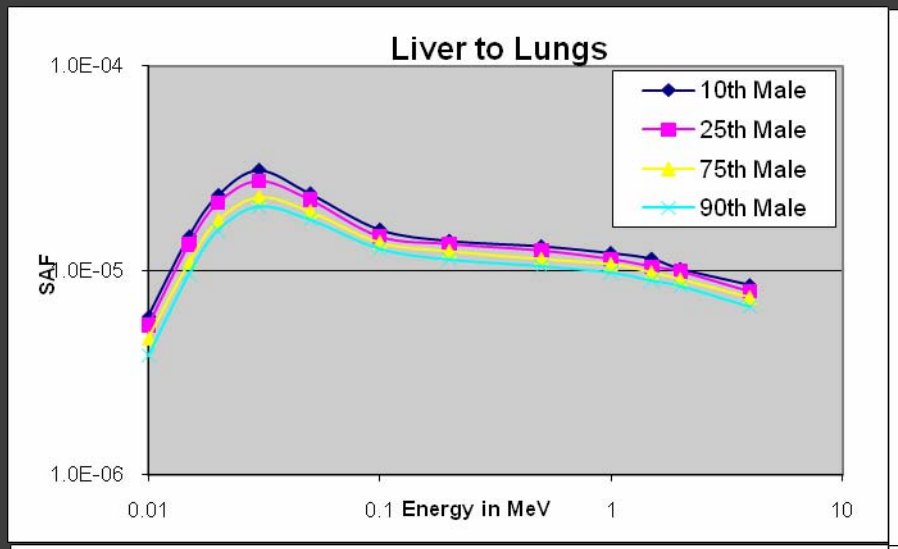

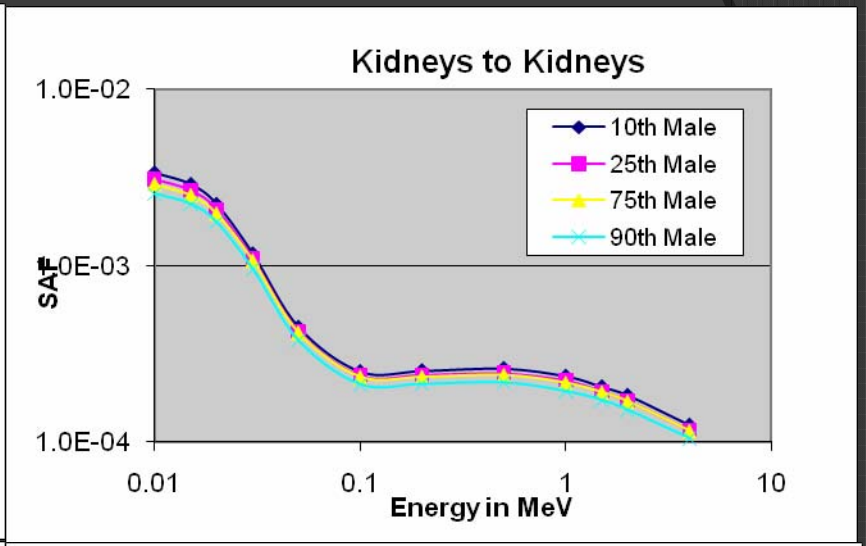

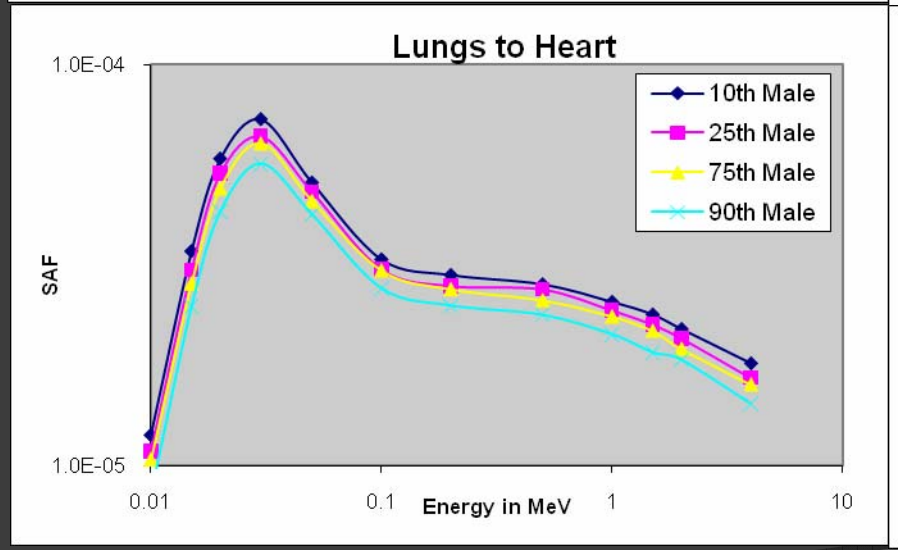

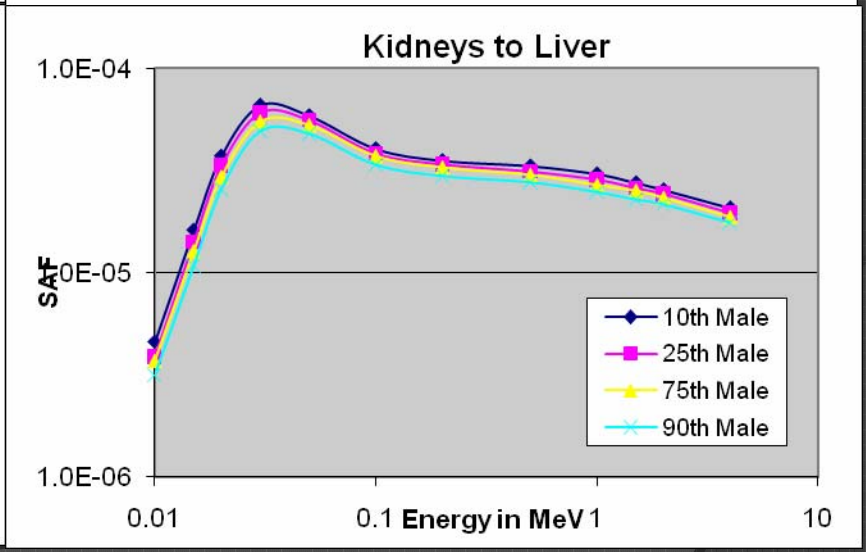

Phantoms of moderate and severe obesity:

The visceral adipose tissue (VAT) areas, comprising the abdominal organs at the T-4 vertebra, for each BMI group were found1 and used to expand the large and small intestines in the AP and lateral dimensions from the median individual using an ellipsoidal shape.

Calculation of Visceral Abdominal Tissue (VAT)
Men: VAT = -453.7+(6.37 x waist)
Women: VAT = -370.5+(4.04 x waist)+(2.62 x age)

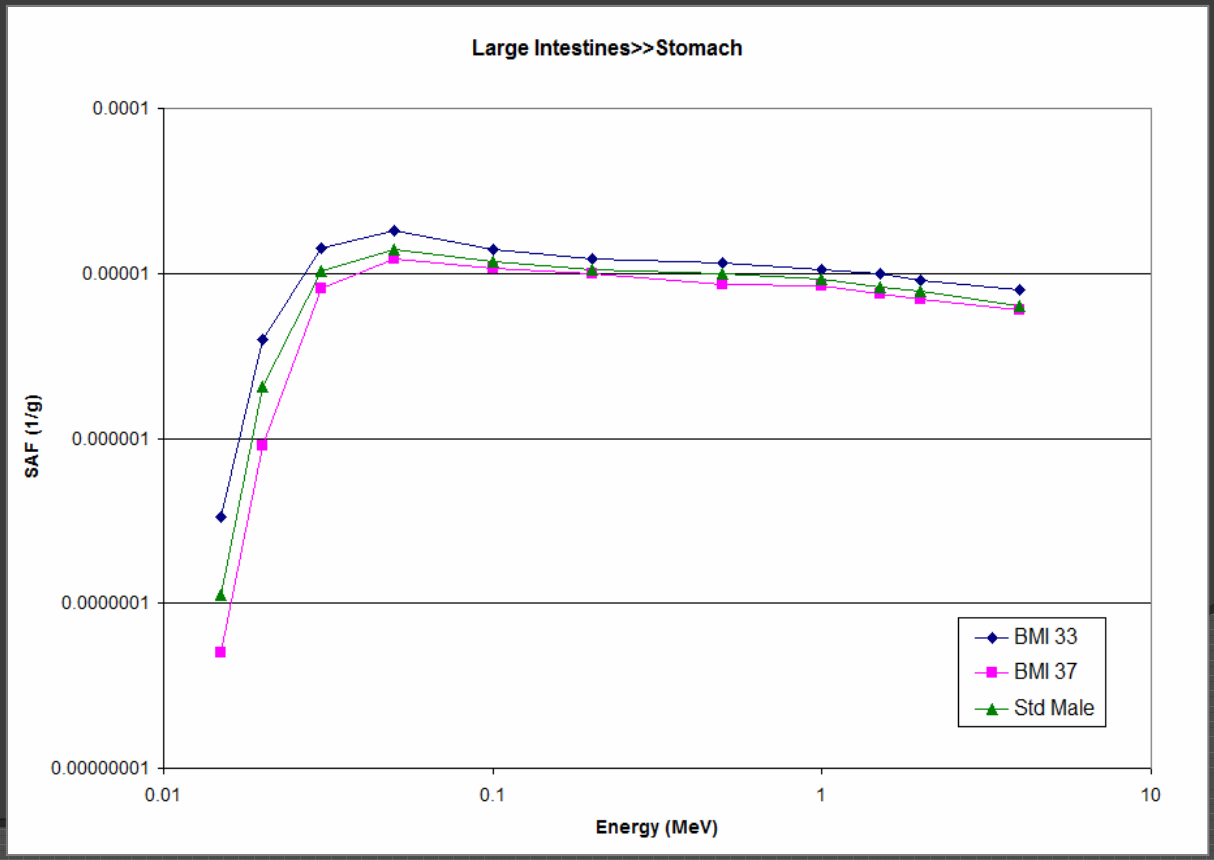

	Percent Difference per kg Difference in Total Body Mass from 10th to 90th Percentile Adult Male Phantom					
	Kidneys	Liver	Lungs	Pancreas	Heart	Spleen
Kidneys	0.59	0.85	0.34	0.63	0.44	0.75
Liver	1.01	0.89	0.91	1.09	0.62	1.02
Lungs	0.46	0.74	0.69	0.52	0.62	0.21
Pancreas	0.47	1.08	0.65	0.52	0.39	0.72
Heart	0.40	0.45	0.66	0.51	0.62	0.39
Spleen	0.62	0.72	0.31	0.70	0.51	1.09

	Absolute Percent Difference from 10th to 90th Percentile Phantom					
	Kidneys	Liver	Lungs	Pancreas	Heart	Spleen
Kidneys	17.7	25.4	10.2	18.9	13.1	22.6
Liver	30.4	26.7	27.4	32.8	18.6	30.7
Lungs	13.7	22.2	20.6	15.6	18.6	6.4
Pancreas	14.0	32.3	19.4	15.5	11.6	21.5
Heart	12.1	13.6	19.8	15.4	18.7	11.7
Spleen	18.7	21.7	9.3	21.1	15.4	32.6

RADAR Realistic Animal Model Series for Dose Assessment

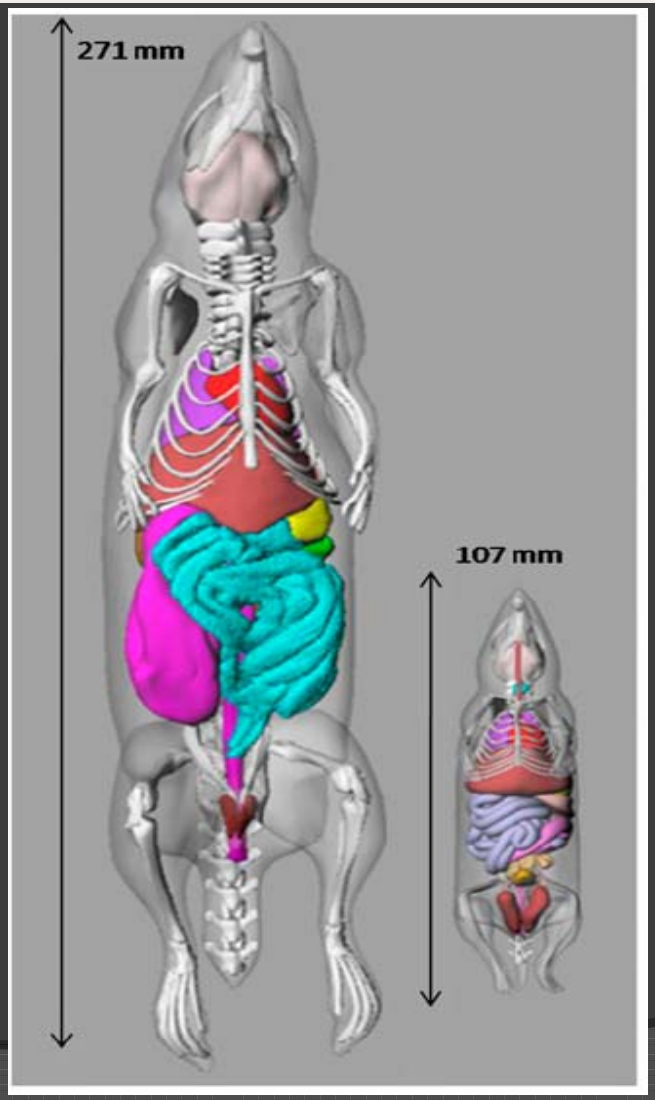

FIGURE 3. Images of unmodified ROBY and MOBY models (*13*), showing length of each model.

Scaled Models - Mouse

Lil MOBY
Body 22.7 g

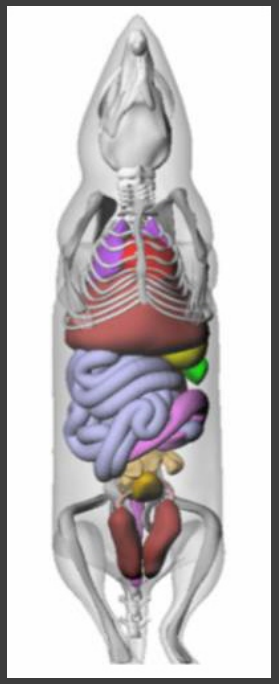

MOBY
Body 28.1 g

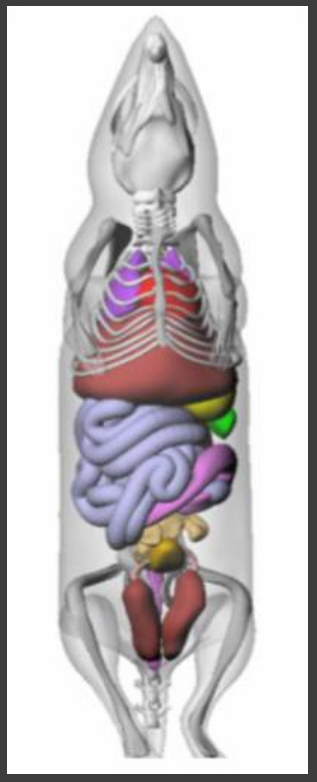

Big MOBY
Body 33.2 g

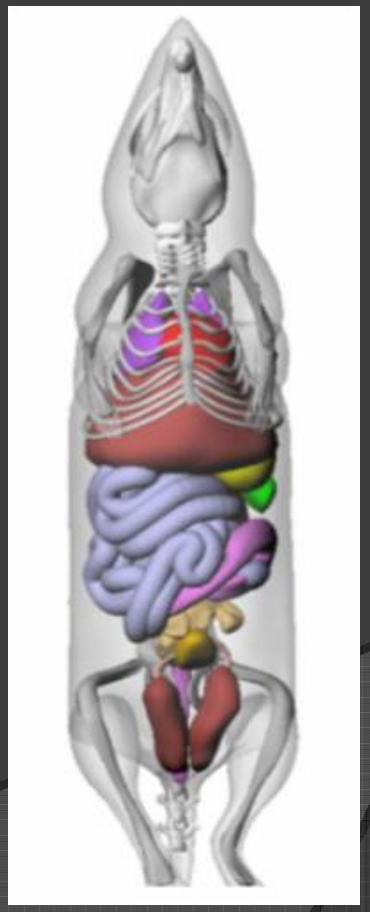

TABLE 1. Organ Masses in 3 Mouse Models

Organ	Organ mass (g)		
	25-g mouse	30-g mouse	35-g mouse
Brain	0.466	0.568	0.666
Heart	0.235	0.291	0.342
Stomach	0.055	0.069	0.082
Small intestine	1.74	2.12	2.49
Large intestine	0.583	0.709	0.830
Kidneys	0.302	0.374	0.432
Liver	1.74	2.15	2.57
Lungs	0.087	0.107	0.131
Pancreas	0.305	0.378	0.450
Skeleton	2.18	2.61	3.01
Spleen	0.111	0.136	0.157
Testes	0.160	0.197	0.228
Thyroid	0.014	0.016	0.020
Bladder	0.060	0.075	0.088
Body	24.11	29.80	35.27

TABLE 2. Organ Masses in 5 Rat Models

Organ	Organ mass (g)				
	200-g rat	300-g rat	400-g rat	500-g rat	600-g rat
Brain	1.57	2.32	3.16	3.93	4.54
Heart	1.80	2.64	3.55	4.39	5.28
Stomach	0.941	1.40	1.89	2.37	2.86
Small intestine	10.6	15.5	20.8	25.6	30.8
Large intestine	7.86	11.5	15.5	19.2	23.1
Kidneys	2.06	3.03	4.09	5.06	6.09
Liver	7.55	11.2	15.2	18.8	22.8
Lungs	0.594	0.884	1.21	1.50	1.82
Pancreas	0.368	0.535	0.732	0.908	1.10
Skeleton	15.3	22.0	29.2	35.2	38.7
Spleen	0.607	0.884	1.18	1.45	1.74
Testes	0.174	0.245	0.321	0.386	0.460
Thyroid	0.191	0.275	0.368	0.457	0.549
Bladder	0.475	0.682	0.916	1.12	1.34
Body	226	335	443	547	643

Photon SAF Comparison across Mouse Model Sizes

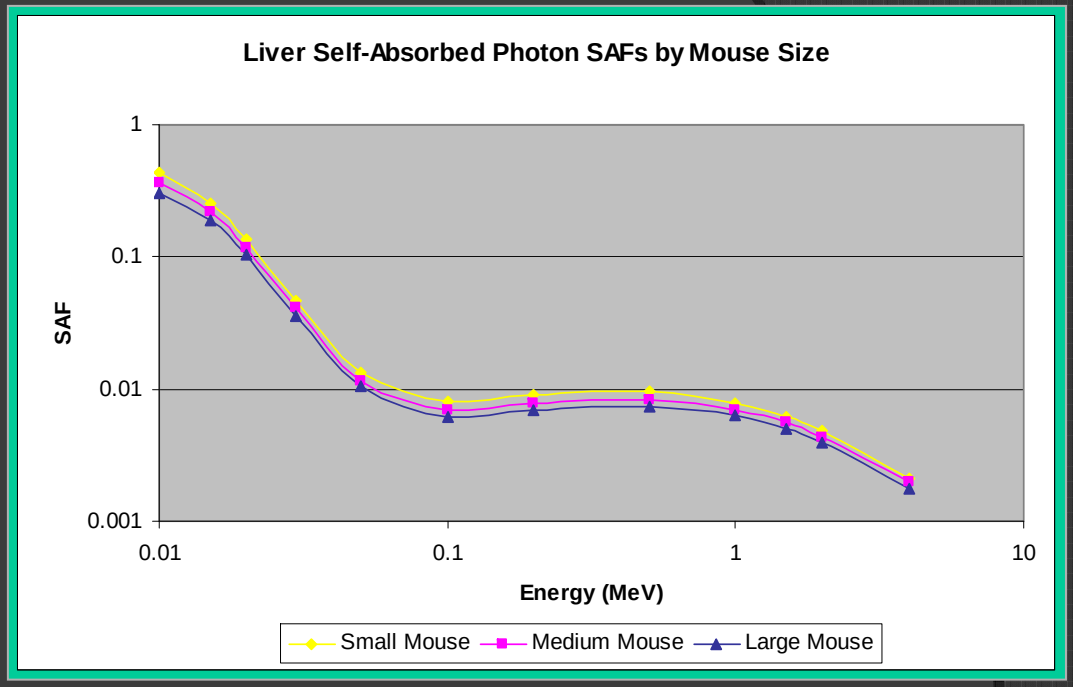

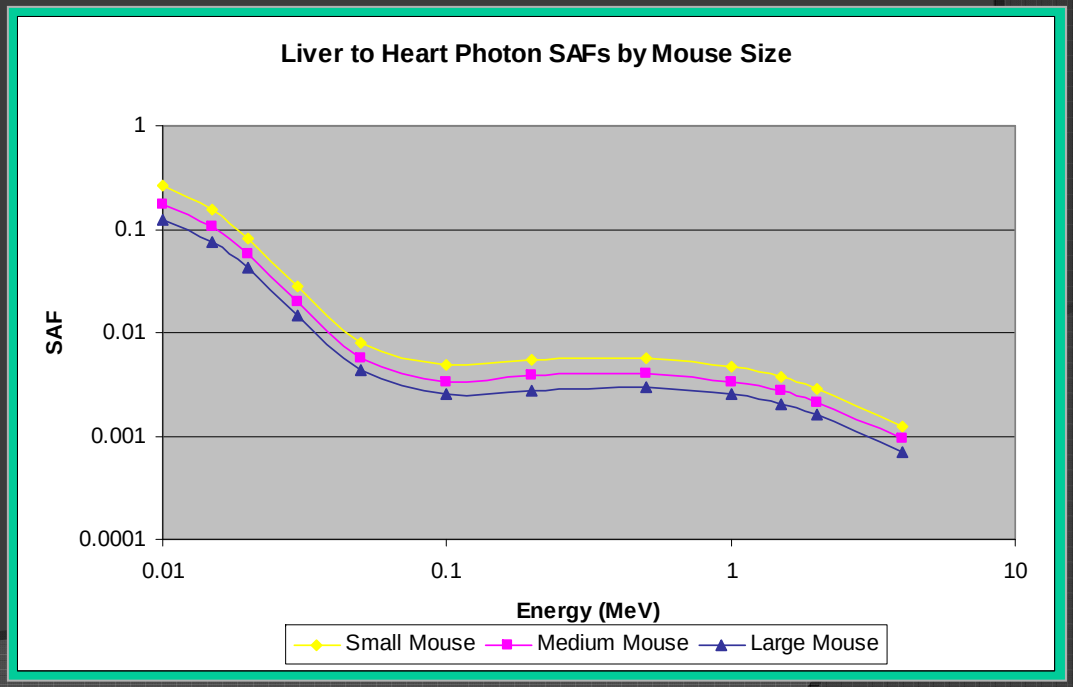

Electron SAF Comparison across Rat Model Sizes

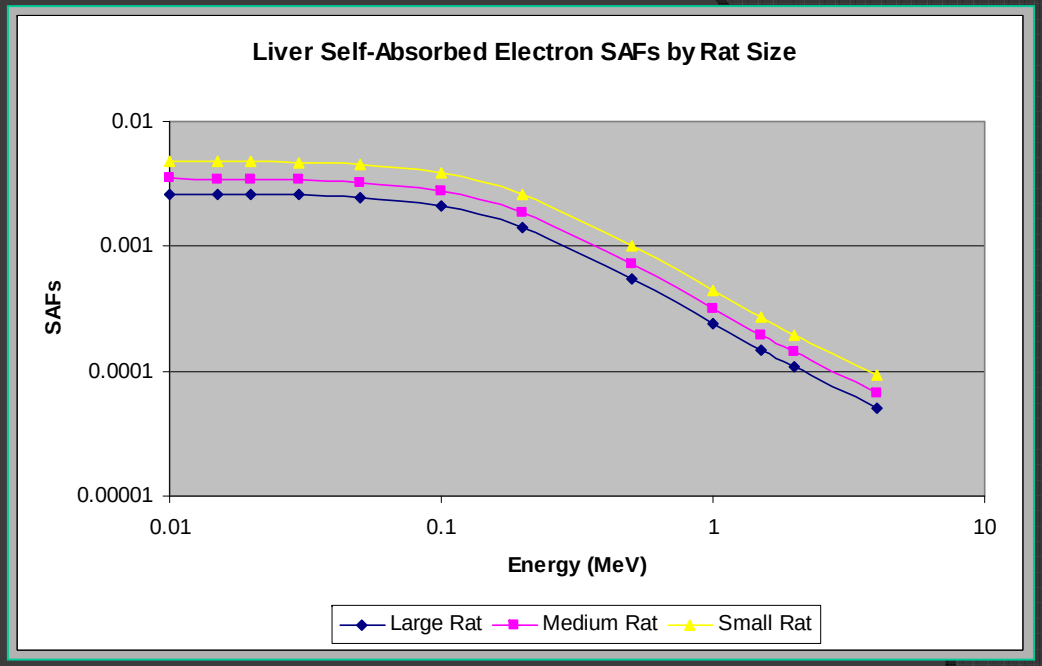

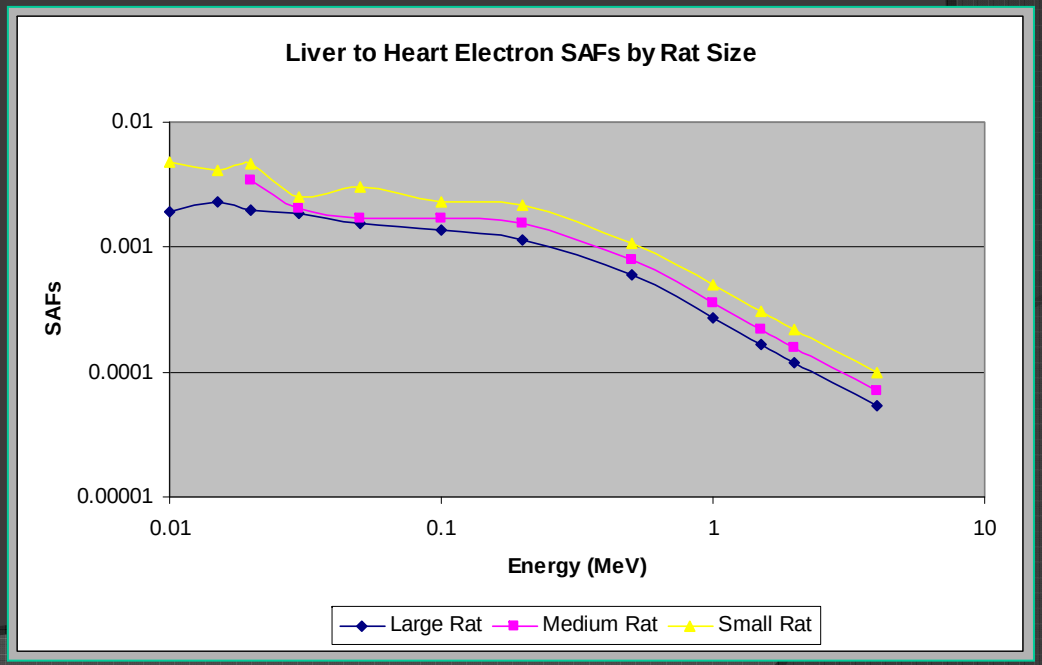

ICRP 30 Kinetic model for the GI tract

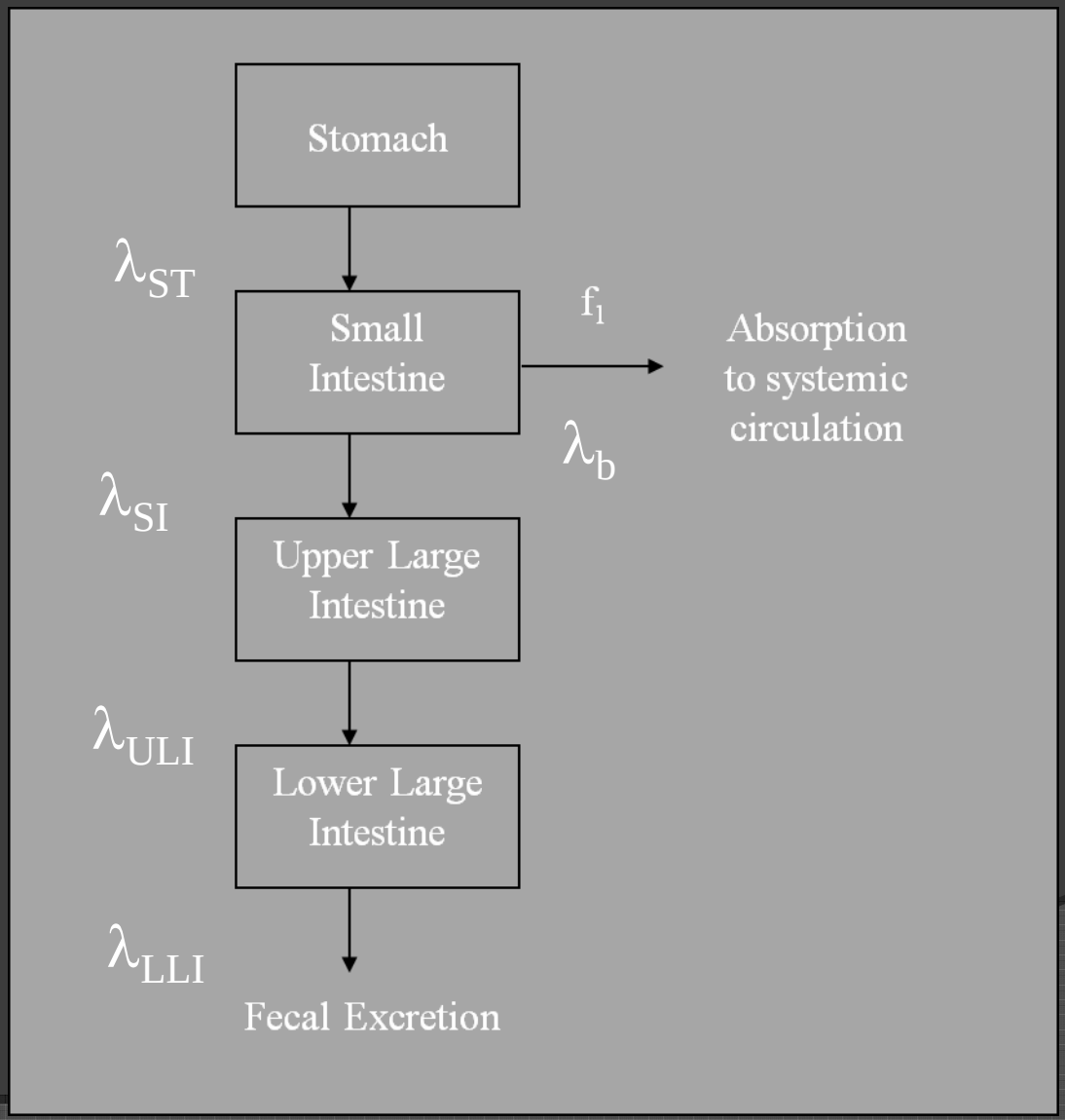

ICRP 100 – New Human Alimentary Tract (HAT) model

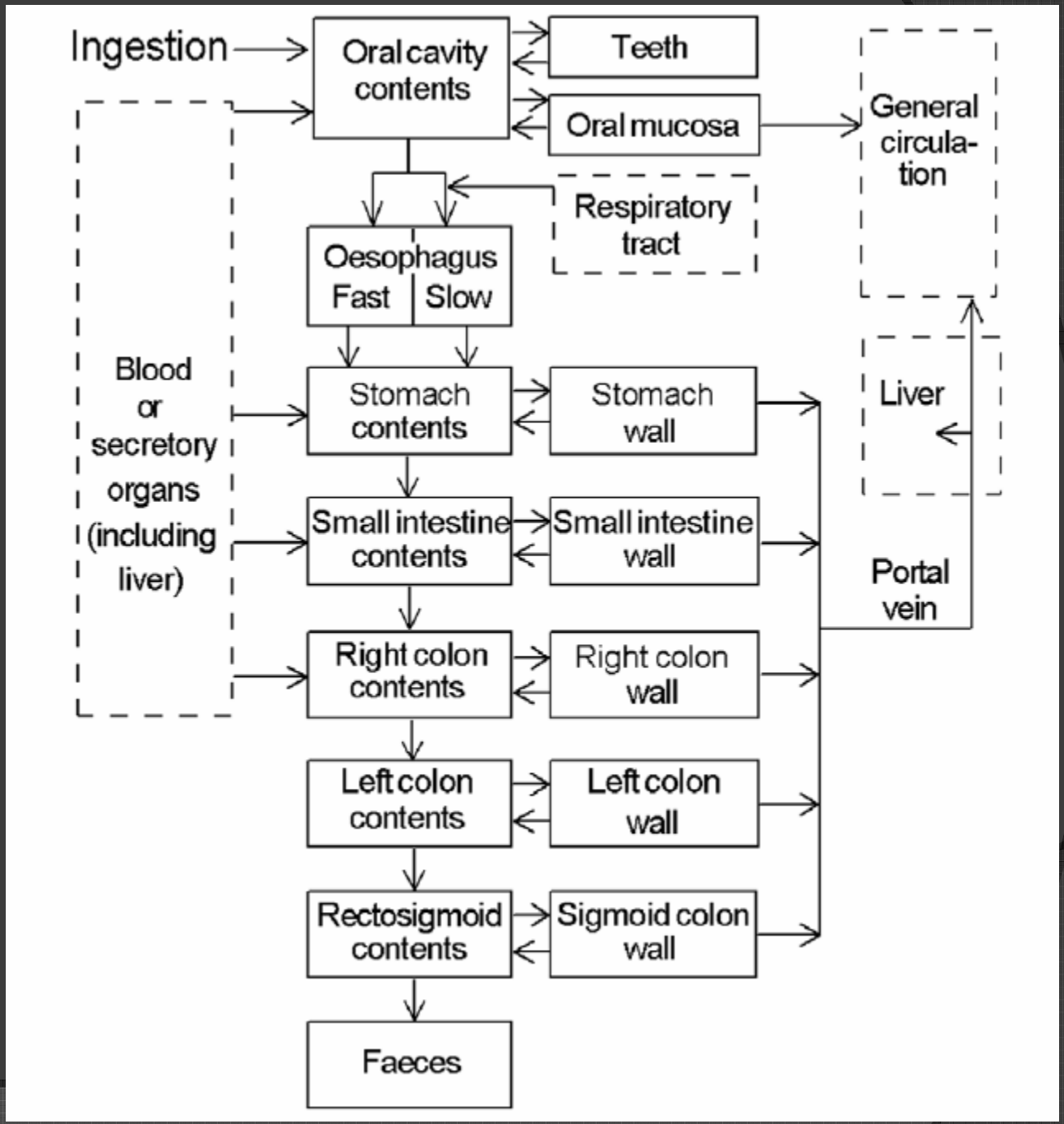

Urinary Bladder – Voiding Model

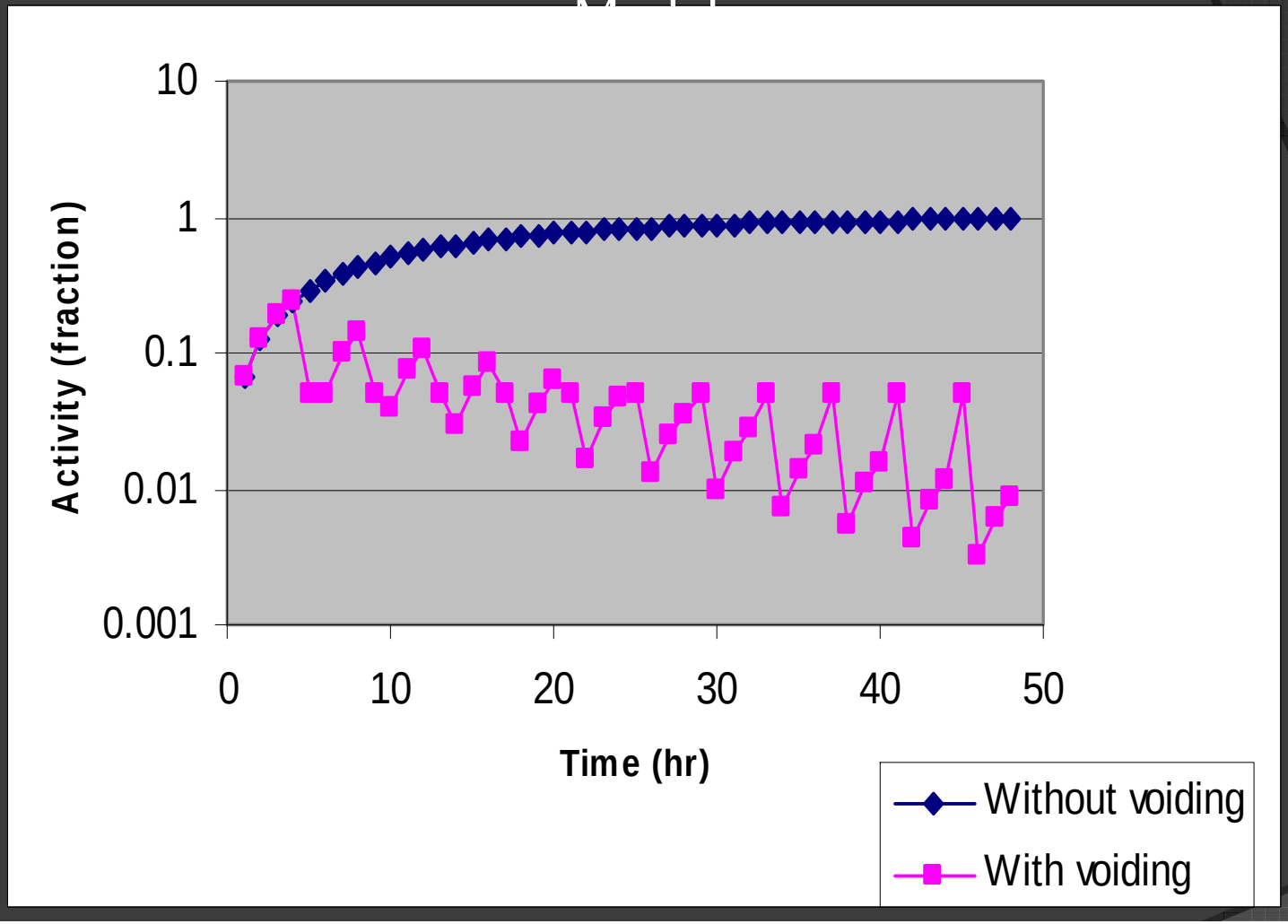

$$N = A_0 \sum_i f_i \left[\frac{1 - e^{-\lambda_i T}}{\lambda_i} - \frac{1 - e^{-(\lambda_i + \lambda_p)T}}{\lambda_i + \lambda_p} \right] \left[\frac{1}{1 - e^{-(\lambda_i + \lambda_P)T}} \right]$$

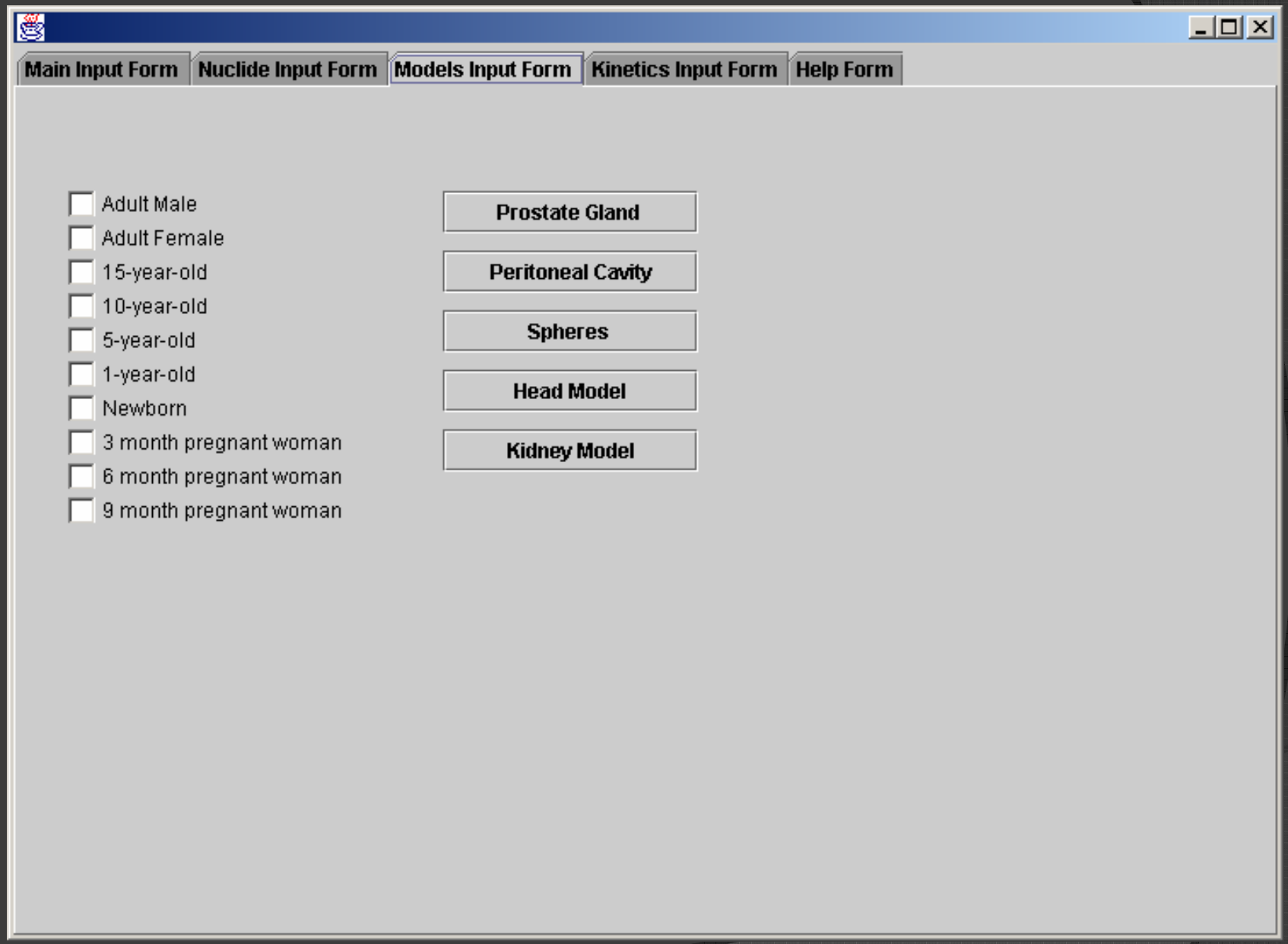
Main Input Form
Nuclide Input Form
Models Input Form
Kinetics Input Form
Help Form
Adult Male
Adult Female
15-year-old
10-year-old
5-year-old
1-year-old
Newborn
3 month pregnant woman
6 month pregnant woman
9 month pregnant woman
Prostate Gland
Peritoneal Cavity
Spheres
Head Model
Kidney Model

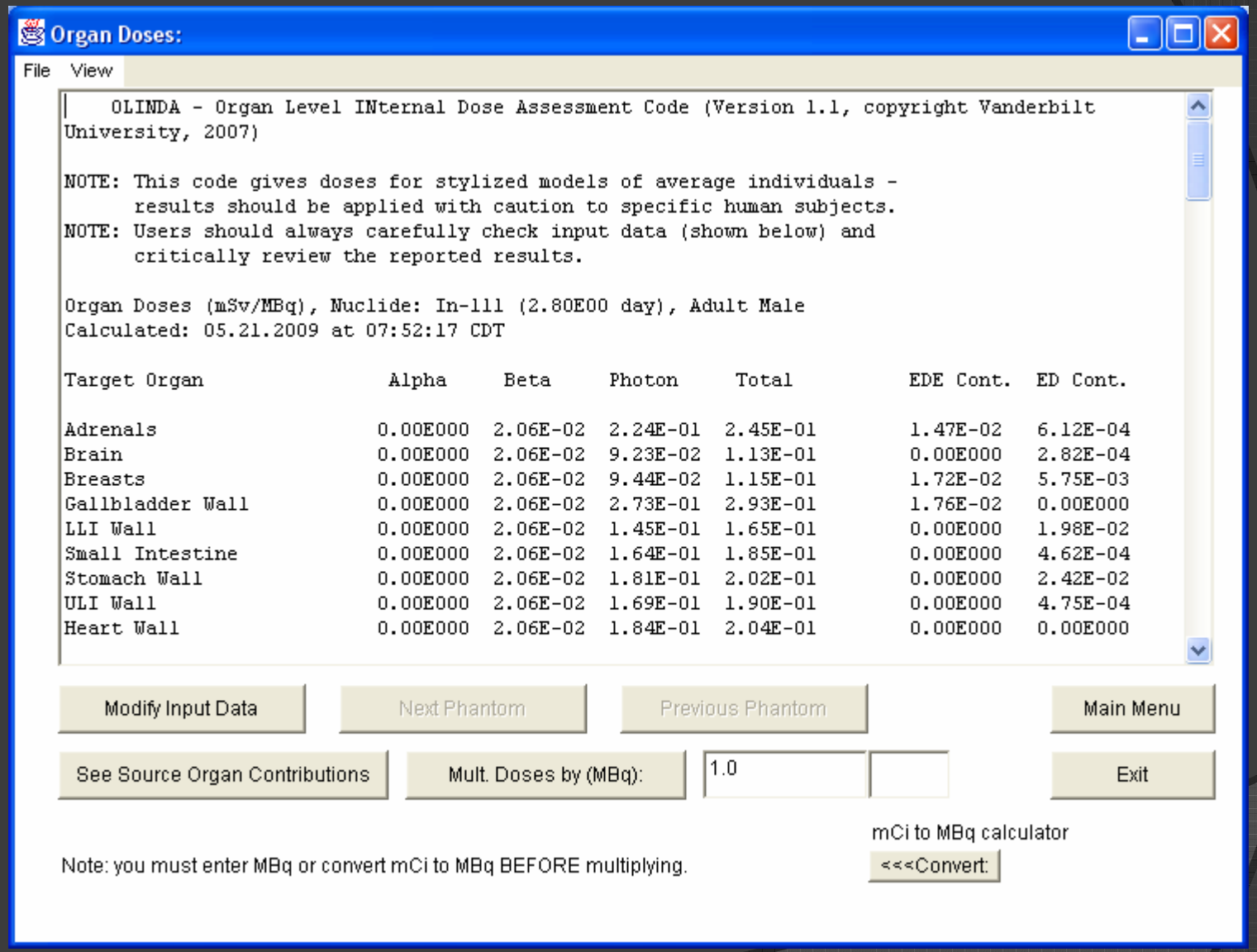
Organ Doses:
File View
OLINDA - Organ Level INternal Dose Assessment Code (Version 1.1, copyright Vanderbilt University, 2007)
NOTE: This code gives doses for stylized models of average individuals - results should be applied with caution to specific human subjects.
NOTE: Users should always carefully check input data (shown below) and critically review the reported results.
Organ Doses (mSv/MBq), Nuclide: In-111 (2.80E00 day), Adult Male
Calculated: 05.21.2009 at 07:52:17 CDT
Target Organ Alpha Beta Photon Total EDE Cont. ED Cont.
Adrenals 0.00E000 2.06E-02 2.24E-01 2.45E-01 1.47E-02 6.12E-04
Brain 0.00E000 2.06E-02 9.23E-02 1.13E-01 0.00E000 2.82E-04
Breasts 0.00E000 2.06E-02 9.44E-02 1.15E-01 1.72E-02 5.75E-03
Gallbladder Wall 0.00E000 2.06E-02 2.73E-01 2.93E-01 1.76E-02 0.00E000
LLI Wall 0.00E000 2.06E-02 1.45E-01 1.65E-01 0.00E000 1.98E-02
Small Intestine 0.00E000 2.06E-02 1.64E-01 1.85E-01 0.00E000 4.62E-04
Stomach Wall 0.00E000 2.06E-02 1.81E-01 2.02E-01 0.00E000 2.42E-02
ULI Wall 0.00E000 2.06E-02 1.69E-01 1.90E-01 0.00E000 4.75E-04
Heart Wall 0.00E000 2.06E-02 1.84E-01 2.04E-01 0.00E000 0.00E000
Modify Input Data
Next Phantom
Previous Phantom
Main Menu
See Source Organ Contributions
Mult. Doses by (MBq):
1.0
Exit
mCi to MBq calculator
Note: you must enter MBq or convert mCi to MBq BEFORE multiplying.
<<<Convert:

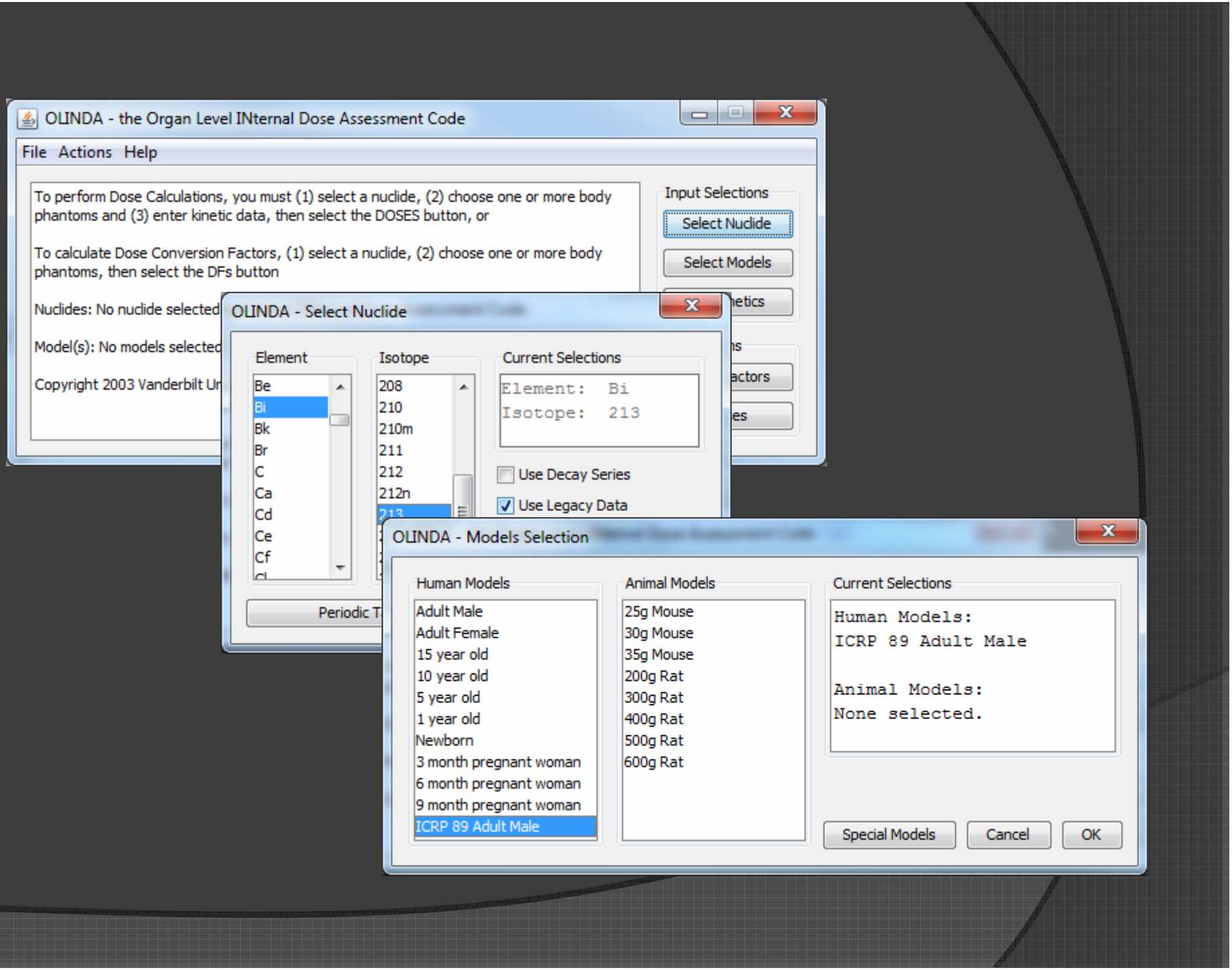
OLINDA - the Organ Level INternal Dose Assessment Code
File Actions Help
To perform Dose Calculations, you must (1) select a nuclide, (2) choose one or more body phantoms and (3) enter kinetic data, then select the DOSES button, or
To calculate Dose Conversion Factors, (1) select a nuclide, (2) choose one or more body phantoms, then select the DFs button
Nuclides: No nuclide selected
Model(s): No models selected
Copyright 2003 Vanderbilt Ur
Input Selections
Select Nuclide
Select Models
OLINDA - Select Nuclide
Element
Be
Bi
Bk
Br
C
Ca
Cd
Ce
Cf
Isotope
208
210
210m
211
212
212n
213
Current Selections
Element: Bi
Isotope: 213
Use Decay Series
Use Legacy Data
Periodic T
OLINDA - Models Selection
Human Models
Adult Male
Adult Female
15 year old
10 year old
5 year old
1 year old
Newborn
3 month pregnant woman
6 month pregnant woman
9 month pregnant woman
ICRP 89 Adult Male
Animal Models
25g Mouse
30g Mouse
35g Mouse
200g Rat
300g Rat
400g Rat
500g Rat
600g Rat
Current Selections
Human Models:
ICRP 89 Adult Male
Animal Models:
None selected.
Special Models
Cancel
OK

Patient-Specific Adjustments to Standard Models

Uncertainty

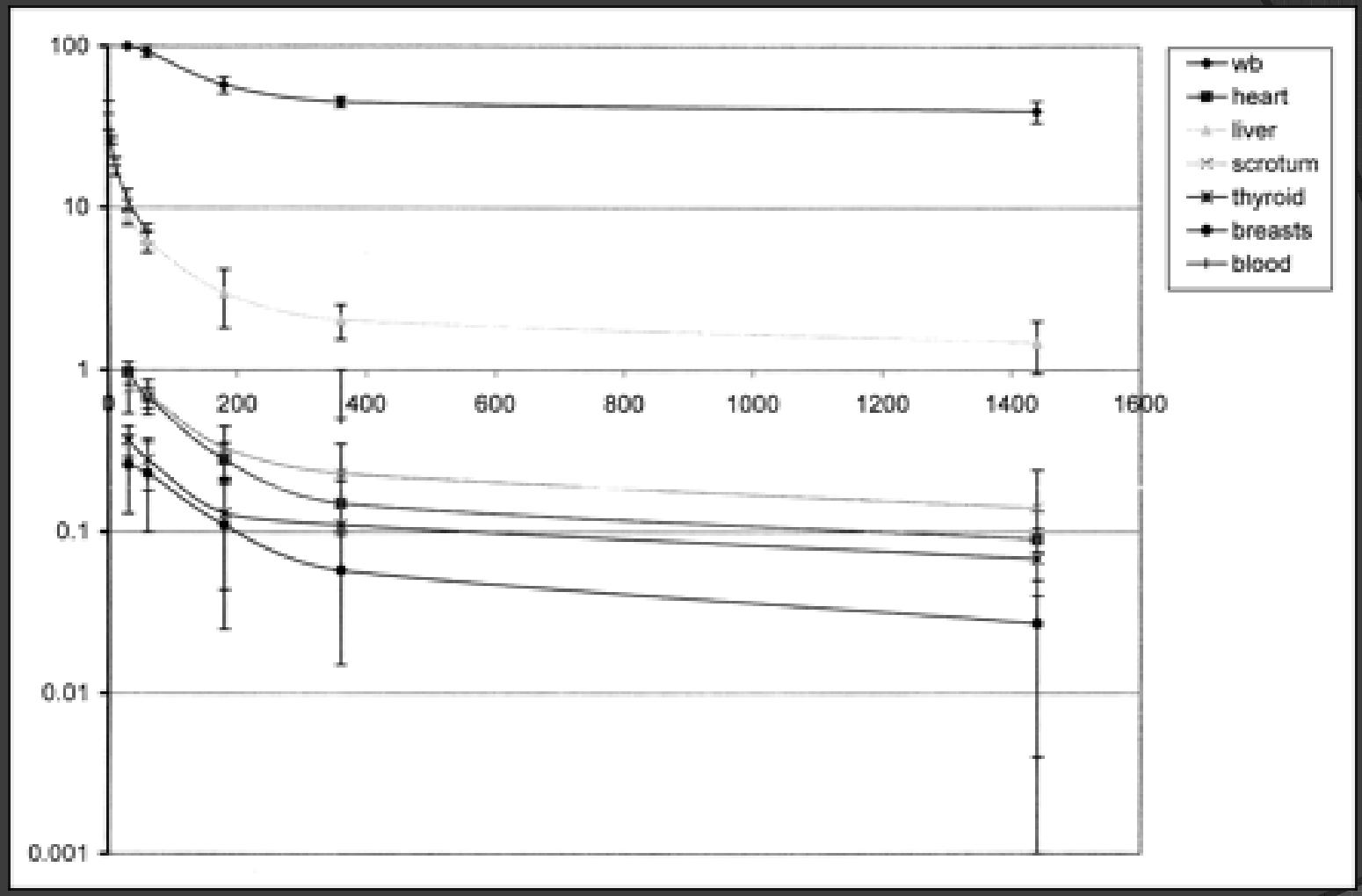

Uptake and retention of ^{99m}Tc-RP527, a gastrin-releasing peptide (GRP) agonist for the visualization of GRP receptor–expressing malignancies in various subjects, as reported by Van de Wiele et al.

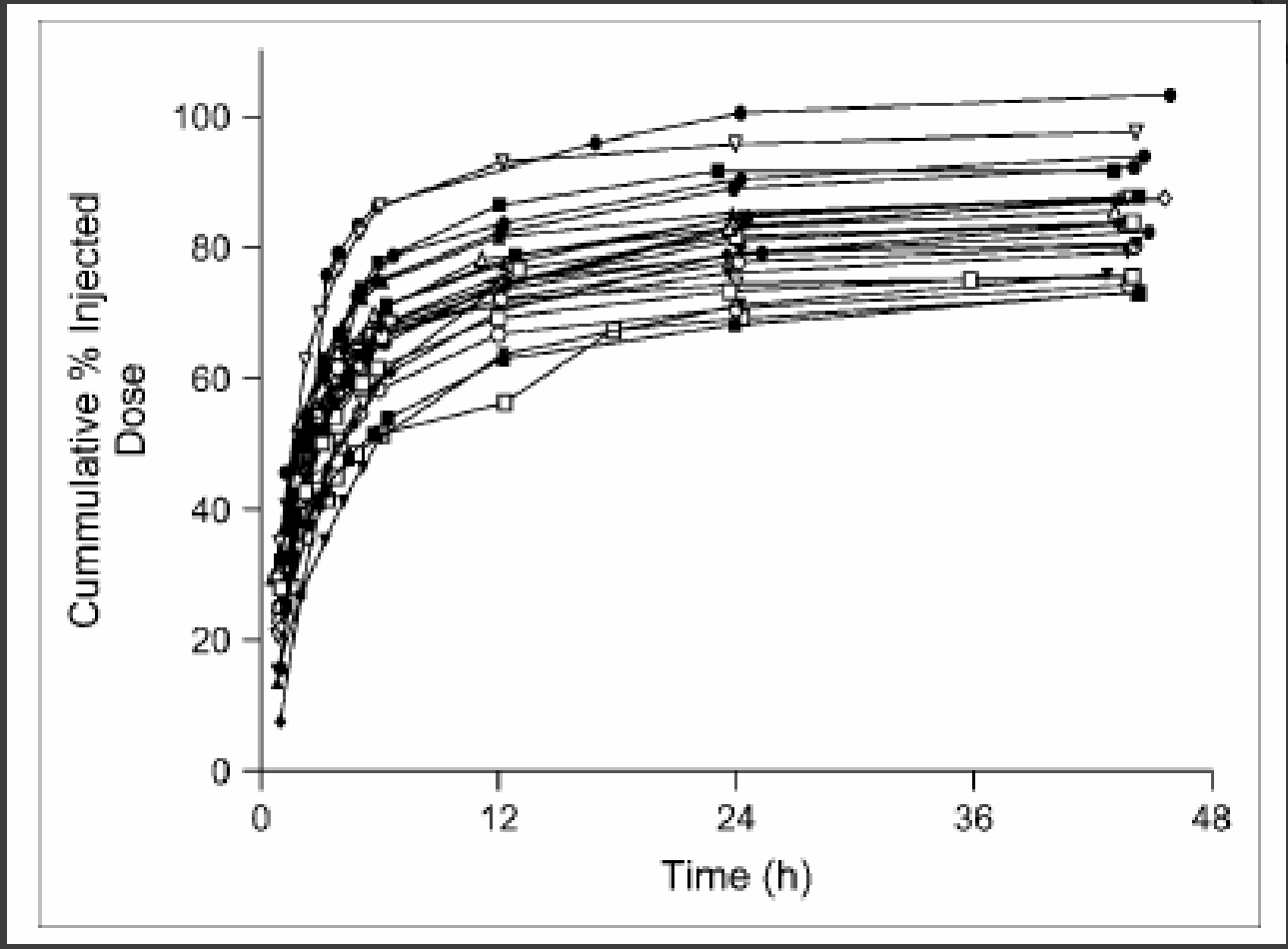

Cumulative excretion of Ho-166 DOTMP in twelve subjects (6 ♀, 6 ♂) with multiple myeloma. Breitz et al. J Nucl Med 2006

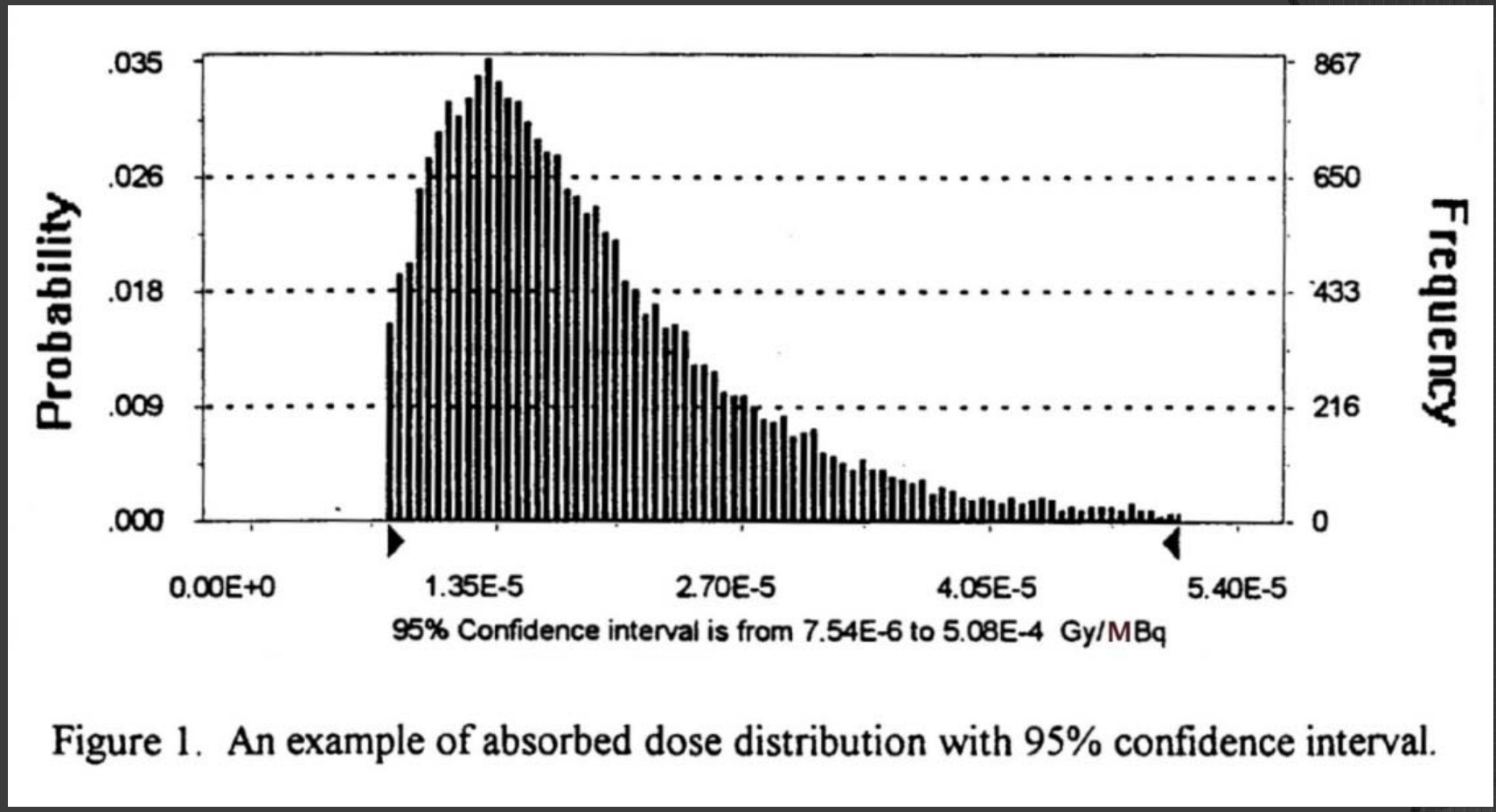

Figure 1. An example of absorbed dose distribution with 95% confidence interval.

Aydogan B, Sparks RB, Stubbs JB and Miller LF. Uncertainty analysis for absorbed dose from a brain receptor agent. Sixth Dosimetry Symposium 1999.

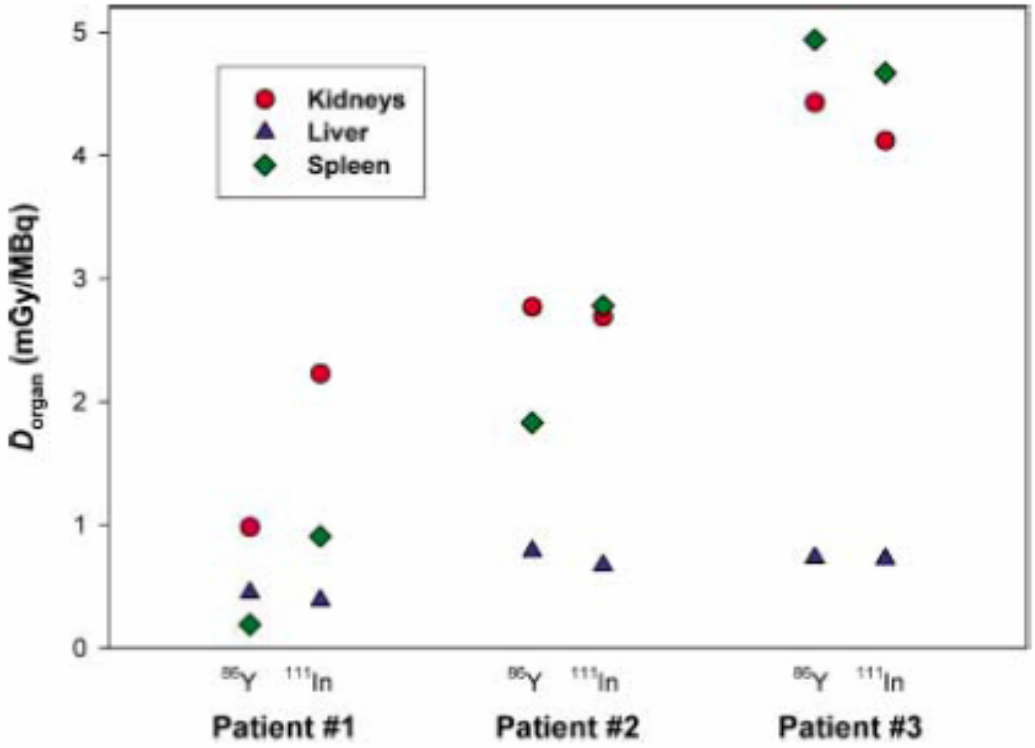

Fig. 4. Estimated absorbed doses to critical organs (D_{organ}) for ^{90}Y-DOTATOC therapy. The plots show the individual absorbed doses based on investigation with ^{86}Y-DOTATOC PET (^{86}Y) and ^{111}In-DTPA-octreotide scintigraphy (^{111}In)

Forster et al. 2001

Organ Mass Scaling

For electrons, the scaling is:

$$DF_2 = DF_1 \frac{m_1}{m_2}$$

For photons, the scaling is:

$$\phi_2 = \phi_1 \left(\frac{m_2}{m_1} \right)^{1/3} \qquad \Phi_2 = \Phi_1 \left(\frac{m_1}{m_2} \right)^{2/3}$$

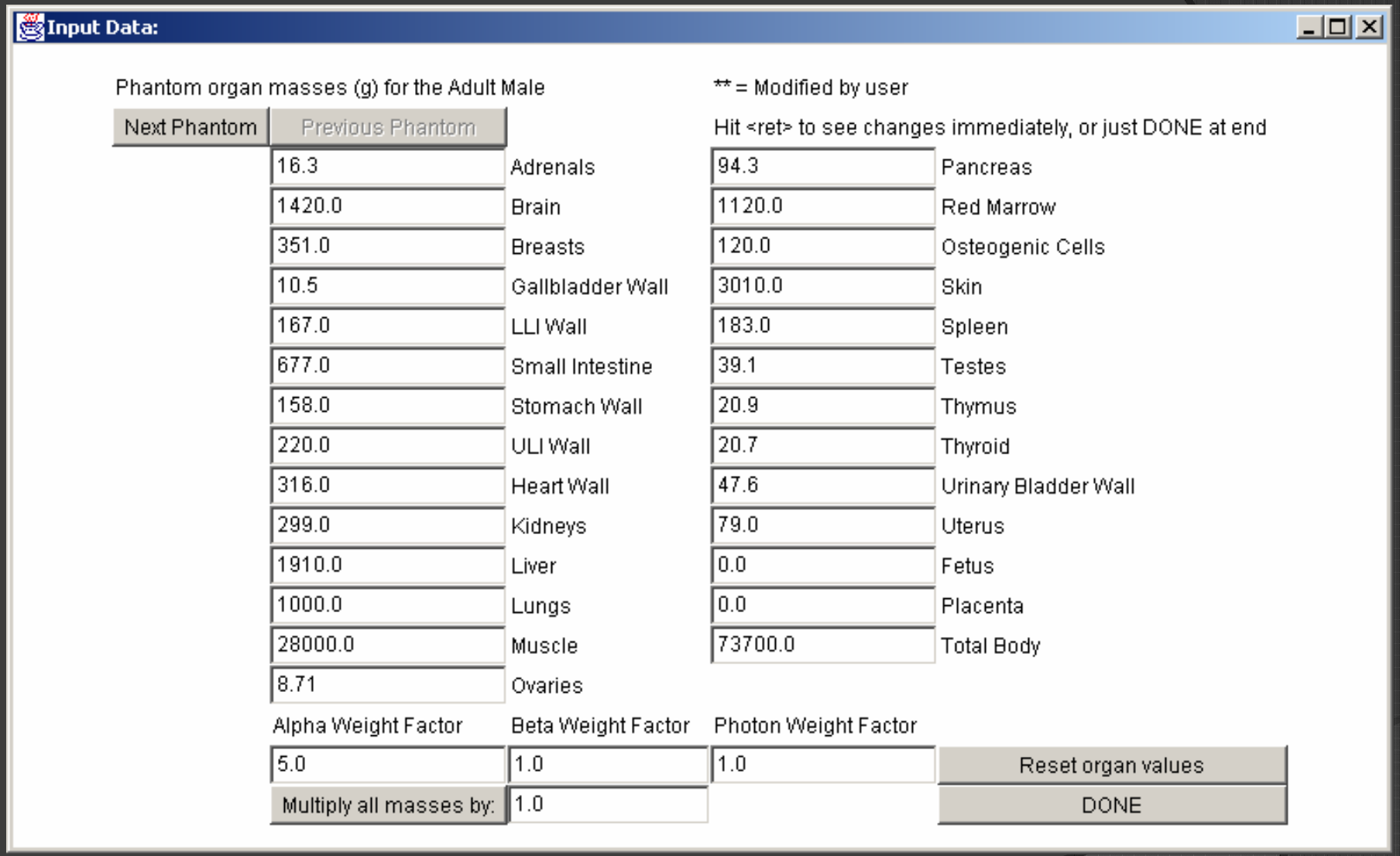
Input Data:
Phantom organ masses (g) for the Adult Male
** = Modified by user
Next Phantom
Previous Phantom
Hit <ret> to see changes immediately, or just DONE at end
16.3 Adrenals
1420.0 Brain
351.0 Breasts
10.5 Gallbladder Wall
167.0 LLI Wall
677.0 Small Intestine
158.0 Stomach Wall
220.0 ULI Wall
316.0 Heart Wall
299.0 Kidneys
1910.0 Liver
1000.0 Lungs
28000.0 Muscle
8.71 Ovaries
94.3 Pancreas
1120.0 Red Marrow
120.0 Osteogenic Cells
3010.0 Skin
183.0 Spleen
39.1 Testes
20.9 Thymus
20.7 Thyroid
47.6 Urinary Bladder Wall
79.0 Uterus
0.0 Fetus
0.0 Placenta
73700.0 Total Body
Alpha Weight Factor
Beta Weight Factor
Photon Weight Factor
5.0
1.0
1.0
Reset organ values
Multiply all masses by:
1.0
DONE

Uncertainties in Internal Dose Calculations for Radiopharmaceuticals

J Nucl Med 2008; 49:1–8

- ..the combined uncertainties in any given radiopharmaceutical dose estimate are typically, at a minimum, a factor of 2 and may be considerably greater, in general because of normal human variability, and particularly in disease states.
- In therapy applications, if patient-individualized dosimetry is performed, …the total uncertainty in an individual dose estimate can be reduced to a value of perhaps ~10%–20%.

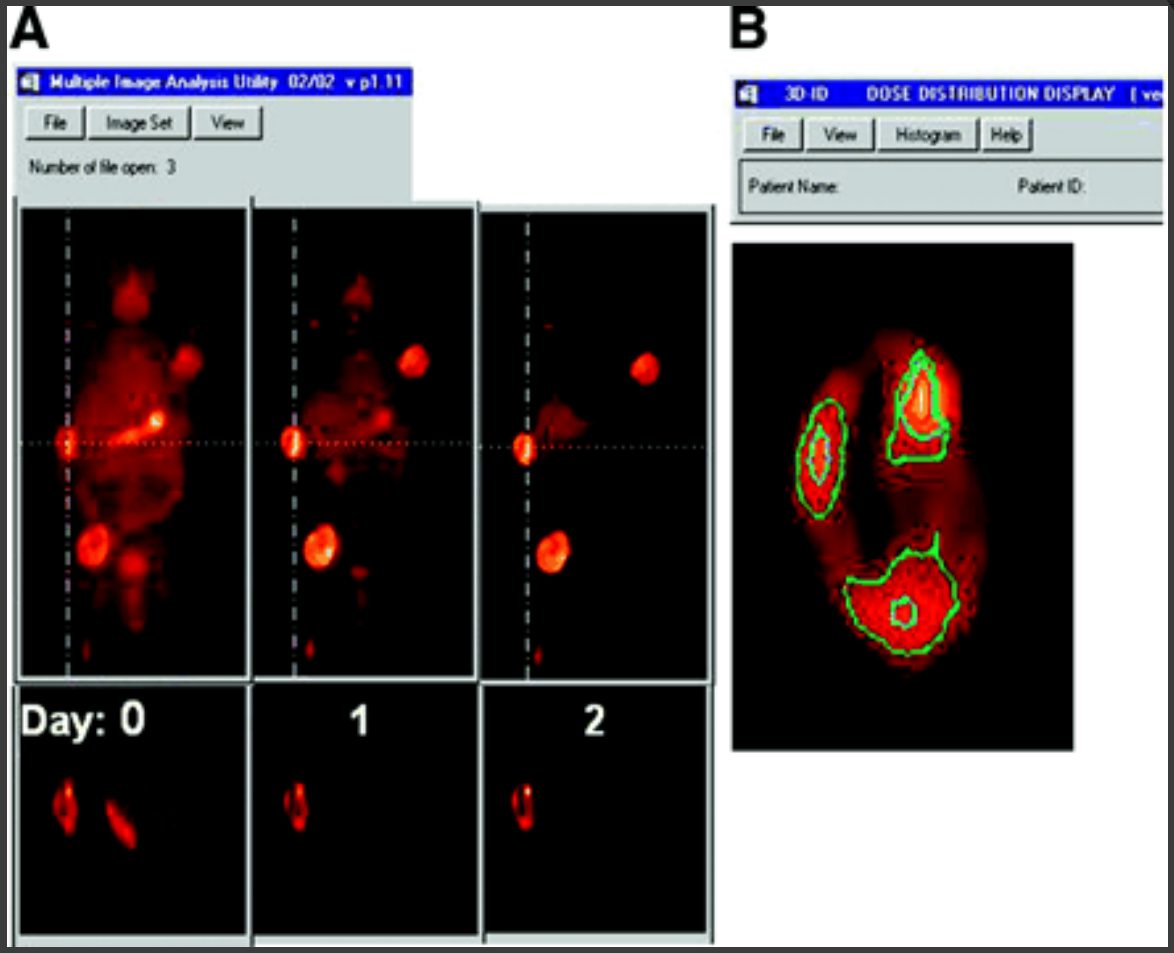

FIGURE 3. (A) Summed coronal ^{124}I PET image slices obtained on day of ^{124}I administration (day 0) and on subsequent 2 days are depicted using same intensity level. Cross-hairs show plane of intersection for corresponding transverse slices through tumor 2, shown immediately below coronal images. (B) Image of absorbed dose distribution in tumor 2, magnified to highlight spatial distribution of absorbed dose within this tumor. Color-coded isodose contours are superimposed as follows: yellow = 75%, red = 50%, blue = 25%, and green = 10% of maximum absorbed dose to tumor (400 Gy). Three different foci of enhanced absorbed dose are observed and designated 1–3 as shown. Kolbert et al. J Nucl Med Vol. 45 No. 8 1366-1372.

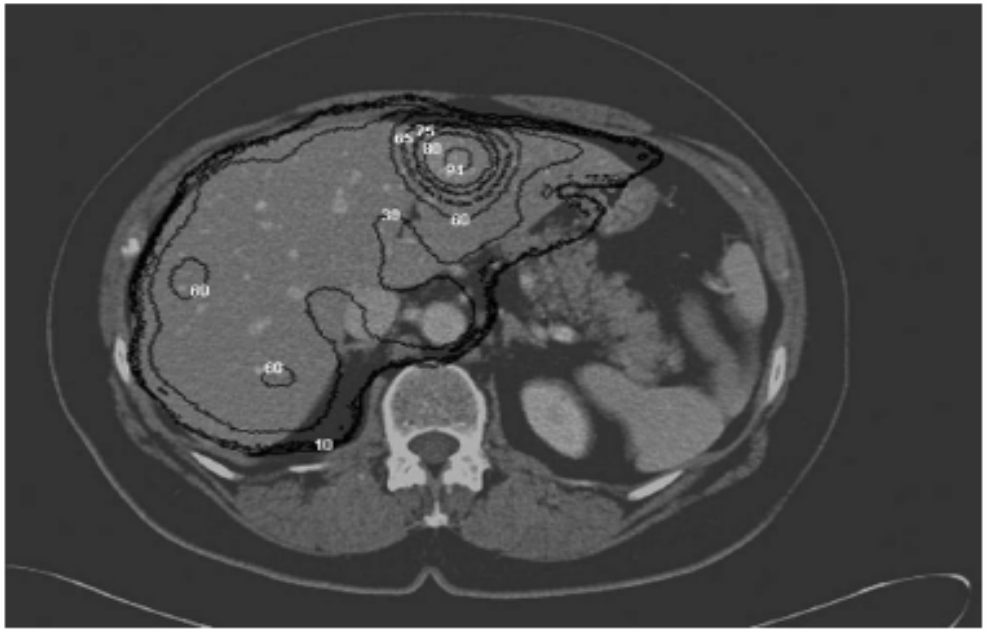

FIG. 7. Calculated dose distribution after administration of ^{131}I-MIBG superimposed on axial CT scan.

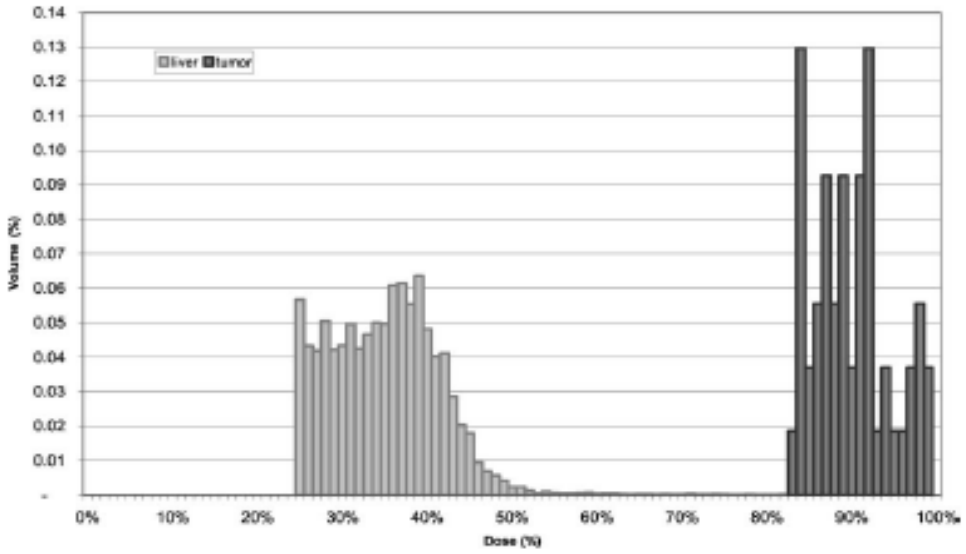

FIG. 8. Differential dose volume histogram for normal liver and metastasis of the case presented in this study.

Strigari *et al.*: Tumor control probability in systemic radiotherapy Medical Physics, Vol. 33, No. 6, June 2006

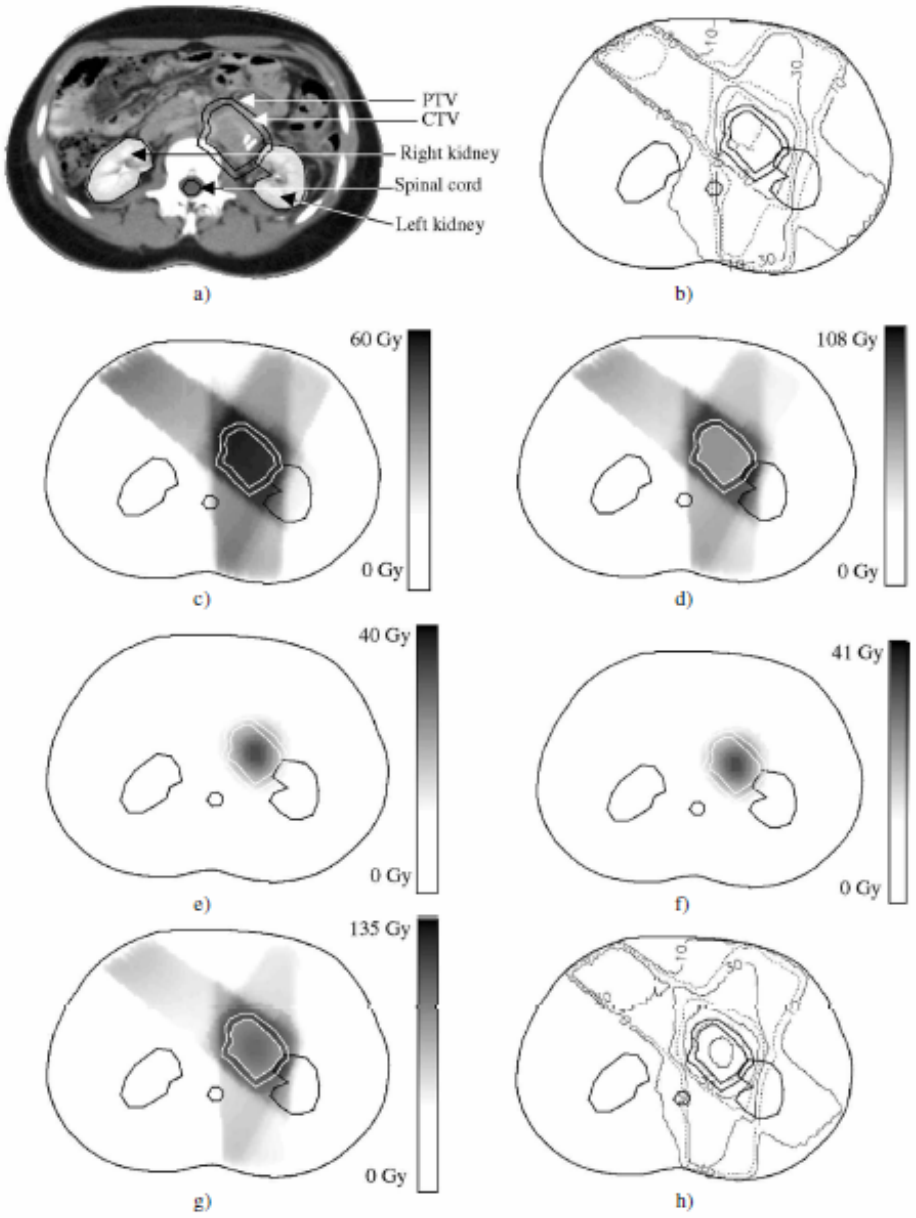

Figure 1. Data for Patient A with CTV, PTV, spinal cord and kidneys outlined. a) CT image of corresponding slice; b) XBT isodose plot showing dose levels in Gy; c) XBT dose distribution; d) XBT BED distribution; e) TRT dose distribution; f) TRT BED distribution; g) Combined BED distribution; h) Equivalent external beam isodose plot for the combined therapy showing dose levels in Gy.

Bodey et al. 2003

Patient-Specific Biological Response

- "Dose" – necessary, not sufficient – interest in biological response functions to modify dose
  - Biologically Effective Dose (BED)
  - Time-dose-fractionation (TDF) factors

Biologically Effective Dose (BED)

Protracted irradiation at a decaying dose rate

$$\ln(SF) = -\alpha D - \frac{\lambda}{\lambda + \mu}\beta D^2$$

$$BED_{TRT} = D\left(1 + \frac{D\lambda}{(\mu + \lambda)(\alpha / \beta)}\right)$$

BED for a fractionated high dose rate treatment

$$BED_{XTB} = D\left(1 + \frac{D / n}{\alpha / \beta}\right)$$

α,β are radiosensitivity parameters
λ is the effective dose-rate decay constant
μ is the repair constant

Time-dose-fractionation (TDF) factors

$$\mathrm{TDF} = 0.122 \sum_{i} r_{0}^{1.35} \, T_{eff}$$

$$\mathrm{TDF} = 1.554 \sum_{i} D^{1.35} \, T_{eff}^{-0.35}$$

r_0 is the initial dose rate in cGy/h
T_{eff} is the effective half-time in days
D_i is the absorbed dose (Gy) delivered for treatment cycle i

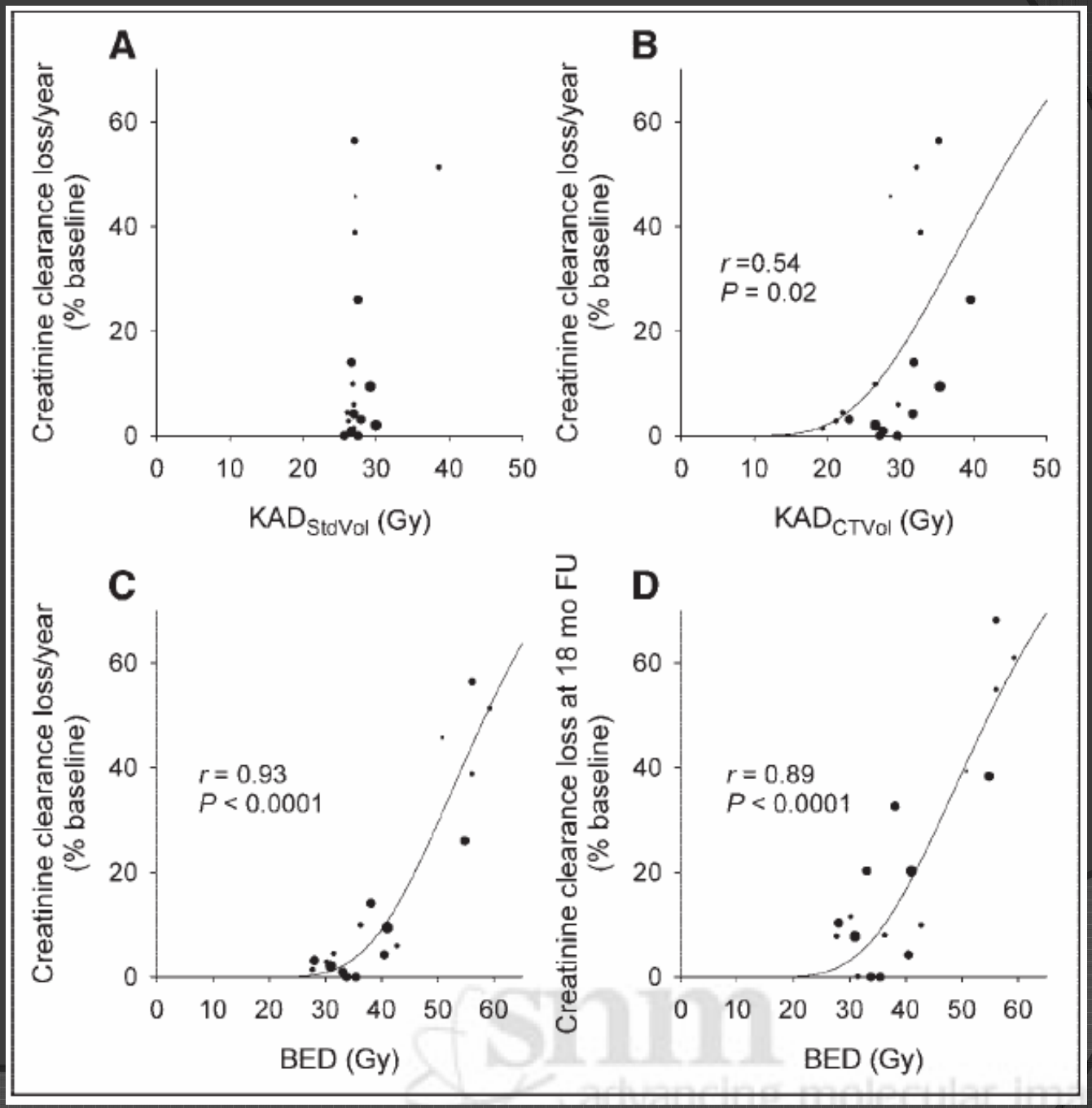
A
Creatinine clearance loss/year (% baseline)
KAD$_{StdVol}$ (Gy)
B
Creatinine clearance loss/year (% baseline)
r =0.54
P = 0.02
KAD$_{CTVol}$ (Gy)
C
Creatinine clearance loss/year (% baseline)
r = 0.93
P < 0.0001
BED (Gy)
D
Creatinine clearance loss at 18 mo FU (% baseline)
r = 0.89
P < 0.0001
BED (Gy)

Difficulty: Effects clearly not related to dose

AAPM Report No. 49 - Dosimetry of Auger-Electron-Emitting Radionuclides:

"Cellular and organ studies have demonstrated that when Auger emitters are introduced into the cytoplasm of cells, the effects are typical of those caused by radiations of low-linear-energy transfer (LET).

In contrast, when Auger emitters are incorporated into the DNA of cells, the resulting survival curves are similar to those for high-LET alpha particles.

Finally, recent *in vivo* studies with radioprotectors show that the intense local damage imparted by Auger cascades can be mitigated despite the fact that they impart high-LET-type effects."

"The absorbed dose from Auger emitters must be calculated at a level suited to the biological system employed. Hence, a number of target volumes are of interest:

individual strands or bases of the DNA molecule,

supercoiled DNA,

cell or cell nucleus,

bulk tissue.

Choosing the target volume, however, is complex. The radiation properties of the radionuclide certainly play a role in this regard. Just as important is the distribution of the radioactivity within the cells, which in turn depends on the chemical nature of the radiocompound. Hence, the appropriate target volume must be determined on a case-by-case basis."

Bystander Effects – in vitro studies

Hall:

"The plethora of data now available concerning the bystander effect fall into two quite separate categories, and it is not certain that the two groups of experiments are addressing the same phenomenon."

1. Medium transfer experiments
2. Microbeam irradiation experiments

Bystander Effects – in vitro studies

Medium transfer:

- Irradiated cells secreted a molecule into the culture medium that was capable of killing cells when that medium was transferred onto unirradiated cells.
- The effect produced by epithelial cell cultures is dependent on the cell number at the time of irradiation, can be observed as soon as 30 min post irradiation, and is still effective if taken from the irradiated cells up to 60 h after irradiation.
- This bystander effect can be induced by radiation doses as low as 0.25 mGy and is not significantly increased up to doses of 10 Gy.
- In addition to increased levels of cell death and reduced cloning efficiency, medium transfer experiments have shown an increase in neoplastic transformation as well as genomic instability in cells that have not themselves been irradiated.

Bystander Effects – in vitro studies

Microbeam studies

- Irradiated human fibroblasts - cells of one population were lightly stained with cyto-orange, a cytoplasmic vital dye, while cells of another population were lightly stained blue with a nuclear vital dye.
- The two cell populations were mixed and allowed to attach to the culture dish, and the computer controlling the accelerator was programmed to irradiate only blue-stained cells with 10 alpha particles directed at the centroid of the nucleus.
- The cells were fixed and stained 48 h later, at which time micronuclei and chromosome bridges were visible in a proportion of the nonhit (i.e., orange-stained) cells!

Bystander effects – in vivo studies

Irradiation of the lung base in rats, marked increase in the frequency of micronuclei in the shielded lung apex.

However, radiation of the lung apex did not result in an increase in the chromosome damage in the shielded lung base.

This suggests that a factor was transferred from the exposed portion of the lung to the shielded part and that this transfer has direction from the base to the apex of the lung.

Bystander Effects

- In another experiment, exposure of the left lung resulted in a marked increase in micronuclei in the unexposed right lung.
- Experiments suggest that bystander effects are limited to the organ irradiated, and have been demonstrated primarily in experiments with alpha particles.
- These results challenge the traditional notion of the relationship of dose and effects.

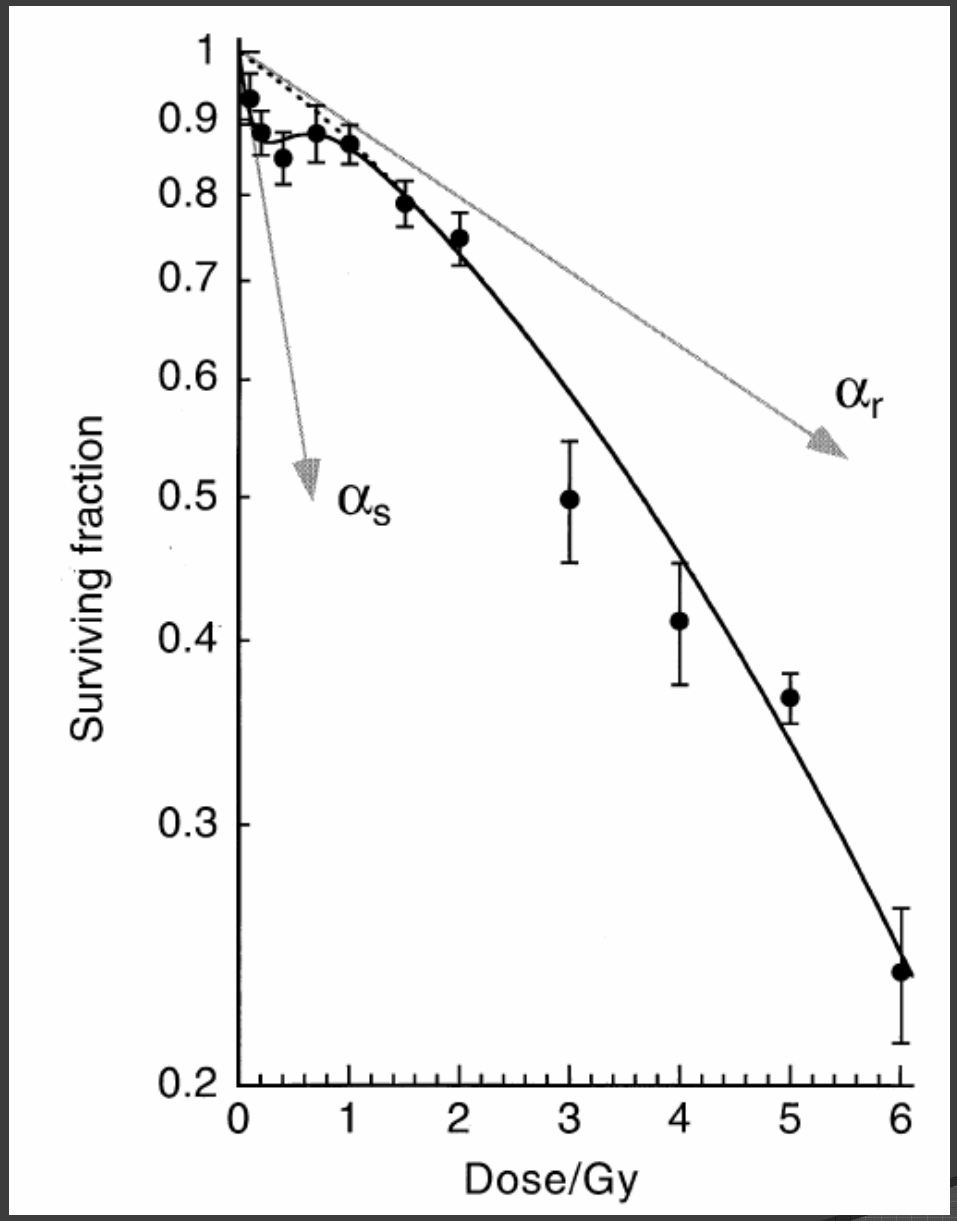

Marples et al. Int. J. Radiation Oncology Biol. Phys., Vol. 49, No. 2, pp. 379–389, 2001

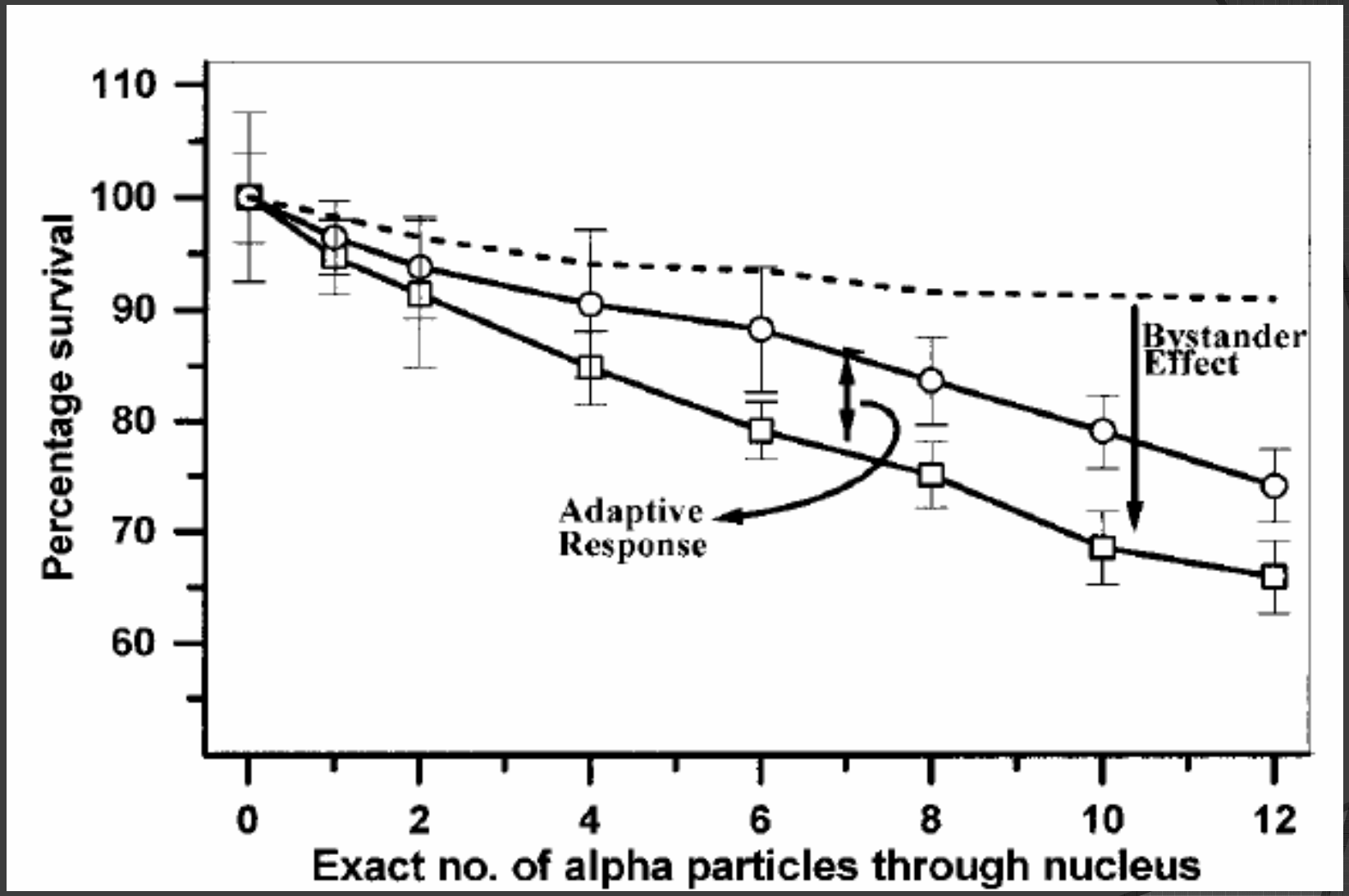

Sawant et al. Radiation Research, 156, 177–180 (2001)

In Vivo Bystander Effects: ^{123}IUdR and ^{125}IUdR

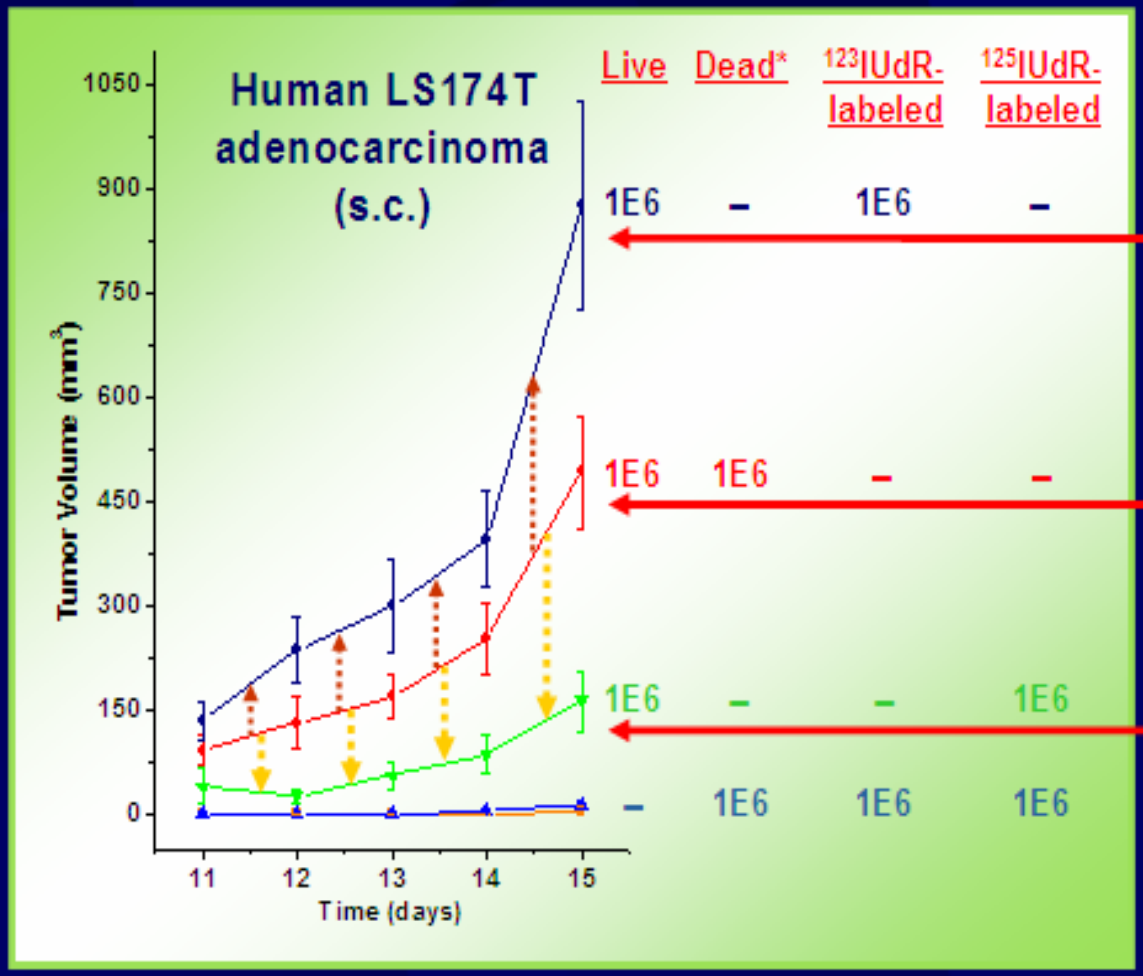

^{123}I → *sBE*

(Stimulatory Bystander Effect)

Control

^{125}I → *iBE*

(Inhibitory Bystander Effect)

* Freeze–defrost 3 times

Relevance of Dosimetry to Clinical Practice

What is the Role of Dosimetry in Targeted Therapy?

- Goal: optimize patient therapy, maximize therapeutic efficacy.
- Radiotherapy:

Anniversary Paper: Fifty years of AAPM involvement in radiation dosimetry

G. Ibbott et al.
Radiological Physics Center, University of M. D. Anderson Cancer Center, Houston, Texas 77030-4009

Med. Phys. 35 (4), April 2008

- "The most important role of the clinical radiotherapy medical physicist is to ensure the accurate delivery of the prescribed dose distribution to the patient…there is a clinical need for accurate dose delivery to the tumor. The often stated goal is for 5% accuracy."

What is the Role of Dosimetry in Targeted Therapy?

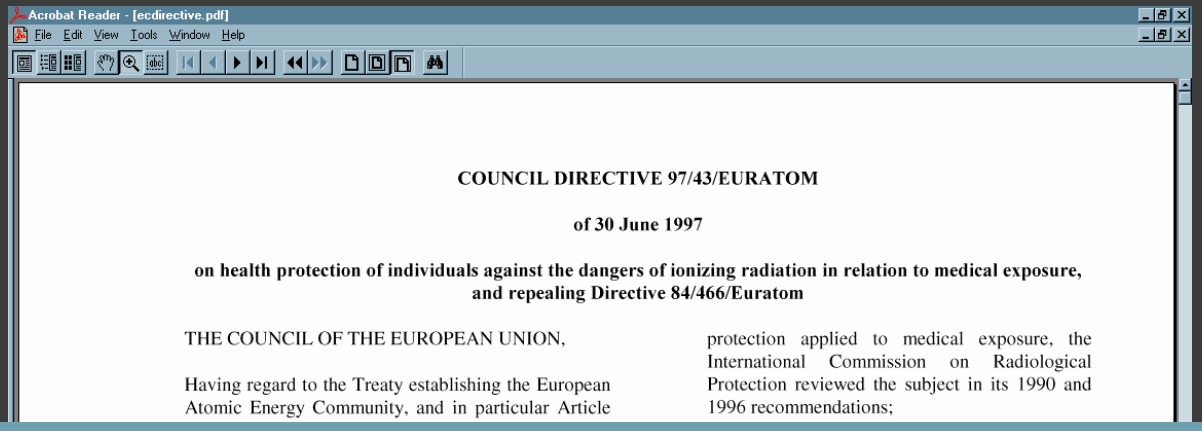
Acrobat Reader - [ecdirective.pdf]

File Edit View Tools Window Help

COUNCIL DIRECTIVE 97/43/EURATOM

of 30 June 1997

on health protection of individuals against the dangers of ionizing radiation in relation to medical exposure, and repealing Directive 84/466/Euratom

THE COUNCIL OF THE EUROPEAN UNION,

Having regard to the Treaty establishing the European Atomic Energy Community, and in particular Article

protection applied to medical exposure, the International Commission on Radiological Protection reviewed the subject in its 1990 and 1996 recommendations;

EURATOM Council Directive 97/43: medical exposures for radiotherapeutic purposes, including nuclear medicine, “exposures of target volumes shall be individually planned”.

What is the Role of Dosimetry in Targeted Therapy?

- Brans et al. 2007: Targeted therapy: "…distinct similarities to, but also profound differences from the more commonly used external radiotherapy…[more evidence is needed that] that applied clinical dosimetry results in better patient outcome than is achieved with fixed activity dosing methods."
- Flux et al. 2007: "It is essential that dosimetry studies are sufficiently resourced and are performed with adequate scientific rigour that the results can be judged with confidence."

What is the Role of Dosimetry in Targeted Therapy?

- Individual patient dosimetry has the following goals:
  - To establish individual minimum effective and maximum tolerated absorbed doses
  - To establish a dose–response relation to predict tumour response and normal organ toxicity on the basis of pretherapy dosimetry
  - To objectively compare the dose–response results of different radionuclide therapies, either between different patients or between different radiopharmaceuticals, as well as to perform comparisons with the results routinely obtained with external radiotherapy
  - To increase the knowledge of clinical radionuclide radiobiology, in part with the aim of developing new approaches and regimens

Flux et al. Z Med Phys 2006;16:47–59

What is the Role of Dosimetry in Targeted Therapy?

The Case for Patient-Specific Dosimetry in Radionuclide Therapy

CANCER BIOTHERAPY & RADIOPHARMACEUTICALS
Volume 23, Number 3, 2008

- "Treating all nuclear medicine patients with a single, uniform method of activity administration amounts to consciously choosing that these patients be treated with a lower standard of care than patients who receive radiation externally for cancer treatments."

What is the Role of Dosimetry in Targeted Therapy?

DeNardo and DeNardo 2010:

- "Although the accuracy of radionuclide dosimetry can be improved, it is precise …and correlates with tissue response, when carefully performed.
- Treatment planning for an individual patient ("patient-specific radiation dosimetry") for RIT must be the ultimate goal.

Radioiodine Therapy

- Fixed activity protocols are widely used, with reasonable success.
- Benua and Leeper (1986), thyroid cancer: whole body activity at 48 hrs <120 mCi, unless there is metastatic lung involvement (80 mCi).
- Maxon et al., thyroid cancer (1992-3): Dose-based approach needed. 80-300 Gy target dose.
- EANM Dosimetry Committee: target dose 80 Gy, marrow dose <2 Gy.

Radioiodine Therapy

- Jonsson and Mattsson, Graves disease, (n=200) (2004) compared theoretical levels of activity that could be given to patients using patient-specific dose calculations and actual practice to a fixed-activity approach.
- "…most of the patients were treated with an unnecessarily high activity, a mean factor of 2.5 times too high and in individual patients up to eight times too high, leading to an unnecessary radiation exposure both for the patient, the family and the public."

Radioiodine Therapy

- Kobe et al. (2007), Graves disease:
  - 571 subjects, target dose 250 Gy.
  - Relief from hyper-thyroidism was achieved in 96% of patients who received more than 200 Gy, even for those with thyroid volumes > 40 mL.

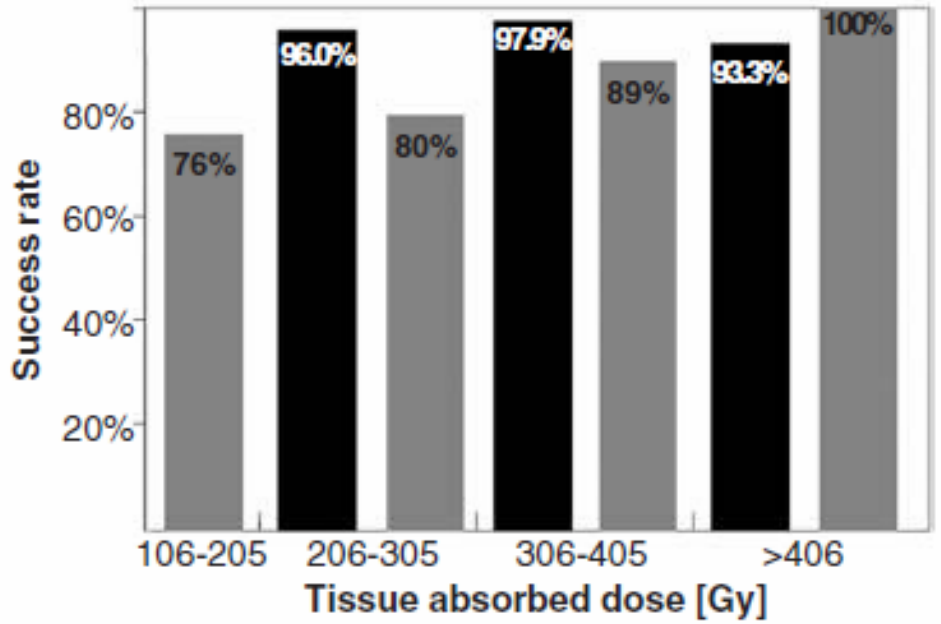

Figure 2. Success rates of Graves' disease therapy at 12 months post-therapy characterized by Kobe et al.[40] using therapy guided by patient-specific dose calculations (black bars), with comparison to those of others (gray bars). Reprinted with permission of Schattauer GmbH.

Radioiodine Therapy

- Since patients are almost always treated successfully in the first treatment and do not have to return multiple times for follow-up treatment, this results in:
  - More favorable outcomes and better quality of life for the patients.
  - Significant monetary savings for the institution.

I-131-mIBG therapy for neuroblastoma and phaeochromocytoma

- Fixed activity fractions (e.g. McCluskey 2005)
  - Simple and easy to implement quickly.
  - No understanding or correlations of dose/effect possible.
- Activity/kg body weight approach (e.g. Sisson et al. 1994)
  - Correlations of marrow toxicity with activity/kg of body weight.
  - Again, no dose/effect correlations possible.

I-131-mIBG therapy for neuroblastoma and phaeochromocytoma

- Dose-based approaches (e.g. Matthay et al. 2001)
  - Total body, marrow, and tumor doses.
  - Hematologic toxicity was correlated with activity/kg, marrow dose, total body dose.
  - Calculated tumor dose predicted response.

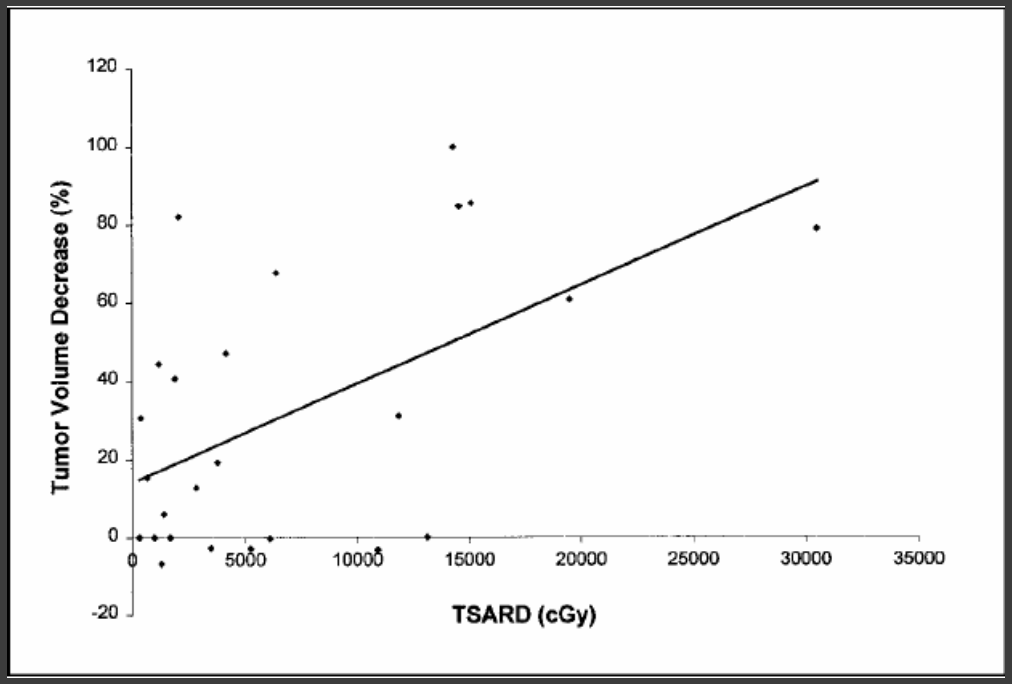

Correlation of TSARD with subsequent tumor volume decrease. Decrease in tumor volume is shown as positive percentage. Spearman rank correlation, *P = 0.02.*

Spearman Rank Correlations Among ^{131}I-MIBG Activity, TSARD, Target Lesion Volume Response, Whole-Body Irradiation Dose, Red Marrow Radiation Dose, and Hematologic Toxicity

Variable (X)	Variable (Y)	r_s	*P*
Red marrow irradiation	Blood irradiation	0.43	0.04
	Neutrophil nadir	−0.47	<0.01
	Platelet nadir	−0.35	0.02
	Volume decrease (%)	0.48	<0.01

Radioembolisation of liver tumors

- Use of ^{90}Y-microspheres has shown significant response rates
- Radiation complications – such as pneumonia, GI ulceration, and liver injury
- Kennedy et al. 2009 – 680 cases, many centers – “a predictive model is not yet possible, given the large variance of the data”.
- Techniques vary – fixed empirical values, patient’s body surface area, average radiation dose to the whole liver, or dosimetric partition model considering liver involvement.

Radioembolisation of liver tumors

- Cases of radiation pneumonia were found at lung doses > 10 Gy (range: 10 to 36 Gy), and one fatal event at 56 Gy.
- Whole liver dose 100-130 Gy typical. "…no dose-limiting organ toxicity has been observed in patients who have received nominal absorbed doses up to 150 Gy"
- Salem et al.: higher doses are tolerated with lower treated volumes.

Radioembolisation of liver tumors

- Young et al.: The results showed that patients with lesser extent of the disease, received a higher cumulative dose than others before worsening of liver function (390 vs. 196 Gy).
- Interestingly, these results also confirm that patients with higher irradiation to the normal liver (because of both, lower liver involvement and higher whole liver dose), but distributed in more cycles, demonstrated higher tolerability.

Radiopeptide therapy for neuroendocrine tumours

- Large interpatient differences in radiopeptide uptake in normal organs and tumour tissues – thus patient-specific dosimetry is necessary for patient selection and therapy planning.
- [^{90}Y-DOTA^{0},Tyr^{3}]-octreotide – pretherapy imaging with ^{111}In or ^{86}Y for dose calculations.
  - ^{111}In – somatostatin receptor binding affinity may be altered.
  - ^{86}Y – good image resolution, but all phases of biological clearance may not be seen due to short half-life.

Radiopeptide therapy for neuro-endocrine tumours

- [^{177}Lu-DOTA^{0},Tyr^{3}]-octreotate
  - Can be used for both imaging and dose delivery
  - Octreotate has a six- to nine-fold higher affinity for somatostatin receptor 2
  - Kidney dose ~3 Gy (Forrer et al. 2005), compare to 20-30 Gy for ^{90}Y-DOTATOC therapy (Barone et al. 2005). Marrow ~60 mGy.

Radiopeptide therapy for neuro-endocrine tumours

- Renal toxicity issues
  - Barone et al. (2005) – importance of patient-specific dose calculations to avoid kidney toxicity with ^{90}Y-DOTATOC
  - Bodei et al., ^{90}Y-DOTATOC (mainly) and ^{177}Lu-DOTATATE in peptide receptor radionuclide therapy (PRRT): to maintain kidney BED values below 28 Gy, a patient-individualized evaluation of dosimetry should always be performed.

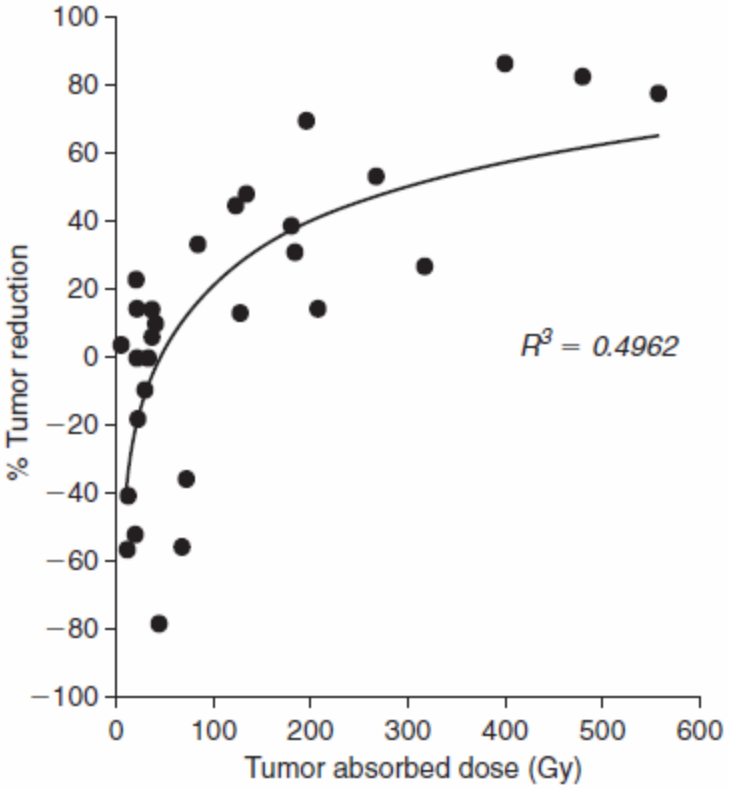

Figure 6. Tumor dose-response characterized by Pauwels et al.[48] with ^{90}Y-DOTATOC. Reprinted with permission of the Society of Nuclear Medicine.

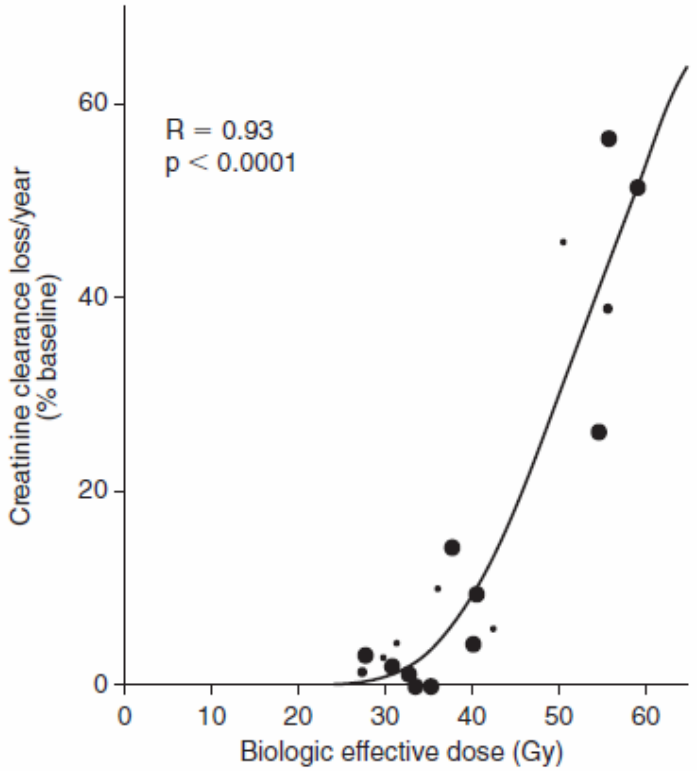

Figure 7. Plot from Barone et al.[51] showing prediction of kidney toxicity from patient-individualized dose calculations in the use of ^{90}Y (DOTATOC). (Larger and smaller dots on the plot were used to indicate the number of treatment cycles received by different patients.) Reprinted with permission of the Society of Nuclear Medicine.

Radioimmunotherapy –non-Hodgkin's Lymphoma

- Goldsmith 2010 – review of several trials
  - both approved agents (Bexxar, Zevalin) have high ORRs.
  - CRs much better for Bexxar
  - Complications for both – antibody response, marrow suppression.
  - Longer beta range of ^{90}Y may be better for bulkier tumors.
  - Dosimetry required for Bexxar, needed in cases of variable T_{eff} for Zevalin.

Radiolabeled antibodies

- Divgi et al (1998) – ^{131}I-labeled Monoclonal Antibody against metastatic renal cell carcinoma:
  - Correlation of marrow toxicity with calculated total body dose.
- Chen et al. (2002) – ^{90}Y-anti-TAG-72 murine antibody against non–small cell lung cancer:
  - Excellent correlations of marrow toxicity with calculated marrow dose, when patient-specific marrow mass estimated.

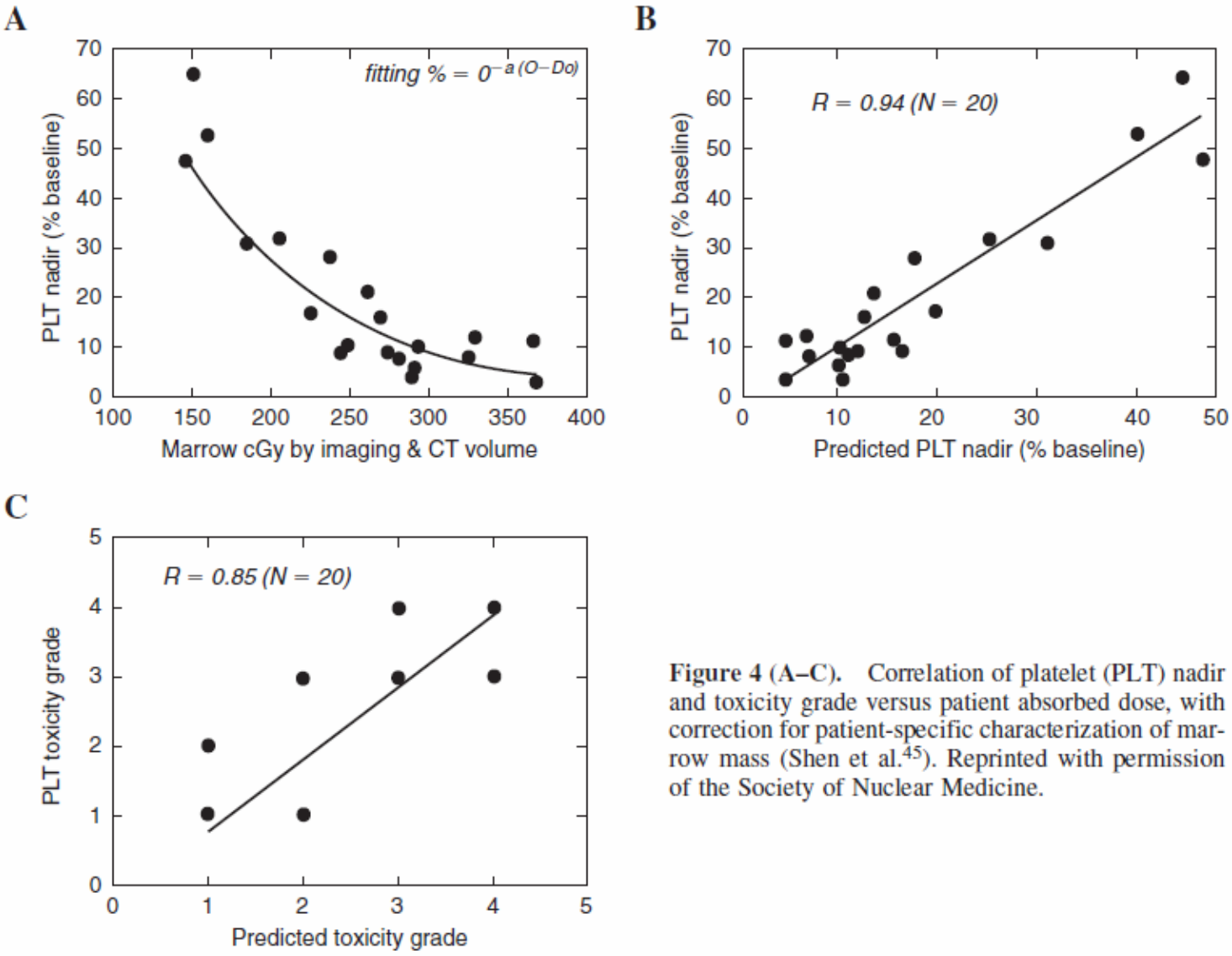

Figure 4 (A–C). Correlation of platelet (PLT) nadir and toxicity grade versus patient absorbed dose, with correction for patient-specific characterization of marrow mass (Shen et al.[45]). Reprinted with permission of the Society of Nuclear Medicine.

Radioimmunotherapy – nonHodgkin's Lymphoma

- Wahl et al. (1998) – Patients receiving a whole-body absorbed dose between 0.65 and 0.85 Gy showed longer CR than patients receiving between 0.25 and 0.55 Gy.
- Liu et al. (1998) – using a myeloablative approach:
  - Markedly improved progression-free survival over 8 years post therapy.
  - Not dosimetric, but demonstrates possibilities if more aggressive therapy is done, using dosimetry.

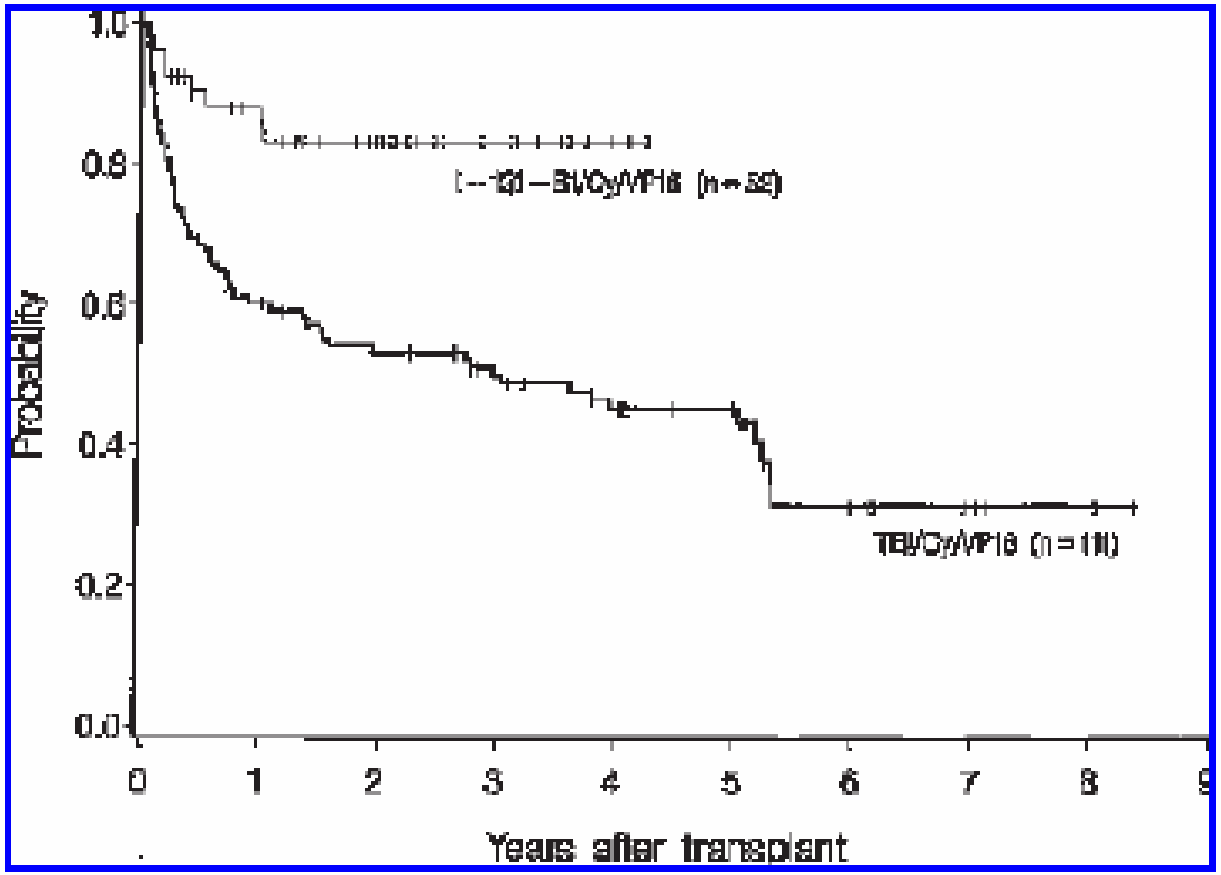

Figure 3. Kaplan-Meier plots from Liu et al.,[44] showing progression free survival after ^{131}I RIT involving myeloablative dose levels, compared with best results with other forms of therapy. © The American Society of Hematology. Reprinted with permission of the Society of Nuclear Medicine.

Conclusions

- Internal dosimetry has come a looooooong way from beta self dose to the thyroid.
- As in occupational internal dose, models are always evolving – more complex and realistic, but more difficult to use.
- Nuclear medicine internal dosimetry has become well standardized and automated.
- More routine use in therapeutic applications is needed.

Conclusions

- Evidence shows that better and more predictable outcomes can be achieved with patient-individualized dose assessment.
- Fixed activity or fixed activity/g or m^2 with no dosimetry cannot yield any meaningful information about dose/response or dose/toxicity.
- Proceeding with therapy with no knowledge of radiation dosimetry not in the best interests of patients.
- Much research is needed to characterize dose/response functions for internal emitters.